Thesis

On

FINITE ELEMENT ANALYSIS AND OPTIMIZATION OF PROCESS PARAMETERS INVOLVED IN ULTRASONIC MACHINING PROCESS

Submitted in partial fulfilment of the requirement for the award of the degree of

Master of Engineering

IN

PRODUCTION & INDUSTRIAL ENGINEERING

Submitted By

KANWAL JEET SINGH

Roll No. 801082017

Under the guidance of

Dr. Vinod Kumar Singla	**Mr. Bikramjit Sharma**
Associate Professor	**Assistant Professor**
Thapar University, Patiala	**Thapar University, Patiala**

DEPARTMENT OF MECHANICAL ENGINEERING

THAPAR UNIVERSITY

PATIALA-147004, INDIA

CERTIFICATE

This is to certify that the thesis entitled **"FINITE ELEMENT ANALYSIS AND OPTIMIZATION OF PROCESS PARAMETERS INVOLVED IN ULTRASONIC MACHINING PROCESS"** is authentic record of my study carried out as requirement for the award of the degree of **Master of Engineering (Production & Industrial Engineering)** to **Thapar University, Patiala,** under the guidance of **Dr.VINOD KUMAR SINGLA** (Associate Professor) and **Mr. BIKRAMJIT SHARMA** (Assistant Professor) Department of Mechanical Engineering, Thapar University, Patiala. This matter embodied in this thesis has not been submitted in part or full to any other University or Institute for the award of any degree.

Kanwal jeet Singh

This is to be certify that above declaration made by the student concerned is correct to the best of my knowledge & belief.

11/07/2012

Dr.VINOD KUMAR SINGLA
Associate Professor,
Department of Mechanical Engineering
Thapar University,
Patiala, 147004

Mr. BIKRAMJIT SHARMA
Assistant Professor
Department of Mechanical Engineering
Thapar University
Patiala, 147004

Countersigned By

Dr.AJAY BATISH
Professor & Head
Department of Mechanical Engineering
Thapar University Patiala 147004

Dr.S.K MOHAPATRA
Dean of Academic Affairs
Thapar University Patiala 147004

ACKNOWLEDGEMENT

With deep sense of gratitude I express my sincere thanks to my guides, ***Dr. Vinod Kumar Singla*** *and* ***Mr. Bikramjit Sharma*** for their valuable guidance, proper advice and constant encouragement during the my thesis work from the initial level to final level. I also feel very much obliged to ***Dr.Ajay Batish***, Professor & Head, of Mechanical Engineering Department and **Dr.S.K.Mohapatra**, Dean Academic Affairs, Thapar University Patiala

I would like to thanks all the members and employees of Mechanical Engineering Department, Thapar University, Patiala for their everlasting support. I am also very thankful to my friends for their cooperation. I offer my regards to all of those who supported me in any respect during the completion of the work.

Lastly, and most importantly, I wish to thank my parents. They supported me and loved me.
To them I dedicate this thesis.

KANWAL JEET SINGH

Registration No. 801082017

ABSTRACT

Ultrasonic Machining is one of the earliest non-traditional machining processes and now days we know that process technology is a very advance, many type of new materials are being developed which have very high strength, high thermal and electrical conductivity. Due to these properties there are difficult to machine by traditional machining. USM also one of the non-conventional machining method which is used to machine such advance hard and brittle materials to satisfy the present day product need like aerospace, mould, dies and other application. The objective of this work is to optimization of process parameters involved in ultrasonic machining process. Some of the process parameters involved are type of slurry used, abrasive grit size, concentration of abrasive slurry, power rate of ultrasonic machine , type of liquid medium used for the slurry. Also the finite element analysis has been used to analyse the results and the modelling of the results has been done for the application in the different fields.

CONTENTS

LIST OF FIGURES

LIST OF TABLES

ABBREVATIONS

ANOVA	Analysis of Variance
CONC	Concentration
DOF	Degree of Freedom
EMA	Experimental Measurement Analysis
FRF	Frequency Response Function
USM	Ultrasonic Machining
FEA	Finite Element Analysis
MIX	Mixture
MRR	Material Removal Rate
TWR	Tool Wear Rate
SR	Surface Roughness
RH	Rockwell Hardness
S/N	Signal to Noise Ratio

NOTATIONS

A	Concentration
B	Type of Abrasive
C	Power Rate
D	Grit Size
E	Young's modulus
F	Force
AxC	Concentration x Power Rate
OR	Orthogonal Array
SS	Sum of Squares
W_i	Initial Weight
W_f	Final Weight
ρ	Density of the material
$[k]_e$	Element Stiffness Matrix
$\{\delta\}_e$	Nodal Displacement Vector
$\{F\}_e$	Nodal Force Vector
σ	Stress
σ_o	Yield Stress
ε	Strain
f_{cur}	Current Natural Frequency
f_{des}	Desired Natural Frequency
ω	Natural Frequency
Φ	Acoustic Loss

CHAPTER 1

INTRODUCTION

1.1 GENERAL

Current techniques for mechanical working of ordinary materials like steels and cast iron are highly developed and machine tools have been greatly improved in recent years. Recent years have seen the introduction of many new materials such as tungsten and titanium carbide, diamonds, rubies, sapphire, hard steels, magnetic alloys and corundum. Another group of material, germanium, silicon, ferrites, ceramics, glass etc give difficulty on account of great brittleness: these materials often cannot withstand the forces needed for machining. Modern materials such as high-strength steel and ceramics, which are developed to meet the needs of advanced industries, are typically string, hard and brittle. Whilst technologically desirable, these characteristics often render the material difficult and sometime impossible, to shape by machining processes into useful components and parts. The cutting action imposed by above said machining processes on brittle materials, for example, will yield components with very poor surface finish and in many cases, results in the chipping and/or fracture of the materials being machined.

In a ductile material, cracking (or material separation at or ahead of the tool tip) proceeds at a speed dictated by the relative velocity between the cutting tool and the work piece, as plasticity at the crack tip (i.e. crack tip blunting) prevents the crack running too far ahead of the crack or tool tip. As the same crack blunting mechanism is not available in hard and brittle materials (because of the lack of plasticity) the crack at the tool tip propagates uncontrollably ahead of the tool tip, giving rise to chipping and fracture.

The improvement of machining quality can be vitally promoted through the conversion of this machining process into one involving controllable high frequency impacts at the cutting zone. This is achieved through the generation and maintenance of ultrasonic vibration in the cutting tool to alter the fracture process in brittle materials to one in which loading of the materials at the tip of tool, repetitive and under control. Engineering ceramic materials have many attractive properties such as high hardness, high thermal resistance, chemical stability and low electrical conductivity etc. Ceramic composites are assuming increasing industrial importance in machine building and engineering field, mainly because of the fact that technological limitation can be overcome by the use of these non-metallic materials. It is for this reason that ceramic composites have gained acceptance in a number of application imposing extreme demands on one or more properties of the material. Despite their outstanding properties as compared to metals, ceramic composites are only gradually gaining acceptance in mechanical engineering application. One reason for this is found to be in the limitation of the forming process which is done prior to sintering, which restricts the limitations of the forming process which is done prior to sintering, which restricts the generation of complex geometries and makes it difficult to ensure adequate accuracy and surface finish.

The need for methods of machining these "unworkable" materials has led to the introduction of special methods e.g. electrochemical, electro erosion, electron beam and ultrasonic machining. Ultra sonic machining is a 'non-traditional' machining technique and is a part of a family of relatively modern material finishing and shaping processes described as 'chip less machining'. These processes don't use cutting tools and don't create residual stresses in the work piece. Ultrasonic machining is often used in combination with other chip less machining technique, such as electric discharge machining, in the manufacturing of precision components.

1.2 HISTORICAL BACKGROUND OF ULTRASONIC MACHINING (USM)

The history of ultrasonic machining (USM) began with a paper by R.W.Wood and A.L Loomis in 1927 and the first patent was granted to L. Balamuth in 1945. The British patent no. 602801 (1945), issued to an American engineer, L.Balamuth, who discovered ultrasonic machining accidentally in 1942, while he was investigating the dispersion of solid in liquid by mean of a magnetostrictively vibration nickel tube. The use of ultrasonic in machining was first proposed by J.O Farrer in 1945. The United States patent, for the process, no.2580716 was issued in 1962.

The first report on the advanced machining equipment and technology appeared by 1954, the machine tools using the ultrasonic principal had been designed and constructed. Originally USM used to be a finishing operation for the component processed by the electro spark machines. But then with the boom in solid state electronics, the machining of electrically non- conducting, semi conductive and brittle material gets more and more important and, for this reason, ultrasonic machining again gained importance and prominence. In recent years, various types of ultrasonic machine tools have been developed.

1.3 USM PROCESS

The research in the field of more efficient material removal processes has been gathering momentum in recent years especially in the ways and mean to reduce the occurrence of faults or cracks in the sub-surface of the machined ceramic composites. Ultrasonic machining process is an abrasive process, and material removal is purely mechanical. The process equipment consists of a vibration horn (the sonotrode), a tool part, abrasive slurry and the work material as shown in figure 1.1

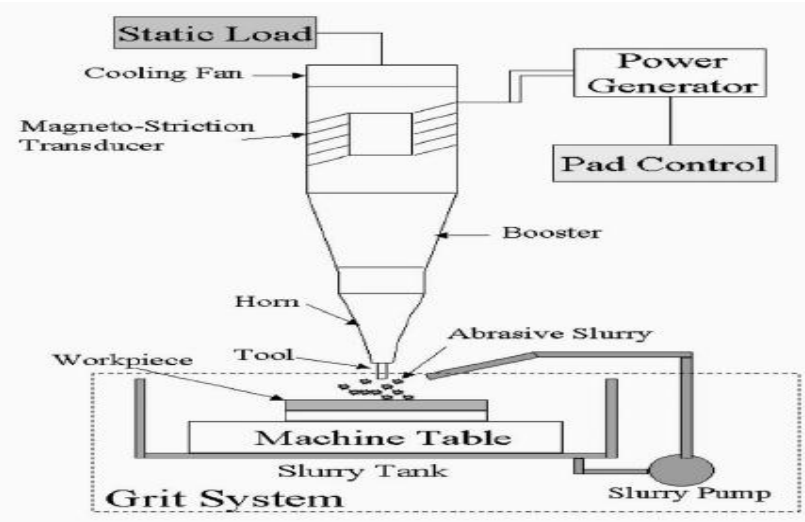

Figure 1.1 Basic features of the ultrasonic machining process [Advanced Machining Processes: Non-traditional and Hybrid Machining Processes, McGraw-Hill Prof Med/Tech, 01-Mar-2005 Vol 1 Page No156]

ultrasonic machining is a process in which abrasive practical in slurry with water are presented to the work surface in the presence of an ultrasonic vibration tool. It is a process which should be of considerable interest, as its potential is not limited by electrical or chemical characteristics of the work material. This machining method can easily perform cutting, drilling and engraving, making it suitable for the processing of ceramics.

As the name implies the process operates at ultrasonic frequencies and typical frequencies used in the ultrasonic machining process range between 20 KHz to 40 KHz. The term ultrasonic is used to describe vibration waves having a frequency above the hearing range of normal human ear i.e. beyond 15 KHz. This would include a wide range of ultrasonic is largely dependent on the generator, practical limitation imposing a maximum frequency in the region of 500 Mc/s. The range of wavelengths in varying media is very wide. For example, when propagated in a solid medium, a wave with the frequency of 25

Kc/s will have a wave length of about 200 mm, while one with a frequency of 500 Mc/s will have a wavelength of the order of 0.008 mm.

The acoustic range of vibration is the one which the human ear perceives i.e. in the frequency range of 30 to 15000 Hz, the ultrasonic range of vibrations lies above this i.e. frequencies beyond 15000 Hz. There is no physical difference between the upper acoustic range 5000 to 15000 Hz and the ultrasonic range 15000 to 30000 Hz. Both the range of frequencies of certain intensities of sound will be heard as loud noise by the human ear and can permanently damage the auditory system. Ultrasonic frequencies of the same intensities of sound cannot be heard by the human ear and they are less harmful.

Ultrasonic frequencies provide satisfactory working condition and hence they are alone used for material removal purposes.

There are two types of waves, namely shear waves and longitudinal waves. Longitudinal waves are mostly used in ultrasonic application since they are easily generated. They can be propagated in solids, liquids and gases and can travel at a high velocity so that their wavelength is short in most media.

The velocity of the wave can be calculated for a given material using the following expression: [Modern Machining Processes By P. C. Pandey, H. S. Shan, Tata McGraw-Hill Education, vol 2, page no 98]

Sonic velocity = $E/\rho\ [m(m-1)/(m^2-m-2)]^{1/2}$ (Equation....1.1)

Where E = Young's modulus,

1/m = Poisson's ratio,

ρ = Density of the material.

1.4 ULTRASONIC MACHINING (USM)

Ultrasonic machining is a 'non-traditional' machining technique and is a part of a family of relatively modern material finishing and shaping processes described as 'chipless machining'. These processes don't use cutting tools and do not create residual stresses in the work piece. Ultrasonic machining is often used in the combination with other chipless machining techniques, such as electro discharge machining, in the manufacturing of precision components.

As the name implies the process operates at ultrasonic frequencies and typical frequencies used in the ultrasonic machining process range between 20 and 40 KHz. The equipment used is based upon a generator energizing a magnetostrictive or piezoelectric transducer which in turn causes an attached tool to vibrate. The vibrating tool transfers energy to abrasive particles carried, within a slurry, underneath the tool tip. The interaction between these particles and the work piece result in the formation of mirror image of the tool tip in the surface of the work piece.

Early design used a magnetostrictive transducer attached to an exponential horn (with a nominal length of one half wavelengths) with a small tool brazed to the tip of the horn. Due to the production of heat within the transducer core, this arrangement tended to have an efficiency of about 50%. Current systems are more likely to use a piezoelectric transducer attached to a 'booster' in the form of a stepped cylinder (nominally one half wavelength long). The booster is, in turn, attached to the tool (again nominally one half wavelengths long). The change in cross-section of the booster causes amplification of the amplitude of vibration at the tool tip. A change in cross-section of the tool can be used to further amplify the vibration. The transducer/booster/tool assembly is located by a clamp around the midpoint or node of the booster.

Ultrasonic machining is a form of abrasion; the brittle material is removed by blows from grains of a harder abrasive, which is under the control of a tool, which vibrates with small amplitude. The abrasive also causes wear in the tool but this is minimized by making the tool of viscous material. The particles of abrasive are themselves cleaved in the process and so must be gradually replaced by running into the working area, a liquid carrying fresh abrasive which also serves to flush away products. The material is cut away as very small particles, but these are produced by many abrasive grains and the tool vibrates at a high frequency so the total rate of removal can be sufficient for practical purposes. Tool may be advanced in the direction of vibration, in which case a cavity is produced whose profile corresponds precisely to that of the tool. Combinations of movements allow one to perform a variety of operations on brittle materials analogous to those of ordinary milling, shaping, profile milling, and so on. The noise resulting from this process is minimized by choosing a frequency in the low ultrasonic range (16-25 Kc/s).

The valuable features of the method possibly of working super hard and very brittle materials ease of piercing and recessing, precision working immediately attracted attention.

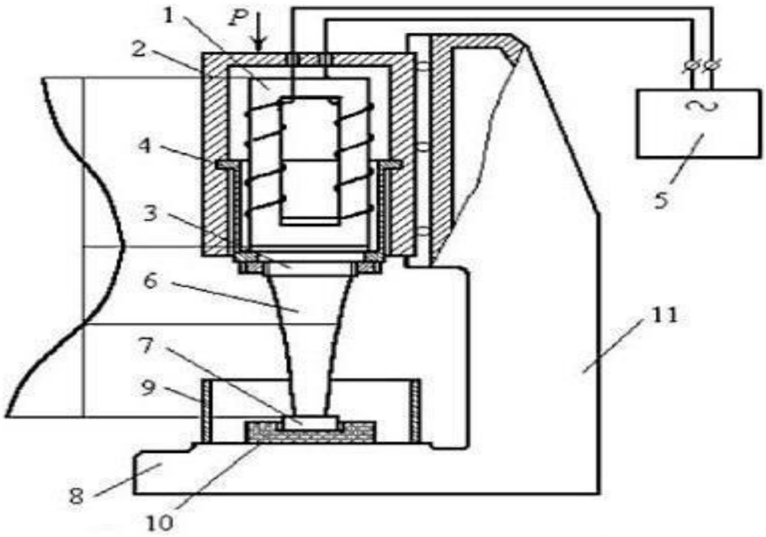

Figure 1.2 Schematic Diagram of USM machine [Modern Machining Processes By P. C. Pandey, H. S. Shan, Tata McGraw-Hill Education, vol 2, page no 99]

magnetostrictive transducer 1, is fixed to the body 2 of the acoustic head using the shoulder 3 and the thin walled cup 4. The winding of the transducer is supplied with an alternating current, at ultrasonic frequency, by the generator 5. The alternating magnetic field induced by the current in the core of the transducer, which is made from magnetostrictive material, is transformed into mechanical vibration in the core. Its main elements are an electromagnet and a stack of nickel plates. The high frequency power supply activates the stack of magnetostrictive material which produces the vibratory motion of the tool. The tool amplitude of this vibration is usually inadequate for cutting purposes, and hence the tool is connected to the transducer by means of a concentrator which is simply a convergent wave guide to produce the desired amplitude at the tool end. The waveguide or concentrator 6 transmits this vibration to the tool 7. The concentrator takes the form of a bar with a variable cross section. It is specially designed to transmit vibration from the transducer, to the tool, with an increase in the amplitude. The selection of frequency and amplitude is governed by practical considerations. The work-piece 10 is placed under the tool, on a plate 8, in a tray 9, with in abrasive slurry. The body of the acoustic head is adjusted to the base's guides 11 and is subjected to a static force P which drives the tool in the direction necessary to machine the work-piece.

The acoustic head is shown in Fig. (1.3) contain the electro mechanical converter which drives the tool via a special holder (waveguide). The feed mechanism applies the necessary force (5-8kgs) between tool and work piece. The abrasive feed system continuously brings in fresh abrasive to the cutting area, removes products and cools the components.

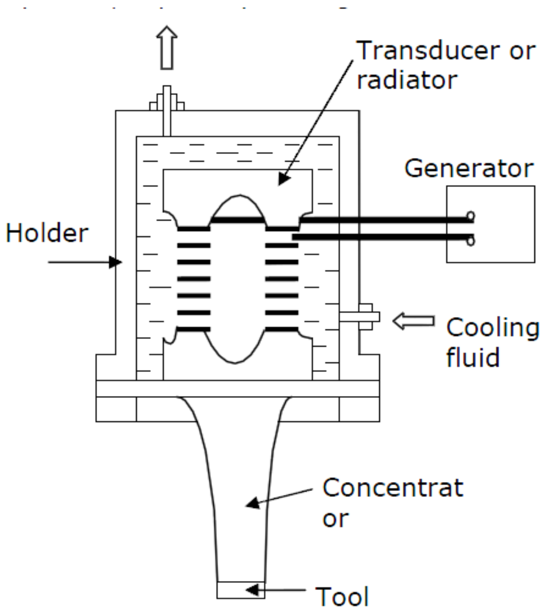

Figure (1.3) Schematic diagram of acoustic head [Modern Machining Processes By P. C. Pandey, H. S. Shan, Tata McGraw-Hill Education, vol 2, page no 99]

The power supplies the ultrasonic current to the acoustic head, various vacuum tube system are in common use and some high power magnetostriction heads have recently been used with high frequency alternators, which appear very promising. Ultrasonic cutting is a technique as yet they are not very reliable and are costly, and are of very low efficiency. Ultrasonic cutting techniques are only beginning to be exploited. No really reliable methods are available for calculating the dimensions of component, especially cutting tools.

1.5 NEED FOR ULTRASONIC MACHINING

The process is regarded as competitive only when an operation cannot be practically and economically performed on conventional machining equipment. The ultimate value of USM lies in the ability to do work that cannot be practically accomplished in any other way because USM is non-chemical and non-thermal. Materials are not altered either chemically or metallurgically during ultrasonic machining. USM is used to machine very hard and difficult to machine by conventional methods. Glass is a material difficult to machine by any means but good result have been obtained as a result of ultrasonic machining.

1.6 APPLICATIONS OF ULTRASONIC MACHINING:

1. Ultrasonic machining
2. Ultrasonic casting, welding, brazing and soldering of metals.
3. Ultrasonic forming of plastics.
4. Measurement of velocity of moving fluids.
5. Measurement of density, viscosity and elastic constant.
6. Measurement of hardness and grain size determination of metals.
7. Non-destructive residual stress determination.
8. Flaw detection, leak detection etc.

The use of ultrasonic in the medical field for the diagnosis and treatment of certain diseases has also been reported.

CHAPTER 2

PRINCIPAL OF ULTRASONIC MACHINING

2.1 PRINCIPAL OF USM PROCESS

In ultrasonic machining, material is removed due to action of abrasive grain which are hammered into the work surface by a tool oscillating at high frequency of 16 KHz to 30KHz and an amplitude in the order of 0.01 mm to 0.06 mm, have been found to be appropriate. The tool is pressed against the work surface under a load of few kilograms and fed downwards continuously as the cavity is cut in the work. The tool is shaped as the approximate mirror image of the configuration of the cavity desired in the work. The tool cross-section is of a shape as the approximate mirror image of the configuration of the cavity desired in the work. The tool cross-section is of a shape similar to that of the desired hole-only it is a little smaller in size in order to compensate for the over cut during the process. The process can cut virtually any material but is most effective on material with hardness greater than HRC= 0.45.

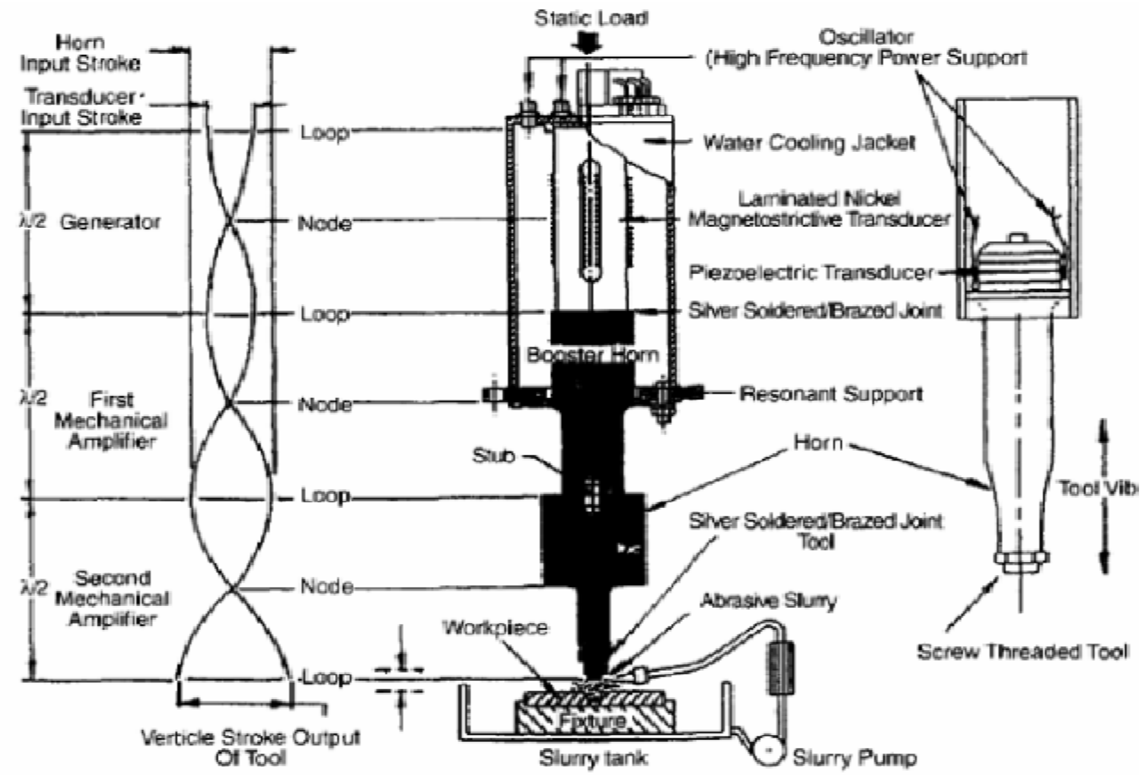

Figure (2.1) Basic features of the ultrasonic machining process [Advanced Machining Processes: Non-traditional and Hybrid Machining Processes, McGraw-Hill Prof Med/Tech, 01-Mar-2005 Vol 1 Page No161]

A simple schematic diagram of this process is shown in Fig.(2.1). The tool is made of soft and tough materials (usually brass, carbide, mild or tool steel). The abrasive grains are carried to the gap (generally in order of 0.02 to 0.10 mm) between the tool and the work piece with the help of a carrier fluid, generally water. The circulation of slurry (mixture of abrasive grains and the carrier fluid) also takes away the worn-out grains and the machining debris, and replaces them by new grains, thus maintaining a good cutting rate. During machining, along with the work piece, the tool also gets reduced in size due to the cutting action of the abrasive grits. Thus the drilled hole by ultrasonic machining is tapered, i.e. larger at the top. By compensating the tool wear properly, close tolerances can be obtained.

The USM equipment consist of an oscillator (high frequency current generator) that converts the 50Hz (c/s) power supply into high frequency (15 KHz to 30 KHz) power which in turn is converted into mechanical oscillations with the help of a magnetostrictive or piezo-electric transducer of the two type, the piezo-electric transducer are most efficient, i.e. they involve less loss of power and hence do not require cooling. The magnetiostrictive transducers generally found in old machines are less efficient due to high eddy current losses and hence may require cooling.

The power rating of modern machines varies from 0.04 to 4 KW. Some of the designs have rating even up to 10 KW. Power supply is: potential volts = 220, current = 12A.

CHAPTER 3

ELEMENTS OF ULTRASONIC MACHINING

The machine for USM ranges from small, table top sized units to large- capacity machine tools as illustrated in Fig.2.1 respectively. In addition to part size capacity of a USM machine, suitability for a particular application is also determined by the power rating. The power of USM machine is rated in watts and can range from 40W to 2400W. The material removal rate is directly related to the power capability of the USM machine. The entire USM machine share common subsystem regardless of the physical size or power. The ultrasonic machining process consists of the following basic element

1. The high frequency oscillating current generator or oscillator.
2. The transducer
3. The velocity transformer
4. The tool holder
5. The tool
6. The abrasive slurry
7. The work-piece

3.1 THE HIGH FREQUENCY OSCILLATING CURRENT GENERATOR OR OSCILLATOR

The power supply for USM is more accurately characterized as a high power sine wave generator that offers the user control over both the frequency and power of the generated signal. It converts low frequency 60 Hz electrical power to high frequency approx. 20 KHz electrical power. This electrical signal is then supplied to the transducer for conversion into mechanical motion.

The main requirements of a generator are:-

(a) Reliability and durability

(b) Efficiency

(c) Simplicity in design and low cost

(d) Compactness and easy to operate

(e) Stable frequency with possibility of being regulated over a specified range.

(f) Controlled power output over a wide range

3.2 THE TRANSDUCER

The transducer is a device that converts energy from one form to another. In the case of transducer for USM, electrical energy is converted to mechanical motion. The two types of transducers used for ultrasonic machining are based on two different principles of operations:

3.2.1 Piezoelectric Transducer

3.2.2 Magnetostrictive Transducer

3.2.1 PIEZOELECTRIC TRANSDUCER

These are used for USM to generate mechanical motion through the piezoelectric effect by which certain materials, such as quartz or lead Zirconate Titanate will generate a small electric current when compressed. When an electric current applied to one of these materials then these materials increases minutely in size. When the current is removed, the material intently returns to its original shape. Piezoelectric transducer, by nature, exhibit an extremely high electro-mechanical conversion efficiency (up to 96%), which eliminates the need for water cooling of transducer. These transducers are available with power capabilities upto 900W.

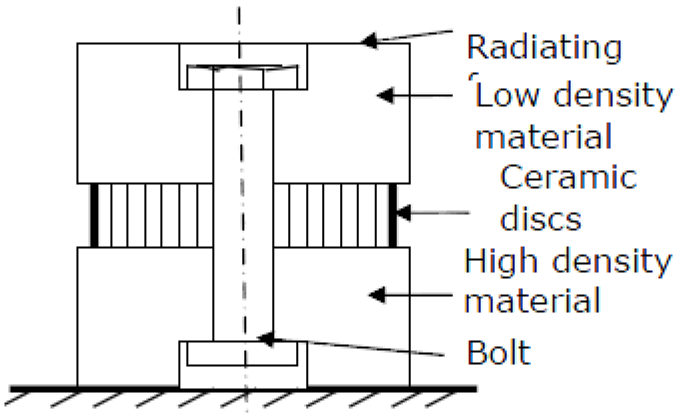

Figure (3.1) Piezoelectric ultrasonic transducer [Nontraditional machining process" E.J. Weller SME, Dearborn, Michigan Second Edition, 156 pages, hardcover, 1984]

3.2.2MAGNETOSTRICTIVE TRANSDUCER

These are usually constructed from a laminated stock of nickel or nickel alloy sheets which, when influenced by a strong magnetic field, will change length. Magnetostrictive transducers are rugged but have electro-mechanical conversion efficiencies ranging from 20 to 30%. The lower efficiency results in the need to water cool magnetostrictive devices to remove the waste heat. Magnetostrictive transducers are available with power capabilities up to 2400W. The magnitude of the length change that can be achieved by both piezoelectric and magnetostrictive transducer is limited by the strength of transducer material. In both types of transducer the limit is approximately 0.025mm (0.01 in).

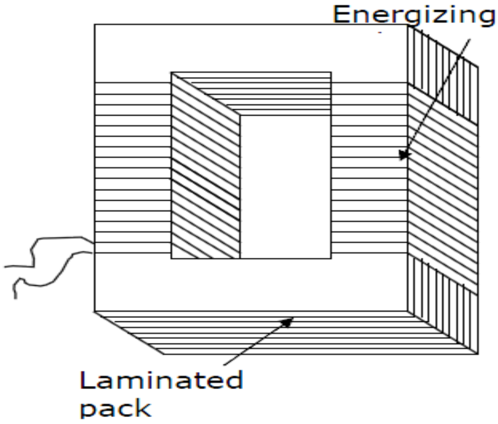

Figure (3.2) Magnetostrictive ultrasonic transducer [Nontraditional machining process" E.J. Weller SME, Dearborn, Michigan Second Edition, 156 pages, hardcover, 1984]

3.3 THE VELOCITY TRANSFORMER (CONCENTRATOR OR TRUNK)

The velocity transformer has got several names like concentrator, trunks. Mechanical focusing device, shank, horn, amplifier, tool cone, transformer stub or convergent wave-guide, etc. it amplifies and focuses the mechanical energy produced by the transducer and imparts this to work-piece in such away that energy utilization is optimum. It is simply a velocity transformer with the exception that it is made slightly shorter than the half wavelength. The amplitude of the vibratory motion of the transducer is small and is usually inadequate for material removal purpose, and hence the tool is connected to the transducer by means of a concentrator which is simply a convergent waveguide to produce the desired amplitude at the tool end. Thus the trunk amplifies and focuses the vibrations of the transducer to intensity necessary to drive the tool to do its work. The increase in amplitude of the vibrations at the tool end is obtained by reducing the cross-section of the trunk at the tool end. The trunks are specially shaped to provide a reduction in cross-section at the tool end because the trunk should be of such sizes and shape that it is mechanically resonant or tuned to the frequency of the transducer vibrations and under working conditions giving maximum amplitude at the tool end with minimum energy losses. The trunk provides increased amplitude in the order of 30 to 120 microns at the tool face.

Trunks may be of different shapes or configurations. Some typical shapes are as follows

1. Exponential (circular)

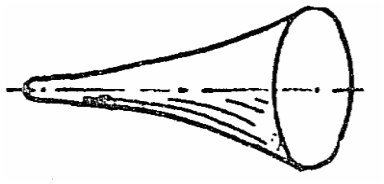

2. Exponential (wedge)

3. Exponential (annular)

Figure (3.3) Exponential Horns

4. Straight conical

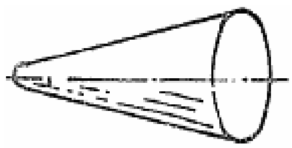

5. Stepped

Figure (3.4) Circular Horns

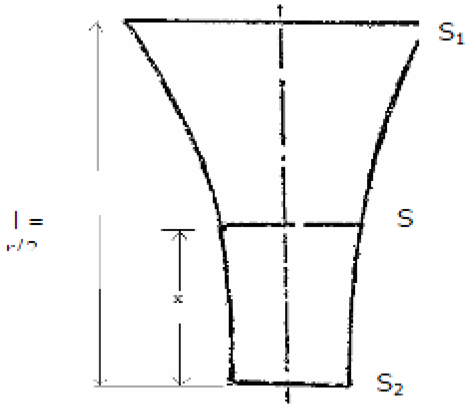

Figure (3.5) Exponential shank

[Nontraditional machining process" E.J. Weller SME, Dearborn, Michigan Second Edition, 161 pages, hardcover, 1984]

μ=Flaring index

λ=Wavelength of sound in the shank material

S_1 = Area of big end

S = Area of any cross-section

S_2 = Area of smaller end (Tool End)

$S_1/S_2=e^{2\mu l}$ (magnification of the shank)

$S/S_2=e^{2\mu x}$

3.4 THE TOOL HOLDER

The tool holder transfers the vibrations to the tool end and therefore, it must have adequate fatigue strength. Tool holder is removable part which is fastened to the concentrator and is made of monel metal or stainless steel. Generally, the shape of the tool holder is cylindrical or conical or a modified cone with the centre of mass of the tool on the centre line of the tool holder. It should be free from nicks, scratches and tool marks to reduce fatigue failures caused by the repeated reversal of stresses. In some ultrasonic machines, the trunk (horn) acts itself as a concentrator as well as the tool holder.

3.5 THE TOOL

For minimum tool wear, tools should be constructed from relatively ductile materials such as stainless steel, brass and mild steel. The harder the tool material the faster its wear rate will be. Depending on the abrasive used, workpiece / tool wear ratios can range from 1:1 to 100:1. Whenever possible, USM tools to be used for hole drilling are constructed from easily obtained materials such as music wire, stainless steel tubing or hypodermic needles. Solid tools used to produce cavities can be fabricated by machining, casting or coining; however finishing or polishing operations are sometimes necessary because the tool holders should be free from scratches, nicks and heavy machining marks, because these produce risers and lead to early fatigue failure.

Because of the overcut that occurs with this process, allowances must be made to use tool are slightly smaller than the desired hole or cavity e.g. to allow for the diameter of tubing to drill holes should be equal to the desired hole diameter minus twice the abrasive particle size. The most desirable method of attaching the tool to the holder is silver brazing. This eliminates the fatigue problems associated with mechanical screw attachment method.

3.6 THE ABRASIVE SLURRY

Several abrasives are available in various sizes for ultrasonic machining (grit). The criteria for selection of an abrasive for a particular application include hardness, usable life, cost and particle size.

In order of hardness, boron carbide, silicon carbide and aluminium oxide are the most commonly used abrasives. The abrasive used for an application should be harder than the material being machined; otherwise the usable life time of the abrasive will be substantially shortened. Boron carbide is selected when machining the hardest work piece materials or when the highest material removal rates are desired. Although the cost is five to ten times greater than the next hardest abrasive, silicon carbide, the usable life of boron carbide is 200 machine operating hours before cutting effectiveness is lost and disposal is necessary. This compares with a usable life time of approximately 60 hours for silicon carbide. Combination of high removal rates and extended life time justify the higher cost of boron carbide.

The size of abrasive particles influences the removal rate and surface finish obtained. Abrasive for USM are generally available in grit sizes ranging from 240 to 800 while the coarser grit exhibit the highest removal rates, they also result in the roughest surface finish and are therefore, used only for roughing operation, conversely, 800 grit abrasives will result in fine surface finishes but at a drastic reduction in metal removal rate. The most popular general purpose abrasive used, based on the above considerations, 320 grit Boron carbide. The abrasive material is mixed with water to from the slurry.

The abrasive material is mixed with water to form the slurry. The most common abrasive concentration is 50% by weight; however, this can vary from 30 to 60 percent. The thinner mixtures are used to promote efficient flow when drilling deep holes or when forming complex cavities. Once the abrasive has been selected and mixed with water, it is stored in a reservoir at the USM machine and pumped to the tool work piece interface by re-circulating pumps at rates up to 26.5 lit/min. higher power ultrasonic machine require the addition of a light-duty cooling system to remove waste heat from the abrasive slurry.

3.7 THE WORK PIECE

There is no limitation to the range of material that can be machined by USM process, expect that they should not dissolve in the slurry media or react with it. While USM can be applied to ductile materials such as soft steel, copper, and brass but it is best suited to machining operation on hard, brittle materials that are not practical to process by other method. In general, USM is not recommended on the work materials which are softer than

Rockwell Hardness Number HRC 45. Ultrasonic machining can be used for metals and non-metals, electrical conductors or non-conductor. The ultrasonic drilling technique is especially suited for hard materials like tungsten carbide, titanium carbide, ceramic and diamond. Materials which exhibit high hardness and which have impact brittleness can be successfully machined by this technique. Such materials are germanium, ferrites, glass and quartz. These materials often cannot withstand the forces needed for ordinary mechanical working. Materials that can be machined by ultrasonic drilling efficiently are shown the table (3.1).

Table (3.1) Material that can be machined by USM process [Advanced Machining Processes: Non-traditional and Hybrid Machining Processes, McGraw-Hill Prof Med/Tech, 01-Mar-2005 Vol 1 Page No156]

Agate	Alabaster	Barium Carbide(Sintered)
Ceramics	Corundum	Diamond
Earthenware	Felspar	Ferrites
Fluorites	Garmanium	Glass
Glass-Micanite	Granite	Graphite
Gypsum	Hard Alloy (Tungsten and Titanium Carbide)	Marble
Jadeite	Jasper	Mother-of Pearl
Nephrite	Onyx	Porcelain
Quartz (Crystalline And Fused)	Rock Crystal	Ruby
Sapphire	Silicon	Stealite
Thermo Corundum	Tourmaline	Zirconium Boride

CHAPTER 4

FINITE ELEMENT ANALYSIS

4.1 INTRODUCTION

The finite element analysis is a numerical technique. In this method all the complexities of the problems, like varying shape, boundary conditions and loads are maintained as they are but the solutions obtained are approximate. Because of its diversity and flexibility as an analysis tool, it received much attention in engineering. The fast improvements in computer hardware technology and slashing of cost of computers have boosted this method, since the computer is the basic need for the application of this method. A number of popular brand of finite element analysis packages are now available commercially. Some of the popular packages are ABAQUS, STAAD-PRO, GT-STRUDEL, NASTRAN, NISA and ANSYS. Using these packages one can analyse several complex structures. [44]

The finite element analysis originated as a method of stress analysis in the design of aircrafts. It started as an extension of matrix method of structural analysis. Today this method is used not only for the analysis in solid mechanics, but even in the analysis of fluid flow, heat transfer, electric and magnetic fields and many others. Civil engineers use this method extensively for the analysis of beams, space frames, plates, shells, folded plates, foundations, rock mechanics problems and seepage analysis of fluid through porous media. Both static and dynamic problems can be handled by finite element analysis. This method is used extensively for the analysis and design of ships, aircrafts, space crafts, electric motors and heat engines.

4.2 GENERAL DESCRIPTION OF THE METHOD

In engineering problems there are some basic unknowns. If they are found, the behaviour of the entire structure can be predicted. The basic unknowns or the Field variables which are encountered in the engineering problems are displacements in solid mechanics, velocities in fluid mechanics, electric and magnetic potentials in electrical engineering and temperature in heat flow problems.

In a continuum, these unknowns are infinite. The finite element procedure reduces such unknowns to a finite number by dividing the solution region into small parts called elements and by expressing the unknown field variables in terms of assumed approximating functions (Interpolating functions/Shape functions) within each element. The approximating functions are defined in terms of field variables of specified points called nodes or nodal points. Thus in the finite element analysis the unknowns are the field variables of the nodal points. Once these are found the field variables at any point can be found by using interpolation functions.

After selecting elements and nodal unknowns, next step in finite element analysis is to assemble element properties for each element. For example, in solid mechanics, we have to find the force-displacement i.e. stiffness characteristics of each individual element. Mathematically this relationship is of the form

$$[k]_e \{\delta\}_e = \{F\}_e \qquad \text{(Equation....4.1)}$$

Where $[k]_e$ is element stiffness matrix, $\{\delta\}$ e is nodal displacement vector of the element and $\{F\}_e$ is nodal force vector. The elements of stiffness matrix k_{ij} represent the force in coordinate direction *'i'* due to a unit displacement in coordinate direction *'j'*. Four methods are available for formulating these element properties viz. direct approach, variational approach, weighted residual approach and energy balance approach. Any one of these methods can be used for assembling element properties.

In solid mechanics variational approach is commonly employed to assemble stiffness matrix and nodal force vector (consistent loads). Element properties are used to assemble global properties/structure properties to get system equations $[k]\ \{\delta\} = \{F\}$. Then the boundary conditions are imposed. The solution of these simultaneous equations gives the nodal unknowns. Using these nodal values additional calculations are made to get the required values e.g. stresses, strains, moments, etc. in solid mechanics problems. Thus the various steps involved in the finite element analysis are:

I. Select suitable field variables and the elements.
II. Discretise the continua.
III. Select interpolation functions.
IV. Find the element properties.
V. Assemble element properties to get global properties.
VI. Impose the boundary conditions.
VII. Solve the system equations to get the nodal unknowns.
VIII. Make the additional calculations to get the required values.

4.3 A BRIEF EXPLANATION OF FEM FOR A STRESS ANALYSIS PROBLEM

The steps involved in finite element analysis are clarified by taking the stress analysis of a tension strip with fillets (refer Fig.4.1). In this problem stress concentration is to be studies in the fillet zone [44]. Since the problem is having symmetry about both x and y axes, only one quarter of the tension strip may be considered as shown in Fig.4.2. About the symmetric axes, transverse displacements of all nodes are to be made zero. The various steps involved in the finite element analysis of this problem are discussed below:

Step 1: Four noded iso-parametric element (refer Fig 4.3) is selected for the analysis However note that 8 noded iso-parametric element is ideal for this analysis). The four noded iso-parametric elements can take quadrilateral shape also as required for elements 12, 15, 18, etc. As there is no bending of strip, only displacement continuity is to be ensured but not the slope continuity. Hence displacements of nodes in x and y directions are taken as basic unknowns in the problem.

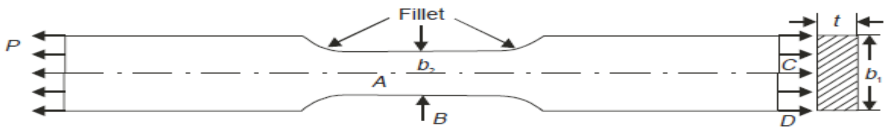

Fig 4.1 Typical Tension Flat [Finite Element Analysis by S.S Bhavikatti, New Age International (P) Limited, Publishers, Vol 1, Page No 156]

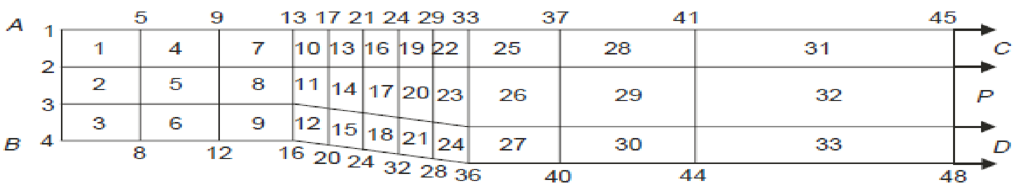

Fig 4.2 Discretisation of Quarter of Tension Flat [Finite Element Analysis by S.S Bhavikatti, New Age International (P) Limited, Publishers, Vol 1, Page No 156]

Step 2: The portion to be analysed is to be discretised. Fig. 4.2 shows discretised portion. For this 33 elements have been used. There are 48 nodes. At each node unknowns are x and y components of displacements. Hence in this problem total unknowns (displacements) to be determined are 48 x 2 = 96.

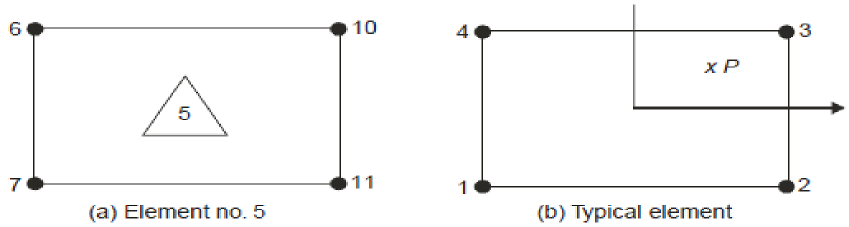

Fig 4.3 Elements of Body [Finite Element Analysis by S.S Bhavikatti, New Age International (P) Limited, Publishers, Vol 1, Page No 156]

Step 3: The displacement of any point inside the element is approximated by suitable functions in terms of the nodal displacements of the element. For the typical element (Fig. 4.3 b), displacements at P are

$$u = \sum N_i u_i = N_1 u_1 + N_2 u_2 + N_3 u_3 + N_4 u_4$$

$$and\ v = \sum N_i v_i = N_1 v_1 + N_2 v_2 + N_3 v_3 + N_4 v_4 \qquad \text{(Equation.....4.2)}$$

The approximating functions N_i are called shape functions or interpolation functions. Usually they are derived using polynomials and u_i in number of nodes. The methods of deriving these functions for various elements are discussed in this text in latter chapters.

Step 4: Now the stiffness characters and consistent loads are to be found for each element. There are four nodes and at each node degree of freedom is 2. Hence degree of freedom in each element is 4 × 2 = 8. The relationship between the nodal displacements and nodal forces is called element stiffness characteristics. It is of the form

$$[k]_e \{\delta\}_e = \{F\}_e ,$$

as explained earlier. For the element under consideration, ke is 8 × 8 matrix and δ_e and F_e are vectors of 8 values. In solid mechanics element stiffness matrix is assembled using variational approach i.e. by minimizing potential energy. If the load is acting in the body of element or on the surface of element, its equivalent at nodal points are to be found using variational approach, so that right hand side of the above expression is assembled. This process is called finding consistent loads.

Step 5: The structure is having 48 × 2 = 96 displacement and load vector components to be determined. Hence global stiffness equation is of the form

$$\underset{96 \times 96}{[k]} \quad \underset{96 \times 1}{\{\delta\}} \quad = \quad \underset{96 \times 1}{\{F\}}$$

Each element stiffness matrix is to be placed in the global stiffness matrix appropriately. This process is called assembling global stiffness matrix. In this problem force vector F is zero at all nodes except at nodes 45, 46, 47 and 48 in *x* direction.

Step 6: In this problem, due to symmetry transverse displacements along AB and BC are zero. The system equation [k] { δ } = {F} is modified to see that the solution for {F} comes out with the above values. This modification of system equation is called imposing the boundary conditions.

Step 7: The above 96 simultaneous equations are solved using the standard numerical procedures like Gauss elimination or Choleski's decomposition techniques to get the 96 nodal displacements.

Step 8: Now the interest of the analyst is to study the stresses at various points. In solid mechanics the relationship between the displacements and stresses are well established. The stresses at various points of interest may be found by using shape functions and the nodal displacements and then stresses calculated. The stress concentrations may be studies by comparing the values obtained at various points in the fillet zone with the values at uniform zone, far away from the fillet (which is equal to P/b_2t).[44]

4.4 FINITE ELEMENT METHOD Vs CLASSICAL METHOD

1. In classical methods exact equations are formed and exact solutions are obtained where as in finite element analysis exact equations are formed but approximate solutions are obtained.
2. Solutions have been obtained for few standard cases by classical methods, where as solutions can be obtained for all problems by finite element analysis.
3. Whenever the following complexities are faced, classical method makes the drastic assumptions' and looks for the solutions:
(a) Shape
(b) Boundary conditions
(c) Loading
Fig. 4.4 shows such cases in the analysis of slabs (plates). To get the solution in the above cases, rectangular shapes, same boundary condition along a side and regular equivalent loads are to be assumed. In FEM no such assumptions are made. The problem is treated as it is.

4. When material property is not isotropic, solutions for the problems become very difficult in classical method. Only few simple cases have been tried successfully by researchers. FEM can handle structures with anisotropic properties also without any difficulty.

5. If structure consists of more than one material, it is difficult to use classical method, but finite element can be used without any difficulty.

6. Problems with material and geometric non-linearities cannot be handled by classical methods.

There is no difficulty in FEM.[44]

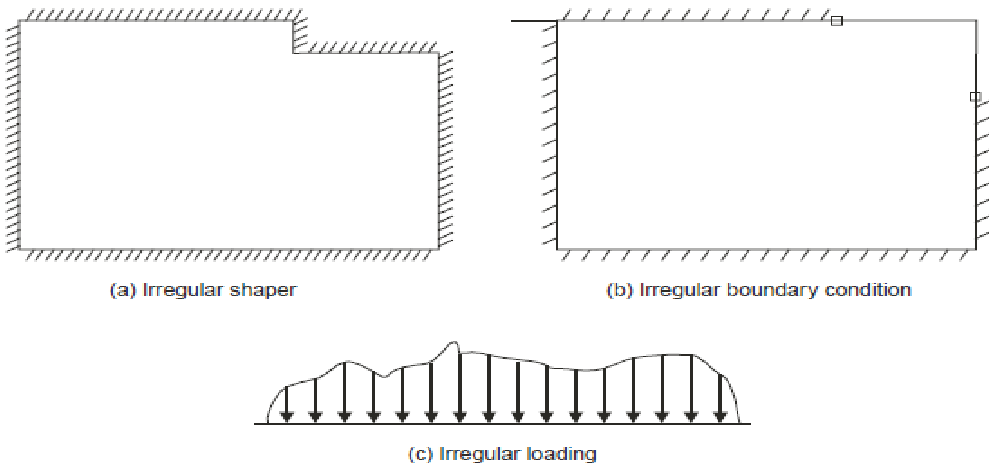

Fig 4.4 such cases in the analysis of slabs (plates) [Finite Element Analysis by S.S Bhavikatti, New Age International (P) Limited, Publishers, Vol 1, Page No 158]

Hence FEM is superior to the classical methods only for the problems involving a number of complexities which cannot be handled by classical methods without making drastic assumptions. For all regular problems, the solutions by classical methods are the best solutions. Infact, to check the validity of the FEM programs developed, the FEM solutions are compared with the solutions by classical methods for standard problems.

4.5 NEED FOR STUDYING FEM

Now, a number of users friendly packages are available in the market. Hence one may ask the question ‘What is the need to study FEA?’

The above argument is not sound.[44] The finite element knowledge makes a good engineer better while just user without the knowledge of FEA may produce more dangerous results. To use the FEA packages properly, the user must know the following points clearly:

1. Which elements are to be used for solving the problem in hand?
2. How to introduce boundary conditions properly?
3. How the element properties are developed and what are their limitations?
4. How the displays are developed in pre and post processor to understand their limitations?
5. To understand the difficulties involved in the development of FEA programs and hence the need for checking the commercially available packages with the results of standard cases.

Unless user has the background of FEA, he may produce worst results and may go with overconfidence. Hence it is necessary that the users of FEA package should have sound knowledge of FEA.

CHAPTER 5

LITERATURE SURVEY

1. Edge-chipping reduction in rotary ultrasonic machining of ceramics: Finite element analysis and experimental verification

Rotary ultrasonic machining (RUM) is one of the machining processes for advanced ceramics. Edge chipping (or chamfer), commonly observed in RUM of ceramic materials, not only compromises geometric accuracy but also possibly causes an increase in machining cost. In this paper, a three-dimensional finite element analysis (FEA) model is developed to study the effects of three parameters (cutting depth, support length, and pretightening load) on the maximum normal stress and von Mises stress in the region where the edge chipping initiates. Two failure criteria (the maximum normal stress criterion and von Mises stress criterion) were used to predict the relation between the edge chipping thickness and the support length. Furthermore, a solution to reduce the edge chipping is proposed based upon the FEA simulations and verified by experiments. As the cutting depth increases, the maximum values of the maximum normal stress and the von Mises stress increase. The effects of pretightening load on the maximum values of the maximum normal stress and the von Mises stress are not significant. There exists a critical support length.[1] As the support length increases before reaching the critical length, the maximum values of the maximum normal stress and the von Mises stress decrease slightly. When the support length exceeds the critical length, there are sharp decreases in the maximum values of the maximum normal stress and the von Mises stress. The edge-chipping thickness can be reduced by increasing the support length.

2. FEM analysis of ultrasonic-vibration-assisted turning and the vibratory tool

Ultrasonic assisted turning (UAT) is an advanced method developed for machining tough and brittle materials such as supper-alloys, ceramics and glass. Using MSC-Marc and Ansys, the authors studied machining of IN738 with a tool vibrating at ultrasonic frequency. The machining forces and stresses acting on the work-piece during the process, and the effect of process parameters such as cutting speed, tool geometry and vibration amplitude were investigated. The authors also worked out the material and the optimum configuration of the vibratory tool being able to operate at an ultrasonic frequency [2] within acceptable range. The results indicate that the forces and the stresses acting on the work-piece follow periodic changes during UAT and are augmented with an increase in the ultrasonic vibration amplitude or the cutting speed. The clearance angle has no significant effect on the magnitude of the machining force, but higher forces are produced with smaller tool rake angles. Conical–cylindrical aluminium horns with concentrically attached tool insert deliver more satisfactory performance. In ultrasonic cutting, machining force and work-piece stress vary periodically and, in most part of the process are significantly less than those occurring in conventional turning. In ultrasonic cutting, machining force depends heavily on the cutting speed and increases with an increase in the latter. The effect of tool clearance and rake angles in UAT is similar to that of conventional turning, i.e., clearance angle has no significant influence on the machining force while rake angle has an inverse effect.

3. Finite element modelling of ultrasonic surface rolling process

Ultrasonic surface rolling (USRP) is a newly developed process in which ultrasonic vibration and static force are applied on work-piece surface through the USRP operator to generate a nanostructured surface layer with mechanical behaviours highly improved. Compared with other surface severe plastic deformation (S2PD) methods, it can realize mechanized machining and be directly used for preparing final product. Notwithstanding the excellent performance of USRP, elaborate relation between process parameters and surface layer characteristics is still inadequacy due to inconvenient and costly experimental evaluation. Therefore, in this paper a three-dimensional finite element model (FEM) has been developed to predict the treatment conditions that lead to surface nanocrystallization. Simulated results of surface deformation, stress and strain are investigated to assess the formation of nanostructured layer. [3] The numerical results from the FEM corresponds well with the values measured experimentally, indicating that this dynamic explicit FEM is a useful tool to predict the processing effects and to relate the treating parameters with the surface layer in terms of the size of nanostructured layer, residual stress and work hardening.

A three-dimensional dynamic FE model was set up to predict the material response affected by USRP. Before simulation, a series of tests were carried out to obtain model parameters. For determination of parameters for combined isotropic kinematic hardening model, static tension tests and cyclic push–pull tests were performed, while for description of loading and boundary conditions, a specific piezoelectric test system was established, aiming at measuring the dynamic impact force. The geometry of this FE model was discreetly decided, followed by an elaborative convergence study of the parameters defining the mesh. The final created model was examined and the comparison with the experimental results showed a favourable consistency. Experimental characterization of the surface layer after

USRP was implemented by means of microscopic observation, residual stress analysis, etc. The overall results indicated that the proposed numerical model can be consulted as a useful approach to predict the formation of nanostructured layer and design process parameters. The induced residual stresses calculated by the FE model were in good agreement with XRD measurements and both results for different repeated processing numbers demonstrated that residual stress profiles form at first few repeated processing times. The accumulated equivalent plastic strain (PEEQ) to estimate the formation of nanostructured layer of material was drawn. It is found that the criterion is able to evaluate the combined ultrasonic impact and rolling process parameters for obtaining nanostructured surface layer. Thus, PEEQ can be used as a favourable assessment method for generation of nanograins.

4. A cutting force model for rotary ultrasonic machining of brittle materials

Knowing cutting force in rotary ultrasonic machining (RUM) can help optimizing input variables .RUM of brittle materials has been investigated both experimentally and theoretically. However, there are no Reports on cutting force models for RUM of brittle materials. Assuming that brittle fracture is the primary mechanism of material removal in RUM of brittle materials, the cutting force model is developed step by step. On the basis of this mechanistic model, relationships between cutting force and input variables (such as spindle speed, feed rate, ultrasonic vibration amplitude, abrasive size, and abrasive concentration) are predicted. Experiments are conducted for model verification and experimental results agree well with model predictions.[4] A physics-based cutting force model for rotary ultrasonic machining (RUM) of brittle materials has been developed. The model is used top redact the influences of input variables on cutting force. These predicted in fluencies are compared with those determined experimentally. The trends of predicted in fluencies of input variables on cutting force agree well with the trends determined experimentally. These predicted trends are cutting force will increase as abrasive concentration, semi-angle of abrasive particle, and feed rate increase and it will decrease as abrasive size, vibration amplitude, and spindle speed increase. This model is the first cutting force model for RUM of brittle materials in the literature. It can serve as a useful spring board for development of more sophisticated cutting force models (such as those that consider the dynamic force in the process) and models.

5. Analysis of ultrasonic-assisted drilling of Ti_6Al_4V

In this study ultrasonic vibration was applied on the drilling of Ti_6Al_4V work-piece samples. Several parameters of ultrasonic-assisted drilling were monitored, including feed force, chip formation by means of high-speed imaging, and temperature measurement on the drill tip by mean so fin fared radiation thermometry. Ultrasonic assistance offered lower feed force and higher process temperatures as compared to conventional drilling. It has also shown higher force reductions and higher temperature increments when vibration amplitude was increased. In situ chip formation was analyzed and no difference was observed with regard to chip geometry. Similarly, when new tools [5] were employed in drilling, burr formation was null. When ultrasonic-assisted drilling was applied, the feed force decreased by 10–20% on average, and the decrease in force was more notorious as the vibration amplitude was higher. Tool tip temperature was higher when ultrasonic-assisted drilling was applied. In this case, the higher the vibration amplitude, the higher the temperature variations at the tool tip. There exists a correlation between temperature variation and feed force variation, but it cannot be explained due to the thermal softening effect of Ti_6Al_4V only. At this point, it is necessary to carry out further research in quantifying the exits the at generation mechanism and its effect on tool wear and work piece tensional state (residual stress, phase transformation, etc.).

6. Ultrasonically assisted turning of aviation materials: simulations and experimental study

Ultrasonically assisted turning of modern aviation materials is conducted with ultrasonic vibration (frequency f 20 kHz, amplitude a 15 lm) superimposed on the cutting tool movement. An auto resonant control system is used to maintain the stable nonlinear resonant mode of vibration throughout the cutting process. Experimental comparison of roughness and roundness for work-pieces machined conventionally and with the superimposed ultrasonic vibration, results of high-speed filming of the turning process and nanoindentation analyses of the microstructure of the machined material are presented.[6] The suggested finite-element model provides numerical comparison between conventional and ultrasonic turning of Inconel 718 in terms of stress/strain state, cutting forces and contact conditions at the work-piece/tool interface. Experimental and numerical studies of conventional turning and ultrasonically assisted turning demonstrate fundamental advantages of the latter technology for machining intractable materials.

Comparative analyses of the quality of the machined surface demonstrated up to 50% improvement in average surface roughness and peak-to-valley roundness for the work-pieces machined with superimposed ultrasonic vibration. Nanoindentation tests of the surface layers of the work-pieces machined with UAT and CT showed a considerably lower influence on the work-piece material microstructure for the case with superimposed ultrasonic vibration. High-speed observations of the cutting region and subsequent SEM analysis of the microstructure of chips produced when CT and UAT demonstrate continuous chip formation and deformation processes concentrated near the work-piece surface for UAT and essentially segmented chip formation affecting deeper layers of the work-piece surface for CT. Numerical simulations of the single cycle of ultrasonic vibration revealed similar maximum stresses arising in UAT and CT processes. However, due to the stresses being significantly lower throughout the considerable part of the cycle of ultrasonic vibration, average cutting forces are up to several times smaller for UAT. Experimental comparison of the temperatures in the cutting tip and chip showed 50% higher temperatures for UAT. This was explained by additional energy coming into the cutting system with ultrasonic vibration and different chip formation processes when ultrasonic vibration is applied.

7. Ultrasonic flow polishing

Dies and moulds used in the fabrication of metal, glass and plastic products require a high quality surface finish in terms of both appearance and integrity. Current manual polishing methods of surface finishing are time consuming and expensive. Consequently, a reduction in operator input and processing time has the potential to significantly reduce the cost of the finished mould. An ultrasonically energised polishing process, suitable for the polishing of complex dies and moulds has been successfully developed and patented.[7] The process is based upon the combination of the two 'non-traditional' techniques of abrasive flow machining and ultrasonic machining. It has proved to be capable of improving surface finishes by factors of up to l & l. This paper describes the development of the process and reports results achieved.

8. Design of rotary ultrasonic milling tool using FEM simulation

This study attempted to design a rotary ultrasonic milling tool using finite element method (FEM). The harmonic piezoelectric vibrations of the ultrasonic milling system are simulated by FEM to shed light on the frequency and amplitude of the vibration as well as stress distribution. Results of the study show that the use of FEM in dynamic simulation of ultrasonic milling is feasible. In addition, increase in tool length will result in increase in mass and resonance amplitude but decrease in resonance frequency. During milling, much longer tool may render the tool to withstand a much bigger bending stress, which would likely cause the tool to break or be damaged. However, increase in resonance amplitude can also be achieved by increase in voltage used.[8] Hence, our findings support that a spherical tool of 30 mm long is most suitable for the milling operation. Moreover, to achieve effective conversion of ultrasonic energy for lateral material removal, the milling plane should be enlarged to reduce the milling angle. A good understanding of the efficiency associated with ultrasonic transmission can help achieve fast and accurate design of milling tool.

9. A Comparative Study on Ultrasonic Machining of Hard and Brittle Materials

Precision abrasive processes are commonly employed to machine glasses, single crystals and ceramic materials for various industrial applications. Until now, precision machining of hard and brittle solids are poorly investigated in Brazil from the fundamental and applied point of views. Taking into account the major technological importance of this subject to the production of functional and structural components used in high performance systems, the present study investigated the ultrasonic abrasion of different work-piece materials - alumina, zirconia, quartz, glass, ferrite and LiF by using a stationary ultrasonic machine. Experiments were conducted using a rectangular shaped cutting toll and SiC particles with mean grain size of 15ìm. The machined surfaces were characterized by surface profile metric and scanning electron microscopy. In the case of alumina, zirconia and quartz, the rates of material removal decrease with the depth of machining. The rate of material removal remained constant for the others materials. The micrographs showed that brittle micro cracking was the primary mechanism involved with material removal.[9] The rates of material removal and the machined surface topographies were discussed as a function of intrinsic stiffness, hardness and fracture toughness of work-piece materials. Ultrasonic machining offers a solution to the expanding need for machining brittle materials such as single crystals, glasses and polycrystalline ceramics, and for increasing complex operations to provide intricate shapes and work-piece profiles. This machining process is non-thermal, non-chemical, creates no change in the microstructure, chemical or physical properties of the work-piece and offers virtually stress-free machined surfaces (Kramer 1995, Thoe et al. 1998). It is therefore used extensively in manufacturing hard and brittle materials that are difficult to cut by other conventional methods. The actual cutting is performed either by abrasive particles suspended in a fluid, or by a rotating diamond-plated tool.

These variants are known respectively as stationary ultrasonic machining and rotary ultrasonic machining (RUM). Stationary (or conventional) ultrasonic machining (USM) accomplishes the removal of material by the abrading action of a grit-loaded slurry, circulating between the work-piece and a tool that is vibrated at small amplitude. The form tool itself does not abrade the work-piece; the vibrating tool excites the abrasive grains in the flushing fluid, causing them to gently and uniformly wear away the material, leaving a precise reverse form of the tool shape. The uniformity of the sonotrode-tool vibration limits the process to forming small shapes typically under 100 mm in diameter (Thoe et al. 1998 and papers herein). The USM system includes the sonotrode-tool assembly, the generator, the grit system and the operator controls.. The sonotrode tool assembly consists of a transducer, a booster and a sonotrode. The electronic generator powers the transducer, creating impulses that occur at a range of 19.5 to 20.5 kHz, and automatically adjusts the output frequency to mach the resonant frequency of the tool, which varies according to the sonotrode shape and material (Thoe et al. 1998 and papers herein). The transducer converts the electrical pulses into vertical stroke. This vertical stroke is transferred to the booster, which may amplify or suppress the stroke amount. The modified stroke is then relayed to the sonotrode-tool assembly. The amplitude along the face of the tool typically falls in a 20 to 50 μm range. The vibration amplitude is usually equal to the diameter of the abrasive grit used. The grit system supplies a slurry of water and abrasive grit, usually silicon or boron carbide, to the cutting area. In addition to providing abrasive particles to the cut, the slurry also cools the sonotrode and removes particles and debris from the cutting area.

The overcut produced with USM is a function of the abrasive particle size, as are the surface finish and the material removal rates (Komaraiah et al. 1988, Thoe et al. 1998). The operator controls provide inputs for manual or automatic sequencing of operations. Controls include variable cutting force, ram position, speed control of the ram movement, cycle timing, retract distance and flush timing. From the tribological point of view, USM can be classified as a three-body abrasive wear. The material removal is assured by direct hammering and impact action of the abrasive particles against the surface of the work-piece (Shawn, 1956; Kainth et al., 1979). Soundararajan and Radhakrishnan (1986) showed that direct hammering of the abrasive particles on the workpiece by the tool, resulting in material removal and particle crushing, may contributes up to 80 % of the stock removal in brittle solids such as glass. Cavitations effects from the abrasive slurry and chemical action associated with the fluid employed have been reported as minor material removal mechanisms. Material removal rate, surface finish and machining accuracy are influenced by various operational parameters such as amplitude and frequency of ultrasonic oscillations, static load applied on the sonotrode, tool design, hardness and size of abrasive particles (Thoe et al, 1998 and papers herein). The effect of material properties on the rate of material removed was analysed by and Komaraiah and Reddy (1993).

Table 5.1 Structural and mechanical properties of work-piece materials.

Material	Chemical Composition	Crystalline Structure	Density (g/cm^3)	*E* (GPa)	*H* (GPa)	K_{Ic} ($MPam^{1/2}$)
Alumina	Al_2O_3	FCC/polycristalline	4.0	210 - 380	14 – 20	3 - 5
Ferrite	-	- / polycristalline	-	~180	6.8	1
LiF	LiF	FCC/single-crystal	2.43	54.6	0.92 ± 0.03	1.5
Quartz	SiO_2	Trigonal/single-crystal	2.65	78.3	15.0 ± 1.0	0.53 ± 0.01
Soda-lime glass	SiO_2+Na_2O+CaO	Amorphous	2.5	69	5.8 ± 0.5	0.48 ± 0.05
Zirconia	ZrO_2	Tetragonal/polycristalline	5.8	140 - 210	10 – 12	8 - 10

E – Young's modulus ; H – static hardness ; K_{Ic} – fracture toughness FCC- face centred cubic, - not determined

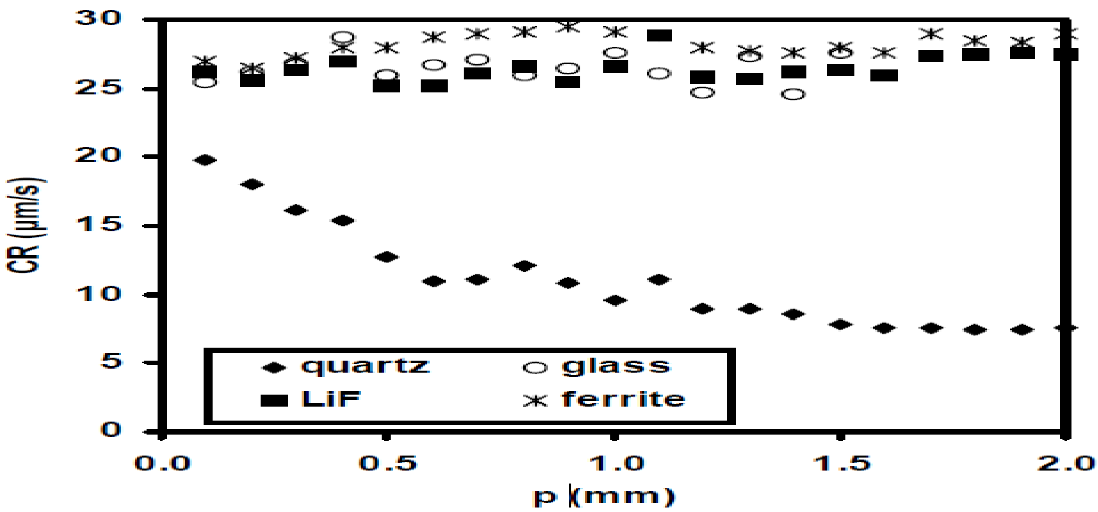

Figure 5.1. Variation of the cutting rate (CR) as a function of the cutting depth (p).

Table 5.2. Mean values for the cutting rate (*CR*) and surface roughness parameters.

Material	*CR* (µm/s)	R_a (µm)	R_z (µm)
Alumina	3.8 (0.4)	1.5 (0.2)	10.9 (1.0)
Zirconia	2.3 (0.4)	1.7 (0.4)	10.7 (1.9)
Quartz	8.4 (1.2)	1.5 (0.2)	9.6 (1.6)
Soda-lime glass	26.5 (1.1)	2.5 (0.4)	14.0 (1.8)
Ferrite	28.2 (0.8)	1.9 (0.2)	11.6 (0.6)
LiF	26.5 (0.9)	0.8 (0.2)	4.6 (1.2)

(-) standard deviation

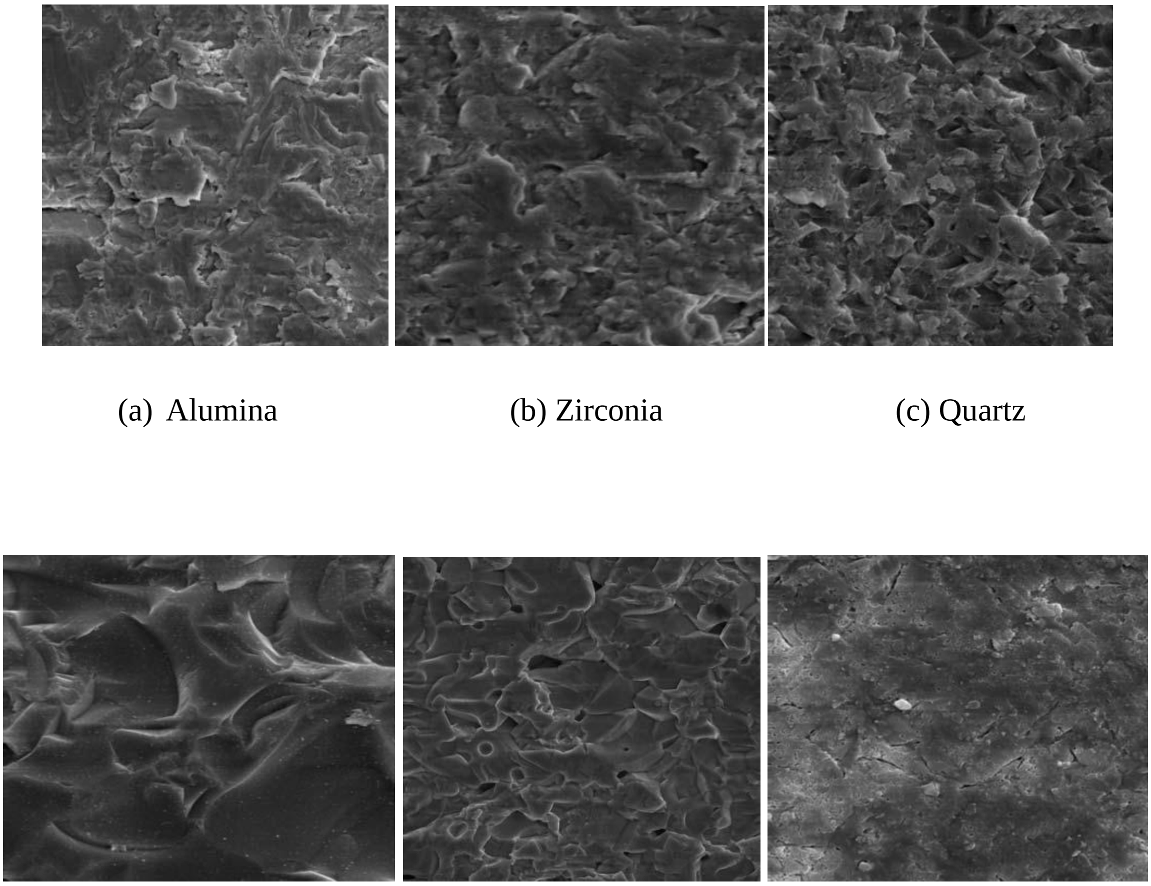

(a) Alumina (b) Zirconia (c) Quartz

(d) Glass (e) Ferrite (f) LiF

Figure 5.2 SEM of different Materials.[P. L. Guzzo and H. Shinohara(2004) A Comparative Study on Ultrasonic Machining of Hard and Brittle Vol. XXVI, No.1]

Preliminary USM experiments carried in different brittle and hard materials revealed the influence of structural and mechanical properties of work-piece materials on the rate of material removal and the topography of machined surfaces. The rate of material removal abruptly decreased with the machining depth for work-piece materials in which hardness is at the same order of magnitude than the hardness of abrasive grits. Under these circumstances, it is believed that abrasive grits lost its cutting power more quickly then the recycling period. It was observed that brittle micro cracking was the dominant mechanism of material removal, except for LiF single crystal. In this case, brittle cleavage is the major mechanism contributing to improve the surface quality. The models used to explain the material removal rate and the surface roughness in relation to material properties did not satisfactorily agreed with the experimental data. Thus, further attempts are required to establish alternative models of machinability of brittle and hard materials under ultrasonic abrasion conditions.

10. STUDY ON ULTRASONIC STEPPED HORN GEOMETRY DESIGN AND FEM SIMULATION

The paper deals with study through Finite Element Method (FEM) of ultrasonic stepped horn used to aid electro-discharge machining (EDM+US). The thermal phenomena are dominant within EDM machining mechanism. The role of US aiding is to intensify the material thermal removal through cavitational phenomena. Several studies were carried on in order to analyze the influence of steps lengths and diameters and corner radius size on own frequency of stepped ultrasonic horns. A good agreement between the FEM results and theoretical and experimental data was emphasized. Methods to adjust the own frequency of stepped horns by adjusting the lengths, diameters and additional machining of a groove at gravity centre level of horn are presented. It is very important to know the resonance frequency and amplitude at every point of the ultrasonic horn, because: it allows precise determination of the nodal plane [10] position for locking in place of the ultrasonic system for desired processing; the parameters of the ultrasonic system can be correlated with technological parameters, especially at EDM+US, in order to avoid short-circuits between electrode-tool and work-piece; finite element method allows testing of various shapes of ultrasonic horns without the need to manufacture a real prototype; it allows the correct selection of the horn shape for a particular machining process demands. It is also important the selection of horn material for desired amplitude of vibration. If the FEM has been performed properly, then the performance predicted by FEM should agree reasonably with the real sonotrode performance.

Agreement between modelling results and real results should be especially good if similar resonators have been previously modelled and validated. Exact agreement should not be expected, either because of limitations of the FEM or because of measurement errors for the real resonator. From our previous studies, it was established that the stability of

EDM+US finishing process was obtained increasing the working gap through ignition voltage growing and amplitude decrease of US oscillations. FEM modelling of sonotrodes described on this paper enables design time and manufacturing costs to be effectively reduced in practical EDM+US technological system achievements. Further studies must be carried on the various geometrical shapes of sonotrodes as one of the most important elements of the ultrasonic assisting system. The main dynamics characteristics (natural frequencies and amplification factors) of sonotrode in the resonant state should be studied according to the geometric shape and dimensions.

11. Ultrasonic horn design for ultrasonic machining technologies

Many of industrial applications and production technologies are based on the application of ultrasound. In many cases, the phenomenon of ultrasound is also applied in technological processes of the machining of materials. The main element of equipments that use the effects of ultrasound for machining technology is the ultrasonic horn so called sonotrode. The performance of ultrasonic equipment, respectively ultrasonic machining technologies depends on properly designed of sonotrode shape. [11] The dynamical properties of different geometrical shapes of ultrasonic horns are presented in this paper. Dependence of fundamental modal properties (natural frequencies, mode shapes) of various sonotrode shapes for various geometrical parameters is analyzed. Modal analyses of the models are determined by the numerical simulation using finite element method (FEM) design procedures. The mutual comparisons of the comparable parameters of the various sonotrode shapes are presented.

12. Study on Ultrasonic Vibration Effects on Grinding Process of Alumina Ceramic (Al_2O_3)

Nowadays, engineering ceramics have significant applications in different industries such as; automotive, aerospace, electrical, electronics and even martial industries due to their attractive physical and mechanical properties like very high hardness and strength at elevated temperatures, chemical stability, low friction and high wear resistance. However, these interesting properties plus low heat conductivity make their machining processes too hard, costly and time consuming. Many attempts have been made in order to make the grinding process of engineering ceramics easier and many scientists have tried to find proper techniques to economize ceramics' machining processes. This paper proposes a new diamond plunge grinding technique using ultrasonic vibration for grinding Alumina ceramic (Al_2O_3)

.For this purpose, a set of laboratory equipments have been designed and simulated using Finite Element Method (FEM) and constructed in order to be used in various measurements. The results obtained have been compared with the conventional plunge grinding process without ultrasonic vibration and indicated that the surface roughness and fracture strength improved and the grinding forces decreased. In this study, a new grinding technique applying ultrasonic vibration along the radius of the grinding wheel was proposed. A compact ultrasonic unit composed of an ultrasonic transducer, acoustic horn and their respective holders was designed and constructed and then installed on a dynamometer surface to measure the normal and tangential grinding forces.

During horizontal grinding, the work-piece was vibrated ultrasonically at the resonant frequency in the vertical direction. Performance of the unit, including the percent reduction in the normal and tangential grinding force and also improvement in the surface roughness and fracture strength has been investigated. The results described below has been confirmed the validity of the proposed new grinding technique, and demonstrated that the designed and constructed unit performed well.

The results can be summarized as follows.[11] The results of the grinding test showed that the surface roughness of Alumina work-pieces was improved by 8% when ultrasonic vibration was applied. The assistance of ultrasonic vibration in the grinding operation reduced the total grinding force. For Alumina (Al_2O_3), particularly, the reduction reached about 22%. The fracture strength of Alumina work-pieces, which had been ground using ultrasonic vibration, was improved by approximately 10% on average.

12. Prediction of Tool and Nozzle Flow Behaviour in Ultrasonic Machining Process

The use of hard and brittle material has become increasingly more extensive in recent years. Therefore processing of these materials for the parts fabrication has become a challenging problem. However, it is time-consuming to machine the hard brittle materials with the traditional metal-cutting technique that uses abrasive wheels.[12] In addition, the tool would suffer excessive wear as well. However, if ultrasonic energy is applied to the machining process and coupled with the use of hard abrasive grits, hard and brittle materials can be effectively machined. Ultrasonic machining process is mostly used for the brittle materials

13. An investigation into the machining characteristics of titanium using ultrasonic machining

Experiments have been conducted to assess the effect of three factors-tool material, grit size of the abrasive slurry and power rating of ultrasonic machine on machining characteristics of titanium (ASTM Grade I) using full factorial approach for design and analysis of experiments. It has been concluded that all factors have significant effect on Material Removal Rate (MRR), Tool Wear Rate (TWR) and surface roughness of the machined surface. Two-way interactions having significant effect on MRR, TWR and surface roughness have also been identified using Minitab14 software.[13] The levels for each factor that contribute the most to the variation in machining performance of USM of titanium have also been established. It has been concluded that titanium is fairly machinable with USM process. Moreover, the surface finish obtained is better than many of the other non-traditional processes. This work presents the identification of process parameters for USM process that put a significant effect on the machining performance of the process for titanium as work material and subsequently, the most significant levels for each parameter undertaken in the study. ANOVA was performed on the response variables data produced from the experimentation which was designed by using full factorials approach.

The significance of all the three parameters studied was confirmed by ANOVA results. For MRR and TWR, all the three parameters were found to be significant for their main effects. Two-way interactions among tool and power rating, tool and grit size and grit size-power rating were also significant for MRR and TWR. For surface roughness, grit size of the abrasive slurry was the only factor found significant. None of the two-factor interactions were found to have any significance for surface roughness.

14. Mechanism of the ultrasonic machining of ceramic composites

This paper intends to further the understanding of the basic mechanism of the ultrasonic machining of ceramic composites. Models representing the shocking force and the material removal rate are deduced and verified. The principles of ultrasonic machining are also stated. The effects on the material removal rate and the surface roughness of the amplitude of the tool tip, the static load applied and the size of the abrasive are measured.[14] It has been concluded that any increase in the amount of work/energy imparted to the machined ceramics in terms of the amplitude of the tool tip. The static load applied and the grit size of the abrasive will result in an increase in the material removal rate and a roughening of the machined surface.

15. Ultrasonic vibrating system design and tool analysis

The applications of ultrasonic vibrations for material removal processes exist predominantly in the area of vertical processing of hard and brittle materials. This is because the power generated by vertical vibrating oscillators generates the greatest direct penetration, in order to conduct material removal on work-pieces by grains. However, for milling processes, vertical vibrating power has to be transformed into lateral (horizontal) vibration to produce the required horizontal cutting force.[15] The objective of this study is to make use of ultrasonic lateral transformation theory to optimize processing efficiency, through the use of the finite element method for design and analysis of the milling tool. In addition, changes can be made to the existing vibrating system to generate best performance under consistent conditions, namely, using the same piezoelectric ceramics.

16. Ultrasonic horn design for ultrasonic machining technologies

Many of industrial applications and production technologies are based on the application of ultrasound. In many cases, the phenomenon of ultrasound is also applied in technological processes of the machining of materials. The main element of equipments that use the effects of ultrasound for machining technology is the ultrasonic horn so called sonotrode. The performance of ultrasonic equipment, respectively ultrasonic machining technologies depends on properly designed of sonotrode shape. The dynamical properties of different geometrical shapes of ultrasonic horns are presented in this paper.[16] Dependence of fundamental modal properties (natural frequencies, mode shapes) of various sonotrode shapes for various geometrical parameters is analyzed. Modal analyses of the models are determined by the numerical simulation using finite element method (FEM) design procedures. The mutual comparisons of the comparable parameters of the various sonotrode shapes are presented.

17. Design of horn for rotary ultrasonic machining using the finite element method

The cutting performance of an ultrasonic machining machine (USM) depends primarily on the ability of the design of the acoustic horn (also known as concentrator or tool holder). A horn is a waveguide-focusing device with a cross-sectional area that decreases from the transducer end to the toe end. It amplifies the input amplitude of vibrations so that at the output end the amplitude is sufficiently large for machining. In the present work, a finite element method (FEM) design procedure has been developed for the design of a horn for rotary ultrasonic machining (RUM). The double conical horn shape has taken as a domain with a hole at the tip for the cooling purpose. [17] The analysis of the various stress components in the horn domain has been studied. The stresses at the middle of the horn are found to be maximum but it is within the allowable stress of the horn material due to the sudden change in the area of the horn. The stresses on the horn for various frequencies are also studied and concluded that at resonance condition the stress is minimum.

18. Study of Micro Rotary Ultrasonic Machining

Product miniaturization for applications in fields such as biotechnology, medical devices, aerospace, optics and communications using a variety of materials has made the advancement of micromachining techniques essential. Machining of hard and brittle materials such as engineering ceramics, glass and silicon is a formidable task. Rotary ultrasonic machining (RUM) is one process capable of machining these materials. It is a hybrid machining process which combines the mechanism of material removal of conventional grinding and ultrasonic machining. Downscaling of RUM for micro scale machining is essential to generate miniature features or parts from hard and brittle materials.

The goal of this thesis is to conduct a feasibility study and to develop a knowledge base for micro rotary ultrasonic machining (MRUM). Positive outcome of the feasibility study led to a comprehensive investigation on the effect of process parameters on the MRUM process performance.[18] The effect of spindle speed, grit size, vibration amplitude, tool tip geometry, static load and coolant on the material removal rate (MRR) of MRUM was studied. In general, MRR was found to increase with increase in spindle speed, vibration amplitude and static load. The machining rate was also noted to depend upon the abrasive grit size, tool tip geometry. During the constant force mode of operation, it was difficult to maintain the force at a constant value. Therefore, a constant feed rate mode of operation was used for machining. The behaviour of the cutting forces was modelled using time series analysis. It was found that the variance associated with the cutting force was least at the highest spindle speed. Capability of MRUM process for machining bone tissue was investigated. Critical issue in bone machining is the thermal damage caused to the tissue because of excessive rise in the machining temperature. Being a vibration assisted machining process, heat generation in MRUM is low and therefore it is a potential option for bone machining. Finally, to estimate the MRR a predictive model was proposed. The experimental and the theoretical results exhibited a matching trend.

Machining

19. Parametric optimization of ultrasonic machining of co-based super alloy using the Taguchi multi-objective approach

Stellite 6 is the most generally useful cobalt alloy, having excellent resistance to many forms of mechanical and chemical degradation over a wide temperature range. Therefore, in particular, their use in aerospace projects worldwide has provided confidence leading to acceptance as prime material for aerospace vehicles in recent years. *Kumar.V , Khamba. J. S. (2009)* This paper outlines the effectiveness of the ultrasonic machining of satellite 6 in terms of tool wear rate of the tool used and the material removal rate of work piece produced. The optimum combination of various input factors as type of abrasive slurry, their size and concentration, nature of tool material and power rating of the machine for the ductile chip formation in the machining of stellite 6 has been determined by applying the [19] Taguchi multi-objective optimization technique and F-test. The analysis of results has been done using the statistic 7.0 software and results obtained are validated by conducting the confirmation experiments. The study shows the considerable improvement in multiple S/N ratio as compared to initial cutting conditions. The Taguchi quality loss function can be used to optimize the multiple quality characteristics. The optimization of the process parameters in the ultrasonic machining of satellite 6 has been done by applying the Taguchi multi-objective optimization technique. The predicted and experimental optimum values of mean signal to noise ratio were found to be 2.784 and 4.876 dB against the initial settings of 3.053 dB. Therefore, the significant increase in mean signal to noise ratio (1.823 dB) has been found at optimum parameter settings. The quality characteristics experimental values of material removal rate and tool wear rate at optimum conditions(0.185 mm^3/min, 0.064 mm^3/min)have been improved considerably in comparison to initial parameter settings of the experiment (0.170 mm^3/ min, 0.100 mm^3/min).

20. Application of Taguchi method in optimization of cervical ring cage

The Taguchi method is a statistical approach to overcome the limitation of the factorial and fractional factorial experiments by simplifying and standardizing the fractional factorial design. The objective of the current study is to illustrate the procedures and strengths of the Taguchi method in biomechanical analysis by using a case study of a cervical ring cage optimization. A three dimensional finite element (FE) model of C_5–C_6 with a generic cervical ring cage inserted was modelled. Taguchi method was applied in the optimization of the cervical ring cage in material property and dimensions for producing the lowest stress on the endplate to reduce the risk of cage subsidence, *Yang.K, Teo.E.C, Konstantin.F (2007)* establishment of objective function, determination of controllable factors and their levels, identification of uncontrollable factors and test conditions, design of Taguchi crossed array layout, execution of experiments according to trial conditions, analysis of results, determination of optimal run, confirmation of optimum run. The results showed that a cage with larger width, depth and wall thickness can produce the lower von Mises stress under various conditions. The contribution of implant materials is found trivial. [20] The current case study illustrates that the strengths of the Taguchi method lie in consistency in experimental design and analysis, reduction of time and cost of experiments, robustness of performance with removing the noise factors. The Taguchi method will have a great potential application in biomechanical field when factors of the issues are at discrete level.

The current case study applied the Taguchi method to determine the optimum dimensions and material for the cervical ring cage to minimize the cage subsidence into the endplate. A cage with larger width, depth and wall thickness can produce the lower von Mises stress under various conditions. The contribution of implant materials to the endplate von Mises stress is found trivial. The results are proven and supported by static analysis and previous studies. the design of the experiment with a mixed matrix of 4 variables with 3 levels and 2 variables with 2 levels, there will be as many as 324 runs of testing if using the conventional full factorial design. The testing of only 36 runs with the Taguchi method greatly reduces the number of tests and increases the efficiency.

21. The use of Taguchi method to optimize the laser welding of sealing neuro-stimulator

Titanium has high strength-to-weight ratio, corrosion resistance, excellent weldability and well biocompatibility. It is applied in various fields, such as medical and aerospace industry. Laser welding is major joint technology for titanium sealing in medical field. It is difficult for sealing thin titanium shell of the neuro-stimulator by laser lap welding. The key point for welding quality is the combination of laser welding parameters. In this paper, the effects of the Nd: YAG laser welding parameters is discussed and analyzed at first, and then a novel application of Taguchi's matrix method is proposed to optimize the selection of laser seal welding thin titanium shell, including the main parameters such as laser power, welding speed, defocusing amount and shield gas, finally the manufacture process for sealing neuro-stimulator is confirmed. The results show that *Xiansheng.N, Zhenggan.Z, Xiongwei.W , Luming.L (2011)* Taguchi method has optimized process parameters of the laser welding on sealing thin titanium shell of the neuro-stimulator, and the device is equipped properly in medical treatments. Conclusions In the paper, [21] the effects of the Nd: YAG laser welding parameters on the bead formation on the neuro-stimulator are analyzed by the Taguchi method. The optimal welding parameters for sealing the neuro stimulator are obtained. The work completed can be concluded as follows. First, according to the Taguchi experiment results, it can be summarized that the laser power and weld speed have the greatest influence on the S/N ratio, and the laser power, defocusing amount and weld speed have influence on average of penetration depth to width.

The Taguchi method has been proved that it is very efficient method to find the dominant factor given the complex interactions within laser welding parameters, such as laser power, welding speed, defocusing amount and pulse frequency. Second, the preliminarily optimal weld parameters for ultra thin neuro-stimulator can be obtained with 80Wlaser power, welding speed at 400 mm/min, a laser focus length at 0 mm, pulse frequency of 100 Hz and a flat type pulse shape. Finally, the verification experiment on product manufacture at the optimal welding parameters is validated that the optimized penetration depth to width can guarantee the mechanical properties and sealing performance.

22. **Optimization of machining parameters in magnetic force assisted EDM based on Taguchi method**

A versatile process of electrical discharge machining (EDM) using magnetic force assisted standard EDM machine has been developed. The effects of magnetic force on EDM machining characteristics were explored. Moreover, this work adopted an L_{18} orthogonal array based on Taguchi method to conduct a series of experiments, and statistically evaluated the experimental data by analysis of variance (ANOVA). The main machining parameters such as machining polarity (*P*), peak current (*I*p), pulse duration (μp), high-voltage auxiliary current (*I*H), no-load voltage (*V*) and servo reference voltage (*S*v) were chosen to determine the EDM machining characteristics such as material removal rate (MRR) and surface roughness (SR). The benefits of magnetic force assisted EDM were confirmed from the analysis of discharge waveforms and from the micrograph observation of surface integrity. The experimental results show that the magnetic force assisted EDM has a higher MRR, a lower relative electrode wear ratio (REWR), and a smaller SR as compared with standard

EDM. In addition, the significant machining parameters, and the optimal combination levels of machining parameters associated with MRR as well as SR were also drawn. Moreover, the contribution for expelling machining debris using the magnetic force assisted EDM would be proven to attain a high efficiency and high quality of surface integrity to meet the demand of modern industrial applications. *Lin.Y.C, Chen.Y.F, WangD.A, Lee.H.S, (2009)* The magnetic force assisted EDM had a better machining stability, since the debris driven by the assisted magnetic force would be expelled more quickly [22] and completely to reduce the abnormal discharge. Moreover, the number of effective discharge waveforms obtained by the magnetic force assisted EDM was higher than that by standard EDM.

The MRR of magnetic force assisted EDM was almost three times as large as the value of standard EDM; the REWR was improved from 1.03% to 0.33% when employed the magnetic force assisted EDM. Moreover, the SR of the magnetic force assisted EDM was less than that of standard EDM. The average value of SR reduced from Ra 3.15 to 3.04µm. The discharge craters obtained by standard EDM were bigger and deeper than those by the magnetic force assisted EDM. Moreover, the machined surface of standard EDM depicted more obvious micro-cracks than that of magnetic force assisted EDM.

23. A study on optimal compensation cutting for an aspheric surface using the Taguchi method.

In this research, the optimization of compensation cutting for eliminating the residual form error of an aspheric surface using the Taguchi method was performed. Three parameters of cutting depth, revolution of work spindle, and compensation ratio were considered as control factors, and the experimental trials based on the $L_9(33)$ orthogonal array were carried out. Based on the results of analysis of variance, the most significant factor is the compensation ratio having a percentage contribution of 49.37%. *Liu.Y.T, Chang.W.C, Yamagata.Y, (2010)* through the confirmation experiment, the rough machining accuracy of 5.81 mm could be significantly improved to 1.53 mm with an improved efficiency of 73.67%. In comparing to the accuracy of 2.60 mm obtained by one of the initial trials, the accuracy efficiency was improved to 41.15%. As presented in this study, the systematic approach to compensation cutting can be applied to various applications [23] of meso-machining or ultra precision machining works performed by ultra precision machines. Even with a feeding resolution of 0.1 µm and a precise straightness accuracy of 2/80 µm/mm along each driving axis, the four-axis desktop ultra precision machine could only achieve a mean PV form error of 5.96 µm by the rough cutting for an OFC aspheric surface. The form error could in part be attributed to the elastic deformations, which might be estimated by the depth difference between the designed curve and the measured curve. According to ANOVA results, the most significant factor in affecting the machining accuracy is the compensation ratio (C) having a percentage contribution of 49.37%.

24. Determination of optimum working conditions R22 and R404A refrigerant mixtures in heat-pumps using Taguchi method

In this study, refrigerants R22 and R404A five of their binary mixtures which contain about 0%, 25%, 50%, 75% and 100% mass fractions of R404A were tested. It is investigated experimentally the effects of gas mixture rate, evaporator air inlet temperature (from 24 to 32 ^{o}C), evaporator air mass flow rate (from 0.58 to 0.74 kg/s), condenser air inlet temperature (from 22 to 34 ^{o}C) and condenser air mass flow rate (from 0.57 to 0.73 kg/s) on the coefficient of performance (COP) and exergetic efficiency values of vapour compression heat-pump systems. To determine the effect of the chosen parameters on the system and optimum working conditions, an experimental design method suggested by Genichi Taguchi was used. In this study, it was observed that the most effective parameters are found to be the condenser air inlet temperature for COP and exergetic efficiency. [24] The collected data were analyzed by using ANOVA-TM computer software package for evaluation of the effect of each parameter on the optimization criteria. *Comakli.K,Simsek.F,Comakli.O, Sahin.B, (2009)* According to the degree of the influence of parameters on the performance statistics. At the first sight, it is difficult and complicated to deduct experimental conditions for the graphs given in these figures. the variation of the performance statistics with parameters on COP. Also, let us try to determine experimental conditions for the first point. The evaporator air inlet temperature for this point is 24 ^{o}C that is level 1 for which column C is 1.

The performance statistics value of the first data point is, thus, the average of those obtained from experimental nos. 1, 10, 14, 18 and 22. The experimental conditions for the second point are the conditions of the experiments for which column C is 2 (i.e., experiments nos. 2, 6, 15, 19 and 23), and so on. The numerical value of the maximum point in each graph shows the best value of that particular parameter, and they indicate the optimum condition in the range of the experimental conditions. The most effective parameters on COP and the exergetic efficiency are found as follows; condenser air inlet temperature, gas mixture ratio, evaporator air mass flow rate, and evaporator air inlet temperature and condenser air mass low rate, respectively. Generally, COP and the exergetic efficiency increases by increasing evaporator air in-let temperature and evaporator air mass flow rate. COP and the exergetic efficiency decreases by increasing gas mixture ratio, condenser air inlet temperature. The condenser air mass flow rate has low effect on the COP and the exergetic efficiency.

25. Parameters optimization of a nano-particle wet milling process using the Taguchi method, response surface method and genetic algorithm.

Nano-particles have been successfully and widely applied in many industrial applications. The wet-type mechanical milling process is a popular method used to produce nano-particles. Therefore, it is very important to improve milling process capability and quality by setting the optimal milling parameters. In this research, the parameter design of the Taguchi method, response surface method (RSM) and genetic algorithm (GA) are integrated and applied to set the optimal parameters for a nano-particle milling process. The orthogonal array experiment is conducted to economically obtain the response measurements. Analysis of variance (ANOVA) and main effect plot are used to *Hou.T.H, Hung S.C, Wang-L. L, (2007)* determine the significant parameters and set the optimal level for each parameter. The RSM is then used to build the relationship between the input parameters and output responses, and used as the fitness function to measure the fitness value of the GA approach. Finally, GA is applied to find the optimal parameters for a nano particle milling process. The experimental results show that the integrated approach does [25] indeed find the optimal parameters that result in very good output responses in the nano particle wet milling process. Using a wet-type mechanical milling process to produce nano-particles is a popular method because of the applicability to all classes of materials. The required qualities of the milling process are that the grain size and the variance of grain size of the nano-particle must be kept small. There are several parameters that may affect these qualities.

However, the effects of these parameters on the output quality responses in the nano particle milling process remain unknown. Moreover, it is also very important to improve the milling process capability and quality by setting optimal milling parameters in the nano particle milling process. In this research, the parameter design of the Taguchi method, response surface method (RSM) and genetic algorithm (GA) are integrated and applied to set the optimal parameters for a nano particle milling process. The orthogonal array experiment is conducted to economically obtain the response measurements and analysis of variance (ANOVA) and main effect plot are used to determine the significant parameters and set the optimal level for each parameter. The RSM is then used to build the relationship between the input parameters and output responses, and used as the fitness function to measure the fitness value in the GA approach. Finally, GA is applied to find the optimal parameters for the nano particle milling process. In this research, there are two output responses and therefore, there are two response models. The two response models are converted into a single fitness function. The experimental results show that these two transformations can obtain similar optimal parameters in a nano-particle milling process. However, this research also finds that there are conflicts between the two output responses. The optimal process parameters that result in a smaller mean grain size may unfortunately result in a larger variance of grain size. Therefore, multi-objective optimization techniques may be applied to solve this problem in future research.

26. Modifications of ITO surfaces in OLED devices by Taguchi methods.

The influences of various surface treatments on indium-tin-oxide (ITO) anodes on the performance of OLED devices are investigated by the Taguchi Method. These surface treatments include chemical and mechanical processes under different conditions. In particular, we find that the chemical treatment producing ultra-smooth ITO film surfaces does not provide the highest efficiency and luminescence. *Ming L.J , Lu.P.L, Weng.W.K, (2001)* The implications of the optimized surface treatment conditions from Taguchi Methods are discussed through device testing. Taguchi Methods were used in this report to provide the robust design for the fabrication of OLEDs. [26] We report that the optimized treatment for the ITO-coated glass substrates is the combination of the mechanical polishing process and the oxygen plasma treatment. The improvement obtained from Taguchi Methods in luminous efficiency is more than 50%.

27. Evaluation of surface roughness in laser-assisted machining of aluminum oxide ceramics with Taguchi method.

This paper evaluates laser-assisted machining (LAM) as an economically viable process for manufacturing precision aluminium oxide ceramic parts. Because it is locally heated by an intense laser source prior to material removal, LAM leads to higher material removal rates, as well as improved control of work-piece properties and geometry. To assess the feasibility of the LAM process and better understand its governing physical phenomena, experiments were conducted to obtain different measures of surface roughness for Al2O3 work-pieces machined by laser-assisted turning using a Nd:YAG laser. The experimental results were analyzed using the Taguchi method, which facilitated identification of optimum machining conditions. The findings indicate that rotational speed, with a contribution percentage as high as 42.68%, had the most dominant effect on LAM system performance, *Chang.C.W, Kuo.C.P(2007)* followed by feed, depth of cut, and pulsed frequency. LAM's most important advantage is its ability to produce much better work-piece surface quality than does conventional machining, together with larger material removal rates (MRR) and moderate tool wear. Laser-assisted machining experiments on aluminium oxide ceramic materials were completed under different operating conditions. Surface roughness and material removal rate were also measured and calculated. The results indicate both that higher rotational speed is appropriate for achieving a good finish and that the optimum machining condition must be properly collocated with the other machining parameters. [27] Thus, it can be inferred that the reduced cutting resistance as temperature increases indicates thermal softening of the material. According to the temperature measurement obtained from the LAM process the temperature on the cutting surface exceeds 850 ^{o}C in each case, ensuring that the laser power provides sufficient energy for the work-piece to reach glass-transition temperature and so be machined successfully.

Using appropriately designed LAM experiments based on the Taguchi orthogonal array, this study developed empirical models to evaluate the effects of the LAM process parameters. The test results reveal the following as optimum operating conditions: a rotational speed of 1500 rpm, a feed of 0.013 mm/rev, a depth of cut of 0.2 mm, and a laser pulsed frequency of 40 kHz. The contribution percentages of the rotational speed, feed, depth of cut, and pulsed frequency to performance were 42.68%, 22.58%, 20.73% and 14.01%, respectively. These findings suggest that the Taguchi method offers much promise for obtaining a wider range of improvement in work-piece quality.

28. A study on kerf and material removal rate in wire electrical discharge machining based on Taguchi method

This paper presents an investigation on the effect and optimization of machining parameters on the kerf (cutting width) and material removal rate (MRR) in wire electrical discharge machining (WEDM) operations. The experimental studies were conducted under varying pulse duration, open circuit voltage, wire speed and dielectric flushing pressure. The settings of machining parameters were determined by using Taguchi experimental design method. The level of importance of the machining parameters on the cutting kerf and MRR is determined by using analysis of variance (ANOVA). *Tosun.N, Cogun.C, Tosun.G, (2004)* the optimum machining parameter combination was obtained by using the analysis of signal-to-noise (*S*/*N*) ratio. The variation of kerf and MRR with machining parameters is mathematically modeled by using regression analysis method. The optimal search for machining parameters for the objective of minimum kerf together with maximum MRR is performed by using the established mathematical models. This paper has presented an investigation on the optimization and the effect of machining parameters on the kerf and the MRR in WEDM operations. The level of importance of the machining parameters on the kerf and the MRR is determined by using ANOVA. [28] Based on ANOVA method, the highly effective parameters on both the kerf and the MRR were found as open circuit voltage and pulse duration, whereas wire speed and dielectric flushing pressure were less effective factors. The results showed that open circuit voltage was about three times more important than the second ranking factor (pulse duration) for controlling the kerf, whereas open circuit voltage for controlling the MRR was about six times more important than the second ranking factor (pulse duration). An optimum parameter combination for the minimum kerf and maximum MRR was obtained by using the analysis of signal-to-noise (*S*/*N*) ratio. The confirmation tests indicated that it is possible to decrease kerf and increase MRR significantly by using the proposed statistical technique. The experimental results confirmed the validity of the used Taguchi method for enhancing the machining performance and optimizing the machining parameters in WEDM operations.

29. The effects of cutter path strategies on surface roughness of pocket milling of 1.2738 steel based on Taguchi method

In pocket milling which is often encountered in plastic mould manufacture, the demand is to narrow the interval between the surface roughness values obtained at finish milling and the surface roughness values will be met by further finishing operations as far as possible. The implementation and selection of cutting path strategies with appropriate cutting parameters have significant effect on surface roughness. *Gologlu.C, Sakarya.N, (2008)* The effect of every single variable on surface roughness is known, however, what kind of results is revealed in their combinations cannot be clearly estimated. The aim of this study is, first, to investigate optimum cutting characteristics of DIN 1.2738 mould steel using high-speed steel end mills. The cutting parameters considered are cutting velocity, feed rate, depth of cut and step over. [29] The second aim is to identify the effects of cutter path strategies when employing in pocket milling. The both aims will be addressed by means of using Taguchi parameter design. Confirmation experiments at optimal conditions were carried out. The outcomes for one direction and back and forth cutter path strategies were better than predicted results. However, the outcome for spiral cutter path was not at the desirable level. One of the reasons was that the chip stayed between the cutter and the periphery of the pocket could worsen the surface. Nevertheless, the surface roughness on the strategy obtained using the optimal cutting conditions were less than the others.

30. Friction and wear studies between cylinder liner and piston ring pair using Taguchi design method.

This paper reports an experimental study of tribological characteristics of cylinder liner (CL)/piston ring (PR) pair. Reciprocating wear process parameters are optimized for minimum weight loss and friction based on mixed L16 Taguchi orthogonal design with three process parameters, sliding velocity, applied load and oil type. It is observed that sliding velocity have the most significant influence on both weight loss and friction characteristics of CL/PR pair. The interaction of sliding velocity and oil type has some significant influence on weight loss of piston ring. The experimental results are in good agreement with the values from the theoretical model *Kapsiz.M, Durat.M,Ficici.F, (2011)* . The optimal combination of parameters is found to be A4B2C1 (highest level of sliding velocity, lowest level of load and lowest level of oil type). [30] Also as a result of the design method ANOVA, the factor sliding velocity has the maximum contribution in controlling the friction and wear behaviour of CL/PR pair. The weight loss of CL was influenced primarily by sliding velocity (44.60%), the applied load (41.54%), and oil type (10.04%).The weight loss of piston ring was influenced primarily by sliding velocity (48.38%), and the applied load (12.10%), and oil type (25.75%).The friction coefficient was influenced primarily by sliding velocity (68.14%), the applied load (6.54%), and oil type (14.15%).

31. Electro deposition of copper on titanium wires: Taguchi experimental design approach

Electro deposition of thin copper layer was carried out on titanium wires in acidic sulphate bath. The influence of titanium surface preparation, cathodic current density, copper sulphate and sulphuric acid concentrations, electrical charge density and stirring of the solution on the adhesion of the electrodeposits was studied using the Taguchi statistical method. A L16 orthogonal array with the six factors of control at two levels each and three interactions were employed. The analysis of variance of the mean adhesion response and signal-to-noise ratio showed the great influence of cathodic current density on adhesion. On the contrary, the other factors as well as the three investigated interactions revealed low or no significant effect. From this study optimized electrolysis conditions were defined. *Rosa. J.L., Robin. A., Silva. M.B., Baldan. C.A., Peres. M.P. (2009)* the copper electro coating improved the electrical conductivity of the titanium wire. This shows that copper electro coated titanium wires could be employed for both electrical purpose and mechanical reinforcement in superconducting magnets. Smooth and adherent copper electro coatings were obtained with high efficiency (>95%) on titanium wires in acidic sulphate bath. The study of the effect of the electrolysis parameters on the deposit adhesion was carried out using Taguchi statistical method and showed that the cathodic [31] current density had the greatest influence. The surface preparation of the wires investigated (degreasing followed or not by pickling), the bath composition ($CuSO_4$ and H_2SO_4 concentrations), the solution stirring and copper thickness presented low or no significance on adhesion. The copper-plated titanium wires are more conductive than the uncoated titanium wires and their resistivity is close to that of copper wires. Copper-plated titanium wires are promising materials for application as mechanical reinforcement and quench-back circuits in superconducting magnets.

32. Effect of micro-powder suspension and ultrasonic vibration of dielectric fluid in micro-EDM processes—Taguchi approach

Solutions are needed for increasing the material removal rate without degrading surface quality in micro-electrical discharge machining (m-EDM). This paper presents a new method that consists of suspending micro-MoS2 powder in dielectric fluid and using ultrasonic vibration during µ-EDM processes. *Prihandana.G.S, Mahardika.M, Hamdi.M, Wong. Y.S.,Mitsui.K, (2009)* The Taguchi method is adopted to ascerta in the optimal process parameter to increase the material removal rate of dielectric fluid containing micro-powder in µ-EDM usingaL_{18} orthogonal array. [32] Pareto analysis of variance is employed to analyze the four machining process parameters: ultrasonic vibration of the dielectric fluid, concentration of micro-powder, tool electrode materials, and work-piece materials. There sults show that the introduction of MoS2 micro-powder in dielectric fluid and using ultrasonic vibration significantly increase the material removal rate and improves surface quality by providing a flat surface free of black carbon spots.

33. Application of Taguchi technique to investigation of geometry and position of V-ring indenter in fine-blanking process

One of the special features of the fine-blanking process is the use of the V-ring indenter. The V-ring geometry, namely its angle and height, in addition to its position, affects features of the fine-blanked surface. In this study, the finite element (FE) simulation, the Taguchi technique, and the analysis of variance (ANOVA) techniques were carried out to investigate the degree of importance of V-ring indenter parameters. The results indicated that the height and position of the V-ring indenter have a major influence on the fine-blanking process, followed by the V-ring indenter angle. *Thipprakmas.S, (2010)* The combination of the FE-simulation, the Taguchi method, and the ANOVA technique was an effective tool to predict the degree of importance of the V-ring indenter parameters in the fine-blanking process, in addition to facilitating an improvement in the quality of the fine-blanked parts by optimization of these V-ring indenter parameters. The FE-simulation method, in association with the Taguchi and the analysis of variance (ANOVA) techniques, was used to examine the degree of importance of the V-ring indenter parameters, namely V-ring indenter angle, height, and position, in the fine blanking process. [33] The ANOVA results illustrated the influence of each V-ring indenter parameter on the smooth shear surface and cracks of the fine-blanked surface, together with their calculated percentage contributions. The V-ring indenter height and position, with their approximately calculated percentage contributions of 40%, have a major influence on the fine-blanking process, followed by the V-ring indenter angle. In addition, the ANOVA results were confirmed again by an additional FE-simulation on the other V-ring indenter parameters. The combination of the FE-simulation, the Taguchi method, and the analysis of variance (ANOVA) technique was an effective tool to predict the degree of importance of the V-ring indenter parameters in the fine-blanking process, in addition to aiding in improvement of the quality of the fine-blanked surface features by optimization of the V-ring indenter parameters.

34. Application of Taguchi's methods to investigate some factors affecting microporosity formation in A360 aluminium alloy casting

A Taguchi design investigation has been made into the relationship between the microporosity and process variables in a sand cast A360 aluminium alloy. The effects of various casting parameters including mold filling, liquid filtering, and solidification time, the dissolved hydrogen level of the liquid alloy and liquid treatments of molten alloy with Sr addition were investigated. Results showed that within these five casting parameters investigated, the local solidification time and the dissolved hydrogen level of the melt were significant on the microporosity. *Savas.O, Kayikci.R, (2007)* accordingly, the other casting parameters have been found to be less influential on the final pore size and their distribution. An A360 aluminium alloy was sand cast under five different design parameters with two level variations to evaluate microporosity formation within the cast part sections. Results showed that the microporosity is overwhelmingly due to the dissolved hydrogen (i.e. no traces of shrinkage porosity was observed) and ranging between 0.04% and 1.72% within the castings. [34] The Taguchi design method revealed that the local solidification time of a casting was the most influential factor upon the microporosity formation. In addition to this, dissolved hydrogen level of the liquid alloy has significant effect on the extent of microporosity.

35. Taguchi analysis of the residual tensile strength after drilling in glass fiber reinforced epoxy composites.

Composites today are replacing several traditional materials due to their superior properties such as high strength to weight ratio, high stiffness to weight ratio, better impact characteristics, corrosion resistance and design flexibility. Drilling is often required to facilitate the assembly of the parts to get the final product. However, drilling induced damage drastically affects the residual tensile strength of the drilled components. The present investigation is an attempt to study the effect of the cutting speed, the feed rate, and the drill point geometry on the residual tensile strength of the drilled unidirectional glass fibre reinforced epoxy composite using the Taguchi method and suggests the optimal conditions for maximum residual tensile strength. *Kishore. R.A., Tiwari. R., Dvivedi. A., Singh I, (2009)* The optimum levels of the drill point geometry, the cutting speed and the feed rate have been established for getting maximum residual tensile strength in drilled UD-GFRP laminates. The maximum residual strength is found with 8-facet drill at cutting speed of 750 rpm and feed rate of 15 mm/min. [35] It can be concluded that the drilling-induced damage at higher cutting speeds severely affects the residual tensile strength of drilled laminates. The optimum selection of the drill point geometry is also important
to ascertain the minimum drilling induced damage and subsequently the maximum residual tensile strength. Confirmation tests were carried out to verify the predicted optimal conditions. Values of estimation gain and confirmation gain were found close each other.

36. EDM machining of carbon–carbon composite—a Taguchi approach

The objective of this paper is to determine the optimal setting of the process parameters on the electro-discharge machining (EDM) machine while machining carbon–carbon composites. The parameters considered are pulse current, gap voltage and pulse-on-time; whereas the responses are electrode wear rate (EWR) and material removal rate (MRR). The optimal setting of the parameters are determined through experiments planned, conducted and analysed using the Taguchi method. It is found that the electrode wear rate reduces substantially, *George P.M., Raghunath B.K., Manocha L.M., Warrier A.M, (2004)* with in the region of experimentation, if the parameters are set at their lowest values, while the parameters set at their highest values increase the MRR drastically. This work shows optimisation of the machining parameters in the EDM machining of C–C composite using Taguchi method. The process variables affecting electrode wear rate and MRR, according to their relative significance, are *V*g, *I*p and Ton, respectively. Among the process parameters Ton is insignificant. [36] The optimum machining conditions for electrode wear rate, with an expected reduction of 89.28% from the current average value of 0.056 mg/min, is *I*p = 1A, Ton = 150 µs and *V*g = 20V. Whereas the same for MRR, with an expected increase of 116.67% from the current average value of 0.09mm3/min, is *I*p = 9A, Ton = 750 µs and *V*g = 100V. The optimum conditions for the two response functions are different. It has been shown that machining parameters set at their optimum levels can ensure significant improvement in the response functions, which is confirmed by the additional experiments.

Optimization

37. Optimization of screen-printing parameters of SN9000 ink for pinholes using Taguchi method in chip on film packaging.

The influence of pinholes on the chip on film (COF) in screen-printing was studied in this paper. Yield improvement is the most challenging part of COF manufacturing in view of its processing complexity, mainly in the screen-printing process. The process parameters such as ink capacity, origin control distance, angle of the squeezer, method of mixing, freshness of ink, speed of printing, and speed of scraper are considered to improve the pinholes. In Taguchi method, a two level orthogonal array is used to determine the signal-to-noise (S/N) ratio. Analysis of variance and the F-test values are used to determine the most significant process parameters affecting the pinholes. *Yen.Y.T, Fang.T.H, Lin.Y.C, (2011)* Confirmation analysis tests with the optimal levels of process parameters are carried out. The results of the experiment show that Taguchi method is a very suitable approach with regard to solving quality problems related to such pinholes. Taguchi method was employed in this work to identify the critical factors of improving the pinholes used in screen-printing COF and to efficiently optimize the process, such as ink capacity, OCD, angle of squeezer, method of mixing, freshness of ink, speed of printing, and speed of scraper.

The S/N ratio was used to analyze experimental results involving multiple runs, and this kind of analysis allows the selection of the optimum level based on least variation around the mean. Combining the critical factors governing pinhole improvement, it was observed that pinhole quantity played a significant role in screen printing. The Cpk better results in improving the pinhole of screen-printing. The models used in Taguchi method were in agreement with the experiments performed. [37] The response was used to examine the relation between the response variables and experimental factors. By means of experiments using Taguchi methods and Cpk approaches, it was found that the generation of the pinholes in COF was strongly related to the screen-printing conditions, especially to the process parameters of a low ink capacity and speed of printing of at least 70 mm/s, etc. The key factor in reducing the size of pinholes was thus to minimize in screen-printing process.

38. Optimization of cutting parameters on delamination based on Taguchi method during drilling of GFRP composite.

Drilling of glass fibre reinforced plastic (GFRP) composite is substantially different from metallic materials due to its mechanical properties. The drilling of this material may generate delamination of drilled holes on work-piece. The purpose of this paper is to investigate the influence of the cutting parameters, such as cutting speed and feed rate, and point angle on delamination produced when drilling a GFRP composite. The damage generated associated with drilling GFRP composites were observed, *Kilickap.E (2010)* both at the entrance and the exit during the drilling. Hence it is essential to obtain optimum cutting parameters minimizing delamination at drilling of GFRP composites. Moreover, this paper presents the application of Taguchi method and analysis of variance (ANOVA) for minimization of delamination influenced by drilling parameters and drill point angle. The optimum drilling parameter combination was obtained by using the analysis of signal-to-noise ratio. The conclusion revealed that feed rate and cutting speed were the most influential factor on the delamination, respectively. The best results of the delamination were obtained at lower cutting speeds and feed rates. [38] The delamination factor at entrance and exit is minimal, both at point angle of 118 ^{o} and 135^{o} .The point angle of 118 ^{o} drill produces less damage on the entrance of GFRP composite than the point angle of 135^{o} drill, the delamination factor is smaller. Based on the S/N, optimal parameters for the minimum entrance damage are the cutting speed at Level 1 (5 m/min) and the feed rate at Level 1 (0.1 mm/rev). Similarly, the optimum cutting parameters for minimum exit damage are cutting speed at Level 1 (5 m/min) and the feed rate at Level 1 (0.1 mm/rev).

39. Multi-response optimization in friction properties of PBT composites using Taguchi method and principle component analysis.

This paper optimizes the injection molding process for friction properties of fiber-reinforced polybutylene terephthalate using Taguchi method and principal component analysis. Four controllable factors of the manufacturing process were studied at three levels each. The single-response optimization of friction property was conducted by Taguchi method. Principal component analysis was employed to correspond to multi-response cases, for transforming the correlated friction properties to a set of uncorrelated components and evaluating the principal components. The optimum combination of process factors and levels for multiple qualities, based on the first principal component, *Fung.P.C, Kang.P.K, (2005)* was determined first. [39] The appropriate number of the principle components, and the influence of the number on the optimum process condition, was subsequently studied by extracting more than one principal component and integrating into a comprehensive index. Finally, the analysis of variance was used to find out the most influential injection-molding parameter for single and multiple responses problems. The anticipated improvement for different recommended process conditions showed that those process conditions extracting more than one principal components have larger S/N ratios. The process condition that extracts only the first principal component is thus not the optimal condition. Consequently, the procedure of process optimization should extract at least all the principal components that correspond to the Eigen values that are larger than one.

40. Optimizing process parameters of hot-bar soldering process through quality function deployment and Taguchi method.

As quality values failed to meet customers' requirements when the hot-bar soldering process (HBSP) was first introduced in the electronic manufacturing service (EMS) company, it is the intention of this study to combine quality function deployment (QFD) and the Taguchi method to analyze the produced quality characteristics and to optimize the process parameters. [40]The product from HBSP is a gate board that transmits vertical signals in thin film transistor liquid crystal display (TFT-LCD) modules. *Jeang.A, Chung.C.P, Chen.C.W, Li. H.C, (2009)* To produce a gate board through HBSP, a film of flexible printed circuit (FPC) is soldered onto the pad of a printed circuit board (PCB) with the hot-bar (HB) which is heated by a pulse heater. When performing a problem analysis, the strength of the solder joints is considered a response value of quality characteristics for the process of HBSP. The critical factors are then identified via the Taguchi method. The results of this study will indicate whether or not the quality of the gate board can be improved significantly and thereby satisfy customers' requirements. This study was carried out at an electronic manufacturing service (EMS) company for quality improvement of gate boards produced by the process of HBSP which is presented in this study. Our approach was to identify the important factors first with the aid of a cause-and effect diagram and QFD, and then the optimal process parameters were determined by the Taguchi method. After implementing optimal process parameter levels in the process of HBSP, the produced quality of gate boards could be greatly improved. Consequently, the yield in satisfying customers quality requirement would be increased significantly.

41. Using Taguchi method to optimize welding pool of dissimilar laser-welded components.

In the present work, CO_2 continuous laser welding process was successfully applied and optimized for joining a dissimilar AISI 316 stainless-steel and AISI 1009 low carbon steel plates. Laser power, welding speed and defocusing distance combinations were carefully selected with the objective of producing welded joint with complete penetration, minimum fusion zone size and acceptable welding profile. [41] Fusion zone area and shape of dissimilar austenitic stainless-steel with ferritic low carbon steel were evaluated as a function of the selected laser welding parameters. *Anawa.E.M, Olabi A.G. (2008)* Taguchi approach was used as statistical design of experiment (DOE) technique for optimizing the selected welding parameters in terms of minimizing the fusion zone. Mathematical models were developed to describe the influence of the selected parameters on the fusion zone area and shape, to predict its value within the limits of the variables being studied.

The result indicates that the developed models can predict the responses satisfactorily. Using laser welding could produce a small welding pool and a narrow HAZ. Welding speed has the stronger effect on the fusion area size among the selected parameters; which is proportional inversely with responses. Laser power has strong effect on fusion area. By changing the P value the response will be changed dramatically, so the P value should be carefully selected. The focusing position parameter has insignificant effect on the total weld pool size. The model developed can be adequately in predicting the responses within the factors domain.

42. Optimization of Nd:YAG laser welding onto magnesium alloy via Taguchi analysis.

The use of an Nd:YAG laser for thin plate magnesium alloy butt welding was optimized using the Taguchi analytical methodology. The welding parameters governing the laser beam in thin plate butt welding were evaluated by measuring of the ultimate tension stress. The effectiveness of the Taguchi method lies in clarifying the factor that dominates complex interactions in laser welding. The factors can be the shielding gas, laser energy, convey speed of work-piece, point at which the laser is focused, pulse frequency, and pulse shape. Furthermore, 18 combinations of these six essential welding parameters were set and Taguchi's method followed exactly. *Pan.L.K, Wang.C.C,Hsiao.Y.C,Ho.K.C, (2004)* The optimal result was confirmed with a superior ultimate tension stress of 169 MPa, 2.5 times larger to that from original set for laser welding. The optimization of Mg alloy thin plate butt welding was studied using Taguchi's analytical method. [42] Various combinations of welding parameters were considered following Taguchi's recommendation, to evaluate the relative importance of welding parameters. The power of the Taguchi method is in its clarifying the dominant factor given the complex interactions which occur in laser welding, involving the shielding gas, laser energy, conveying speed of work-piece, laser focus, pulse frequency and pulse shape. Analytical results indicate that the pulse shape and the energy of the laser contributed most to thin plate butt welding. Accordingly, the optimal combination of welding parameters for laser welding is Ar as the shielding gas, a 360 W laser, a work-piece speed of 25 mm=s, a laser focus distance of 0:0 mm, a pulse frequency of 160 Hz, and a type III pulse shape. The ultimate tension stress was maximum at an overlap of the welding zone of approximately 75%.

43. **Optimizing power consumption for CNC turned parts using response surface methodology and Taguchi's technique—A comparative analysis**

This paper presents the findings of an experimental investigation into the effects of cutting speed, feed rate, depth of cut, nose radius and cutting environment in CNC turning of AISI P-20 tool steel. Design of experiment techniques, i.e. response surface methodology (RSM) and Taguchi's technique; have been used to accomplish the objective of the experimental study. L27 orthogonal array and face cantered central composite design have been used for conducting the experiments. Taguchi's technique as well as 3D surface plots of RSM revealed that cryogenic environment is the most significant factor in minimizing power consumption followed by cutting speed and depth of cut. The effects of feed rate and nose radius were found to be insignificant compared to other factors. *Aggarwal.A, Singh.H, Kumar.P, Manmohan Singh.M, (2008)* Though both the techniques predicted near similar results, RSM technique seems to have an edge over the Taguchi's technique. The analysis of the results for power consumption shows that the techniques, RSM and Taguchi methodology, give similar results. Taguchi's technique revealed that cryogenic environment is the most significant factor followed by cutting speed and depth of cut.

The 3D surface plots of RSM also revealed that cryogenic environment has very significant effect in reducing power consumption. The lowest value of power consumption in the given range of parameters as depicted by ramp function graphs are dry environment (858.07), wet environment (1479.87) and cryogenic environment (658.79). Significance of interactions and square terms of parameters is more clearly predicted in RSM. The RSM shows significance of all possible combinations of interactions [43] In Taguchi's technique only three interactions (*AB*, *AC* and *BC*) are normally studied. Also square of parameters are analyzed in RSM whereas none of them is done in Taguchi's technique. This is owing to the fact that in Taguchi's design, interactions between control factors are aliased with their main effects.

CHAPTER 6

FINITE ELEMENT ANALYSIS OF UNTRASONIC MACHINE TOOL

Ultrasonic components can be turned using equation based on theory derived from the longitudinal vibration of rod. Simple geometric shapes can be tuned accurately using this method, but as the geometry of the blade increases in complexity analytical solution are ineffective. Very complex component geometries can be tuned accurately using the computational FE method.[45]

6.1 LONGITUDINAL VIBRATION OF ROD

When in-plane vibration displacements excite a profile, a uniform rod, longitudinal mode vibration occurs. The displacement, u, is a function of position, x, and time, t.

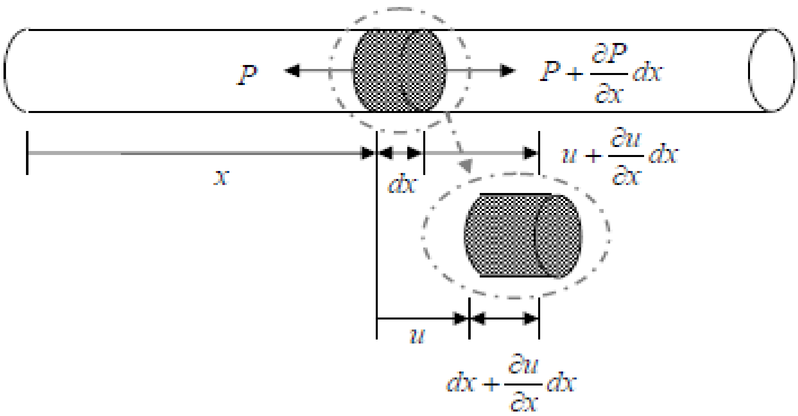

Fig 6.1 Longitudinal motion of a uniform rod.[Experimental and finite element modelling of ultrasonic cutting of food (2008)Euan McCulloch BEngAMIMechE, Department of Mechanical Engineering University of Glasgow.]

For an isotropic, uniform, elastic rod with free- free boundary conditions, the equation of motion can by found by considering a small element of rod, dx, where under an applied force, P, the displacement at x is u and the displacement x+ds is $u+\left(\frac{du}{dx}\right)dx$ .the element dx has now increased in length by $\left(\frac{du}{dx}\right)dx$ and the strain in the elongated element is $\left(\frac{du}{dx}\right)$ as shown in fig 6.1. If σ=εE where σ is the stress in the element, ε is the strain and E is the young's modulus, then for a rod with cross-section area A, and applied force P;

$$\frac{u+\left(\frac{\partial u}{\partial x}\right)dx-u}{\partial x}=\frac{\partial u}{\partial x}=\frac{P}{EA} \qquad \text{(Equation....6.1)}$$

Applying Newton's Second law:

$$P + \frac{\partial P}{\partial x} - P = \rho A dx \frac{\partial^2 u}{\partial t^2} \qquad \text{(Equation....6.2)}$$

Where ρ is the density

Substitute equation 1 in 2

$$AE \frac{\partial^2 u}{\partial t^2} dx = \rho A dx \frac{\partial^2 u}{\partial t^2} \qquad \text{(Equation...6.3)}$$

$$\frac{\partial^2 u}{\partial t^2} = \frac{E}{\rho} \frac{\partial^2 u}{\partial x^2} \qquad \text{(Equation....6.4)}$$

The equation of motion can be define as:

$$\frac{\partial^2 u}{\partial x^2} = \frac{1}{c^2} \frac{\partial^2 u}{\partial t^2} \qquad \text{(Equation....6.5)}$$

Where c^2= E/ρ and is the velocity of the stress wave in the rod.

Separation of variables can be used to solve the partical differential equation and a solution is considered of the form:

$$U(x,t)=G(x)H(t) \qquad \text{(Equation....6.6)}$$

Substituting equarion 6 in 5

$$\frac{1}{G} \frac{\partial^2 G}{\partial x^2} = \frac{1}{c^2} \frac{1}{H} \frac{\partial^2 H}{\partial t^2} \qquad \text{(Equation....6.7)}$$

Each side of equation 7 must be a constant as the left hand side is independent of x and the right hand side is independent of t. Let the constant be $-(\frac{w}{c})^2$, then two ordinary differential equation can be obtained.

$$\frac{\partial^2 G}{\partial x^2} + (\frac{\omega}{c})^2 G = 0 \qquad \text{(Equation....6.8)}$$

$$\frac{\partial^2 H}{\partial t^2} + \omega^2 H = 0 \qquad \text{(Equation....6.9)}$$

The general solution is of the form:

$$G(x) = ASin\frac{\omega}{c}x + BSin\frac{\omega}{c}x \qquad \text{(Equation....6.10)}$$

$$H(t) = CSin\omega t + DCos\ \omega t \qquad \text{(Equation...6.11)}$$

Where A,B,C, and D are dependent on boundary and initial condition. The general solution for u is therefore:

$$u(x,t) = \left(ASin\frac{\omega}{c}x + BSin\frac{\omega}{c}x\right)(CSin\omega t + DCos\ \omega t) \quad \text{(Equation....6.12)}$$

For a free- free rod, the natural frequency is found to be:

$$f_n = \frac{n}{2l}\sqrt{\frac{E}{\rho}} \qquad \text{(Equation....6.13)}$$

Where n is the mode order and l is the tuned length.

For a fixed resonant frequency, the tuned length can be calculated from:

$$l = \frac{n}{2f_n}\sqrt{\frac{E}{\rho}} \qquad \text{(Equation....6.14)}$$

From Eq 13 the natural frequency f_n, is dependent on the length of the component and the material constants E, and ρ. Eq 13 is only accurate for components of low mode order that have length much greater than the diameter of the rod.

All the equations are taken from *Experimental and finite element modelling of ultrasonic cutting of food (2008)Euan McCulloch BEngAMIMechE, Department of Mechanical Engineering University of Glasgow.*

6.2 FINITE ELEMENT MODELLING

The creation of the finite element method in 1943 was by Courant who obtained approximate solution to vibration system by utilising the Ritz method of numerical analysis and minimisation of variational calculus. Further work followed this pioneering work by Courant to establish the FE method for practical use and by the 1970s it was being used by large industries such as aerospace, automotive, defence and nuclear industries at large, mainframe computers. However, with rapid advancements in computational power and the reduced cost of FE software, FEA is now widely used. The FE method works by modelling a structure using a mesh of elements connected together using nodes. The elements can have simple as complex material properties applied to characterise the behaviour of the structure under analysis. Boundary and load conditions can be simulated on the nodes or elements of the mesh and a variety of analytical results can be calculated depending on the type of analysis requested by the user and the parameters the uses is interested in. Several modelling techniques can be used to analyse a structure in using a 2D or 3D modelling domain, the choice of which depends using the FE methods and FEA is now considered to be an essential tool in the arsenal of an engineer especially for design or troubleshooting.

6.3 DESIGN PROCESS FOR ULTRASONIC TOOL.

The literature on ultrasonic component design indicates that for uniform cylinder the gain of the tuned component is 1.i.e theoretically if 1 micron amplitude is supplied by the transducer at one end of the rod then the displacement at the other end is 1 micron, this however in reality never occurs due to slight internal losses. Also, gain is dependent on the rate of change in cross- sectional area from the base of the component, where the input is supplied to the tip. A reduction in cross-sectional area from the base to the tip increases gain and an increase in cross-sectional area reduce gain. Many components profiles exist such as conical, exponential, stepped or combination of each to magnify or reduce amplitude at the tip of the component.

6.4 DESIGN CONSIDERATION FOR USM TOOL

For the experimental cutting tool tuned to the longitudinal mode of vibration at 30 kHz frequency, material Alloy Steel (High Carbon High Chromium Alloy Steel) and work-piece Glass. An increase in gain would allow a large range of amplitude to be investigated. To increase the vibration amplitude of the tool and for simplicity for tuning and comparison studies two symmetric circular cuts were taken from both uniform rod along the longitudinal axis to reduce the cross sectional area from the base to the tip, as shown in fig: 6.2

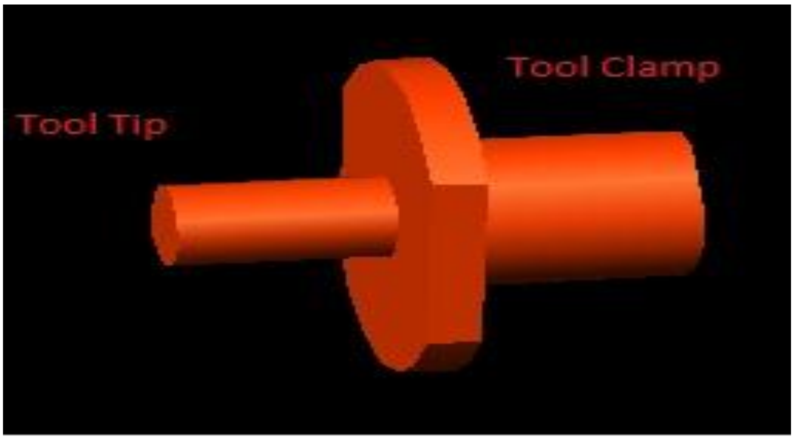

Fig6.2 Symmetric circular cuts through a uniform rod

6.5 TUNING THE ULTRASONIC TOOL

From the basic elementary vibration equation it is standard to tune the waveguide to resonance by scaling the geometry of the tool by a constant. This can be determine by equation 14 where C is the constant, f_{cur} is the current natural frequency of the required mode shape and f_{des} is the desired natural frequency the component will be driven at by the transducer.

$$C = \frac{f_{cur}}{f_{des}} \qquad \text{(Equation....6.15)}$$

Only the longitudinal length was multiplied by the constant to tune the tool whilst the diameter remained constant. To tune the ultrasonic tool the geometry of the tool was created in ABAQUS and then the program executed to determine natural frequencies. The longitudinal mode of the tool was identified and the resonant frequency recorded. Afterwards the length of the tool was rescaled by multiplying the length by the constant as calculated in eq 14 which was the ratio of the calculated output frequency to the desired frequency. The analysis was the resubmitted and the longitudinal mode identified to determine if it was operating at the driving frequency.

6.6 STRESS ANALYSIS USING FEA

After the tool had been tuned to resonance a forcing was applied to the base of the tool as indicated in Equation 15 where F is the force, A the amplitude of the transducer (8 microns), ω the natural frequency and t the time.

$$F = A \sin \omega t \qquad \text{(Equation....6.15)}$$

A steady state dynamics direct step was included in the FE analysis after the frequency step to analysis stress and displacement of the tool due to the applied loading at the longitudinal mode of vibration. The stress distribution in the tool can be plotted using the Von-mises and Hencky criteria as shown in Eq: 16 below where σ_1, σ_2, σ_3 are the principal stresses and σ_o is the yield stress.

$$(\sigma_1 - \sigma_2)^2 + (\sigma 2 - \sigma_3)^2 + (\sigma 3 - \sigma_1)^2 = 2\,\sigma_o^2 \qquad \text{(Equation....6.16)}$$

Assuming the stress distribution lies in-plane along the cross-section of the blade where no traverse movement exists implies that there is only one principal stress, σ_2, acting in one direction always and no shear stress and using Eq: 17

$$\sigma_1, \sigma_3 = 0$$

$$(0 - \sigma_2)^2 + (\sigma_2 - 0)^2 + 0 = 2\,\sigma_o^2$$

$$\sigma_2^2 = 2\,\sigma_0^2$$

$$\sigma_2 = \sigma_0 \qquad \text{(Equation....6.17)}$$

as shown in Eq 17 the Von Mises stress will be the same as the maximum principal stress in the longitudinal direction in the wave guides when excited in the longitudinal mode. Maximum stress limits in components must always be considered in any design and for ultrasonic cutting tool ideally the maximum stress must lies in the elastic region of the material at a safety factor typically of 4 or greater for operational safety. The maximum allowable stress in an ultrasonic component when designed can therefore be considered to the yield stress of the material divided by the safety factor as denoted in Eq:6.18

$$\sigma_{max} = \frac{\sigma_{yield}}{Safety\ Factor} \qquad \text{(Equation....6.18)}$$

6.7 MATERIAL SELECTION FOR ULTRASONIC TOOL

Material selection for ultrasonic components is critical to ensure the tool operate correctly. Material factor such as high strength and high toughness are specified for the design of ultrasonic components especially ultrasonic tool where the components experience extreme loading conditions. Minimising heat generation during operation is often a design specification for ultrasonic tool to restrict burning at the cut interface that can ruin the substrate material, and materials with low internal friction co-efficients are required to minimise temperature rise during operation. However, in some processes such as ultrasonic cutting of glass products a slight temperature increase is sometimes an advantage and for soft materials can locally melt the material at the interface which can often produce a cut surface that is visually appearing to the eye. Ideally during operation an acoustic loss factor zero is prefect as there will be no energy losses due to heat or noise and all energy supplied will be transformed into mechanical vibration but in reality every ultrasonic component will experience acoustic losses and energy will be lost in the system. Often the quality factor is used to characterise the effectiveness of the ultrasonic components and a high mechanical Q is often advantageous for ultrasonic components design. The mechanical Q or quality factor can be calculated using Eq.19, where Q is the quality factor and Φ is the acoustic loss available from material table.

$$Q = 1/\Phi \qquad \text{(Equation....6.19)}$$

Many materials have high quality factor but it is also critical when selecting a material for component design to consider the acoustic impedance, z, of the material which can be determine from Eq: 20 where c is the speed of sound in the material and ρ is the density. $Z = c\rho$ (Equation....6.20)

When several ultrasonic components are connected, usually by using threaded studs where one component is tightened against another, the acoustic impedance should be matched as closely as possible to ensure transfer is maximised between joining components and to ensure the vibration is transferred effectively between one component and the next.

6.8 EXPERIMENTAL ULTRASONIC TOOL

In the investigation Alloy steel (High carbon, High Chromium steel) is used for the ultrasonic tool, used in the experimental cutting trials due to its high strength, high toughness, corrosion resistance, durability and low acoustic loss (or high mechanical Q). The material properties for alloy steel are tabulated in table 6.1.A finite Element model of the ultrasonic tool was made using the FE package ABAQUS and using the procedure described previously to resonate in the longitudinal mode at 30 kHz.

Table 6.1 Material properties of Alloy Steel (High carbon, High Chromium steel)

Alloy Steel (High carbon, High Chromium steel)	
Density	7.8gm/cm^3
Hardness (Vicker’s) HRB	168
Ultimate Tensile Strength	765 MPa
Yield Strength	529 MPa
Young’s Modulus	84.2 GPa
Poisson Ratio	0.321
Fatigue Strength	114 MPa
Specific Heat Capacity	0.359 Kj/Kg^{o}C
Thermal Conductivity	4.5 W/mK

With the help of these material properties, generate the model in the ABAQUS Solver that is shown in the fig: 6.3 these date are taken from the R & D Department, industrial area Ludiana.

6.9 BOUNDARY CONDITIONS AND LOADS

Boundary conditions are the conditions existing at the physical boundary of the domain. In stress analysis problem they refer to displacements or rotation and forces/ moment conditions. Since the upper part of the ultrasonic tool is fixed in the horn therefore no longitudinal movements and no rotational movements are allowed. The boundary conditions were imposed to finite element model by freezing all degrees of freedom of motion at one end (ENCASTRE; U1=U2=U3=UR1=UR2=UR3=0). The same condition was applied to the work piece which was holded at the base. The load applied on the tip of the ultrasonic tool is 100 N/m^2 in the longitudinal direction direct to the work piece. During machining operation pressure is also applied on the sides wall of the ultrasonic tool that is approximately half the force applied on the tip i.e. 50 N/m^2. This happens because the abrasive particles get stuck in the gap between tool and work piece hole and due to this effect the hole diameter generated is always bigger than the required hole diameter. The force is transferred to the abrasive and these abrasives strike with the work piece to remove the material by erosion effect. These are 6586 tetrahedral elements were generated for the studies to ultrasonic tool and 12858 tetrahedral elements were generated for the studies to the glass work-piece. In which 21 tetrahedral elements are come on the surface of the tip of USM tool. The maximum stresses are generated in this part.

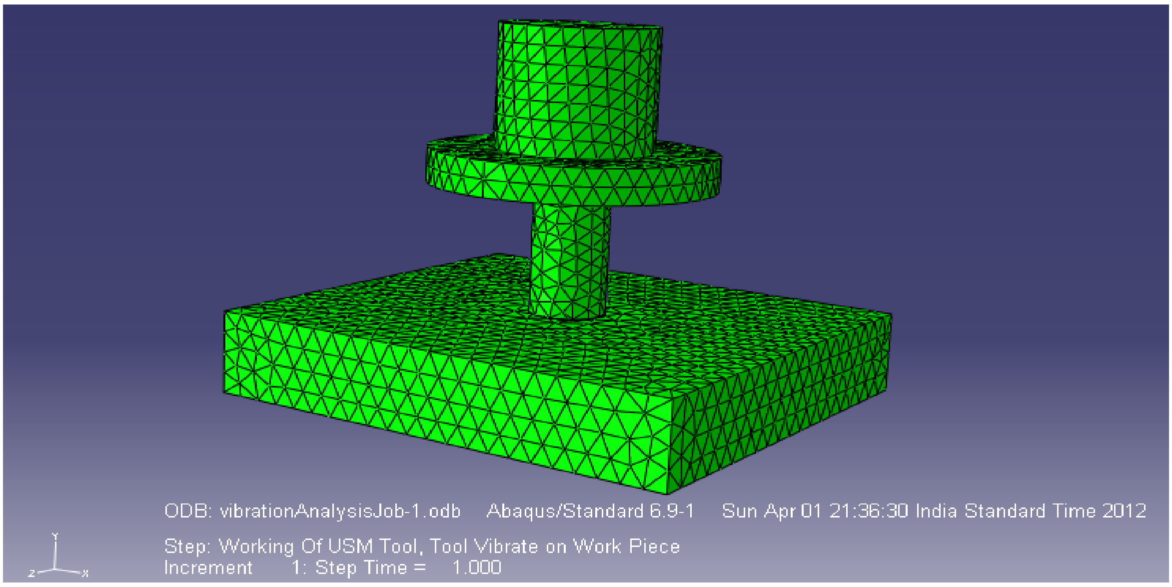

Fig: 6.3 Modal in ABAQUS with boundary condition

6.10 RESULTS

By analysis of the results obtained for the defining and submitting a job where the load applied was represented using a sinusoidal force function as equation using 6.18, the maximum stress, tool displacement were determined. Fig: 6.4 illustrate using contour plots, the locations of maximum stresses and displacement for the 30 kHz tool when excited in the longitudinal mode.

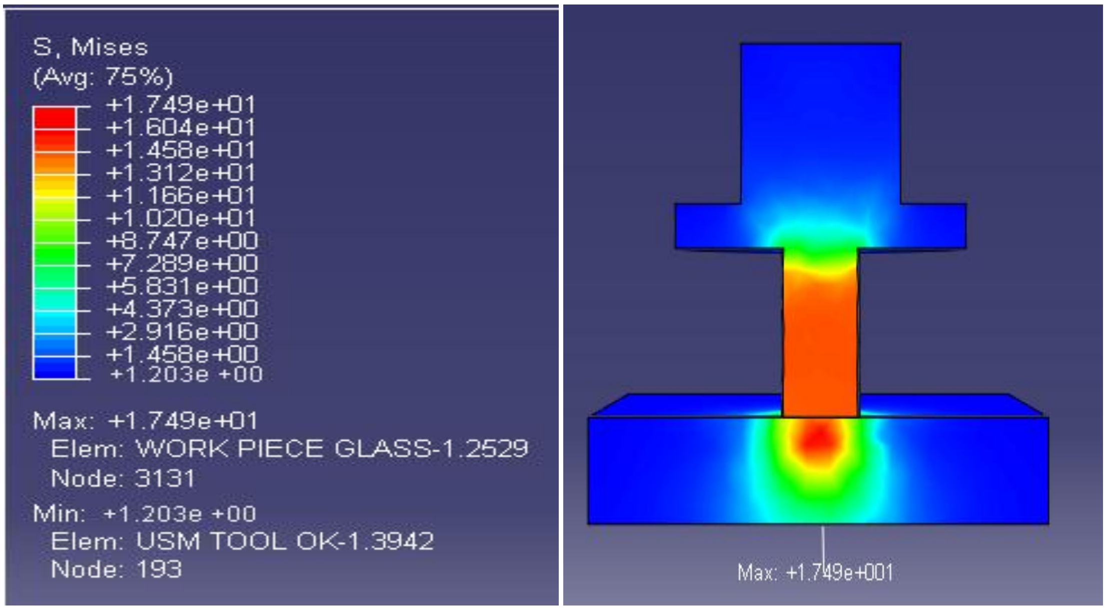

Fig: 6.4 Contour plot of the deformed shape for the tuned 30 kHz ultrasonic machine tool maximum principal stress in the longitudinal direction

From the FE analysis, the maximum stress location along the longitudinal axis of the ultrasonic tool was predicted by plotting the principal stress in the longitudinal direction or the Von Mises stress along a path of node along the centre of the tool at the excited natural frequency.

From the Fig 6.4 it is shown the maximum stress was generated on the tip of the work piece the value of the stress is shown in the table the value is approximately 17.49 Mpa. It observed that stress is decrease when we move in the upward along longitudinal direction. Same way the maximum stress is generated under the tip of the tool at the work piece. These load and conditions (parameters) was used to remove the material from the work piece with the help of erosion effect. The vibration force was transferred in to the abrasive slurry due to the vibration these abrasive particles strike with work-piece and the material start erode.

Similarly, the nodal displacement can also be determined along the same nodal path. Present the nodal displacement, principal stress in the longitudinal direction and Mises stress for the 30 kHz.

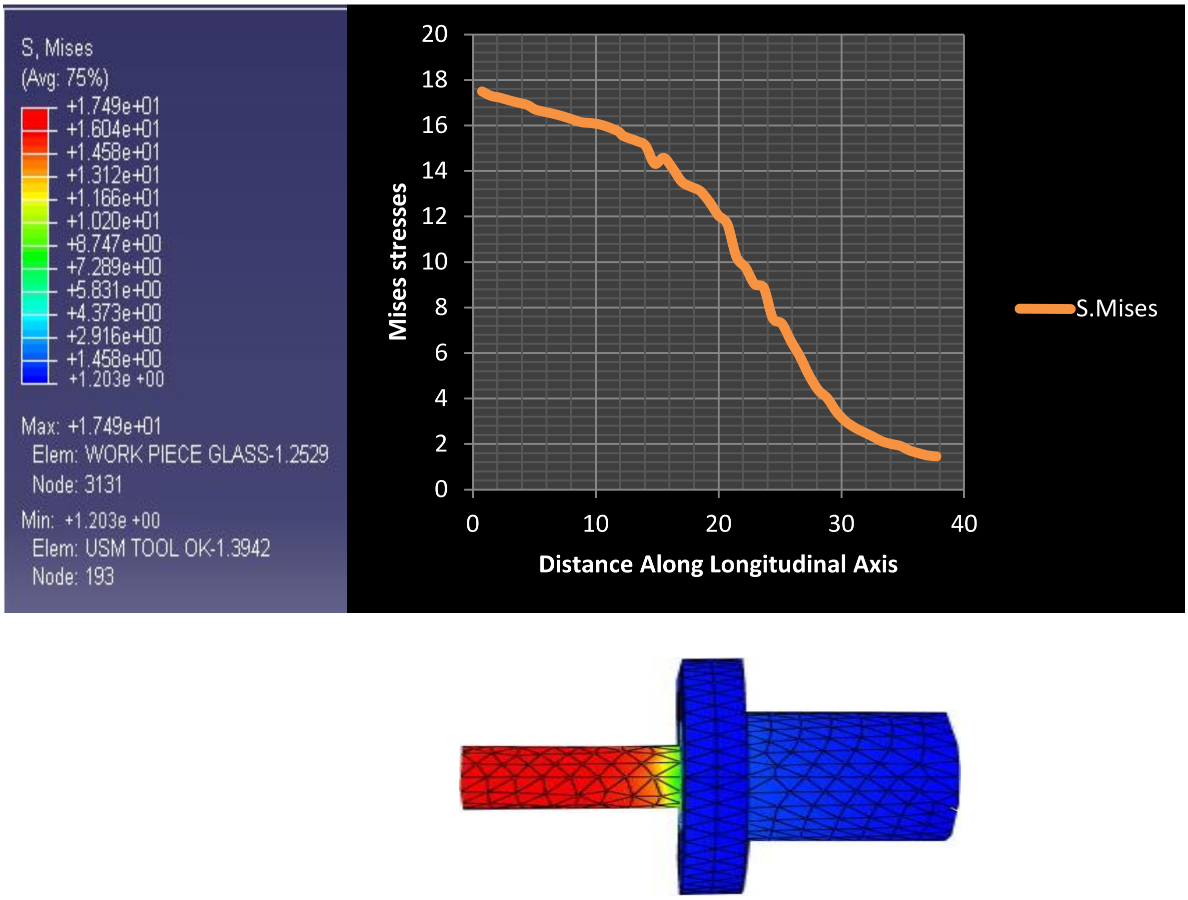

<--------- Longitudinal Axis------------>

Fig: 6.5 Present the principal stress in the longitudinal direction and Mises stress for the 30kHz.

From Fig 6.5.it is observed that maximum stress is generated on the tip of the tool, the maximum stress value at the tip of a tool is 17.49 N/m^2, The value of the stresses is decrease gradually from tip to the end along longitudinal axis. The minimum value of stress is 1.203 N/m^2 at the other end of the tool. In the tool stress diagram different colours show the change in the stress value. For example from the 0.5 mm distance the value is 16.24 N/m^2 it shows with the help of red colour. At the distance 15 mm from the tip of tool the value of stress is 13.85 N/m^2 is shown with the light yellow colour. At distance 25 mm from the tip of tool the value of stress is 8.56 N/m^2 it is shown by the sky-blue colour. The minimum stress value is at 38mm from the tip of the tool the value is 1.25 N/m^2 and it is shown with the blue colour.

From the FE analysis, the maximum stress location along the longitudinal axis of the ultrasonic tool was predicted by plotting the principal stress in the longitudinal direction or the Mises stress along a path of node along the centre of the tool at the excited natural frequency.

The nodal displacement can also be determined along the same nodal path Fig: 6.8 present the nodal displacement, principal stress in the longitudinal direction and Mises stress for the 30 kHz for work piece Glass.

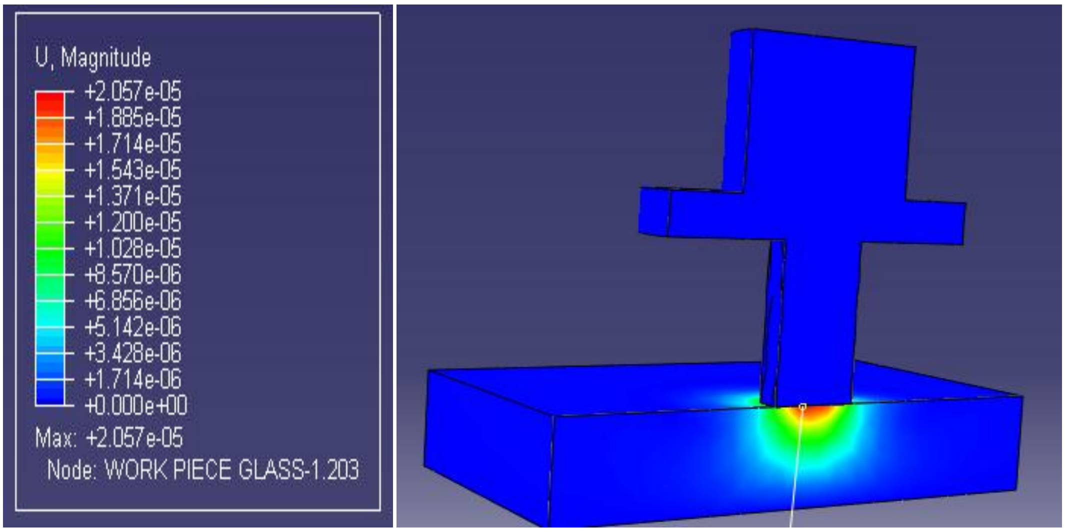

Fig:6.6 Contour plot of the deformed shape for the work piece Glass

Similarly, the nodal displacement can also be determine along the same nodal path for the work-piece (Glass) is shown in Fig: 6.9 present the nodal displacement, principal stress in the longitudinal direction and Mises stress for the 30 kHz

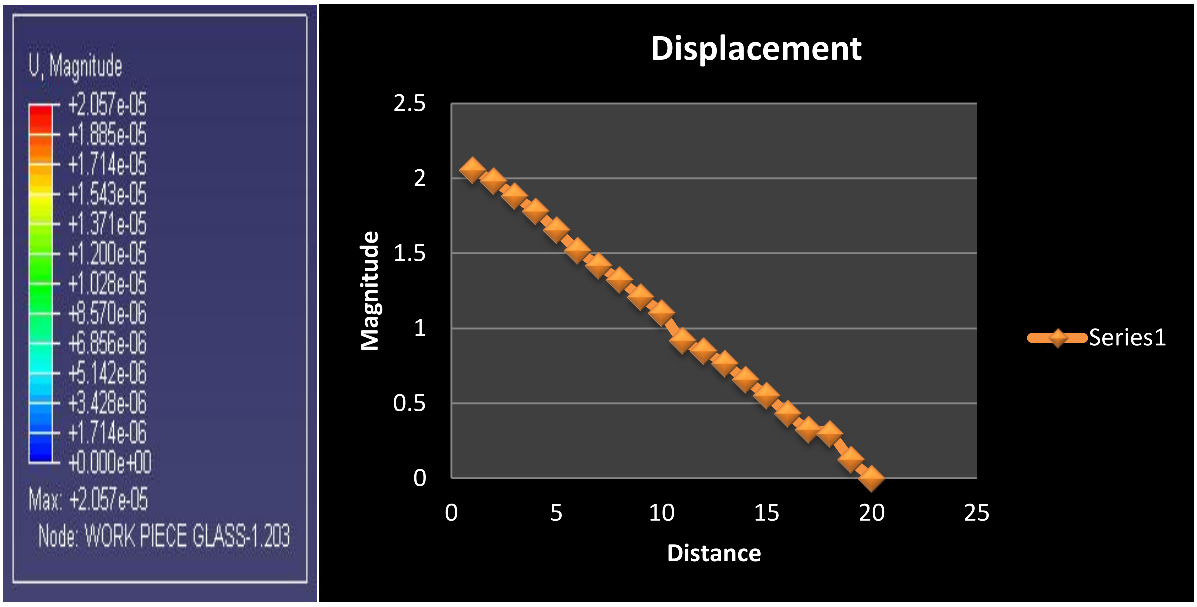

Fig: 6.7 Present the nodal displacement in the longitudinal direction and Mises stress for the 30kHz

At the just below of the tip of ultrasonic tool the maximum stresses is generate, Because the Ultrasonic tool is vibrate and the maximum vibration is transfer at this point, and this vibration is transfer in to the abrasive particle, when these particles are strike with the work piece the material will remove by erosion, the maximum stresses is generate under the tip of tool is +2.05e-05 (0.00205 N/m^2).

6.11 CONCLUSIONS

The ultrasonic tool design process has been introduced and explained in detail in this section with an introduction to FEA based ultrasonic tool analysis. The finite element model was developed with an aim to predict the stresses generated, tool deformations and strains under different operating conditions for example: tip diameter, ultrasonic amplitude, cutting orientation, ultrasonic tool material properties. FEA was used to design ultrasonic tool resonant in the longitudinal mode at 30 kHz for use in experimental work.

The theory of the longitudinal vibration of uniform rods used to calculate the tuned length of a 30 kHz uniform alloy steel rod has been discussed. The calculated lengths of the uniform Alloy steel rod were then modelled using the FE modelling package ABAQUS using tetrahedral elements to determine the resonant natural frequency of the longitudinal mode.

A 30 kHz alloy steel tool for experimental process trials was designed using FEA. A defining and submitting a job was performed on the ultrasonic tool from the initial design concept and tuned to the driving frequency of the transducer to resonate in the longitudinal mode of vibration. The tip displacement, maximum stress and its location along the longitudinal axis in the ultrasonic tool was determine using the FE procedure.. The stress results were analysed for the maximum vibration output of the transducers considering a safety factor of 4 during operation to ensure the stress levels did not exceed the yield point of the tool material.

CHAPTER 7
EXPERIMENT WORK

7.1 METHODOLOGY

The full factorial design is referred as the technique of defining and investigating all possible conditions in an experiment involving multiple factors while the fractional factorial design investigates only a fraction of all the combinations. Although these approaches are widely used, they have certain limitations: they are inefficient in time and cost when the number of the variables is large; they require strict mathematical treatment in the design of the experiment and in the analysis of results; the same experiment may have different designs thus produce different results; further, determination of contribution of each factors is normally not permitted in this kind of design.

The Taguchi method has been proposed to overcome these limitations by simplifying and standardizing the fractional factorial design. The methodology involves identification of controllable and uncontrollable parameters and the establishment of a series of experiments to find out the optimum combination of the parameters which has greatest influence on the performance and the least variation from the target of the design. The effect of various parameters (Power Rate, Grit Size, Type of abrasive, Concentration) and some of the effects of interactions between the main factors were also being studied using parameterization approach developed by Taguchi.

7.2 PROCEDURE OF EXPERIMENTAL DESIGN

The whole procedure of Taguchi method is as under.

1. Establishment of objective functions.
2. Selection of factors and/or interactions to be evaluated.
3. Identifications of uncontrollable factors and test conditions.
4. Selection of number of levels for the controllable and uncontrollable factors.
5. Calculation total degree of freedom needed
6. Select the appropriate Orthogonal Array (OA).
7. Assignment of factors and/or interactions to columns.
8. Execution of experiments according to trial conditions in the array.
9. Analyze results.
10. Confirmation experiments

7.3 ESTABLISHMENT OF OBJECTIVE FUNCTION

The objective of the study is to evaluate the main effects of Power Rate, Grit Size, type of abrasive, Concentration on the MRR, TWR, surface roughness and hardness.

7.4 DEGREE OF FREEDOM (DOF)

The number of factors and their interactions and level for factors determine the total degree of freedom required for the entire experiment. The degree of freedom for each factor is given by the number of levels minus one.

DOF for each factor: k-1

Where k is the number of level for each factor

DOF for interactions between factors: $(k_A-1) \times (k_B-1)$

Where k_A and k_B are number of level for factor A and B

7.5 SELECTION OF FACTORS AND INTERACTION

The determination of which factors to investigate depends on the responses of interest. The factors affects the responses were identified using cause and effect analysis, brainstorming and pilot experimentation. The lists of factors studied with their levels are shown in the Table 7.1.

Table 7.1 Factor interested and their level

Factor	Levels		
	Level 1	Level 2	Level 3
Concentration	20	30	---
Abrasive	Aluminium Oxide	Silicon Carbide	Mix
Power Rate	20	40	60
Grit Size	280	400	600

Some of interactions between the main factors were believed to be of interest. The interaction identified for detailed statistical analysis is as under:

- Concentration and Power Rate, A x C

The minimum DOF required in the experiment are the sum of all the degrees of freedom of factors and interaction. In the present experiment setup, there are three (abrasive, power rate, grit size) 3-level factor and one (concentration) is 2-level factor. The total DOF for the experiment including the interaction is given in Table 7.2, as the DOF for the experiment is 9, the orthogonal array (OA) to be used should have more than 9 DOF. The most suitable orthogonal array that can be used for this experiment is L18 mixed, which have 9 DOF assigned to its various columns. The additional 8 DOF were used to measure the random error.

Table 7.2 Degree of Freedom

Factor	A	B	C	D	A x B	Total
Degree of Freedom	1	2	2	2	1x2=2	9

7.6 ORTHOGOLNAL ARRAY (OA)

OA plays a critical part in achieving the high efficiency of the Taguchi method. OA is derived from factorial design of experiment by a series of very sophisticated mathematical algorithms including combinatory, finite fields, geometry and error correcting codes. The algorithms ensure that the OA to be constructed in a statistically independent manner that each level has an equal number of occurrences within each column; and for each level within one column, each level within any other column will occur an equal number of times as well. Then, the columns are called orthogonal to each other.

OA's are available with a variety of factors and levels in the Taguchi method. Since each column is orthogonal to the others, if the results associated with one level of a specific factor are much different at another level, it is because changing that factor from one level to the next has strong impact on the quality characteristic being measured. Since the levels of the other factors are occurring an equal number of times for each level of the strong factor, any effect by these other factors will be ruled out. The Taguchi method apparently has the following strengths:

1. Consistency in experimental design and analysis.
2. Reduction of time and cost of experiments.
3. Robustness of performance without removing the noise factors.

The selection of orthogonal array depends on:

- The number of factors and interactions of interest
- The number of levels for the factors of interest

Taguchi's orthogonal arrays are experimental designs that usually require only a fraction of the full factorial combinations. The arrays are designed to handle as many factors as possible in a certain number of runs compared to those dictated by full factorial design. The columns of the arrays are balanced and orthogonal. This means that in each pair of columns, all factor combinations occur same number of times.

Orthogonal designs allow estimating the effect of each factor on the response independently of all other factors. Once the degrees of freedom are known, the next step, selecting the orthogonal array (OA) is easy. The number of treatment conditions is equal to the number of rows in the orthogonal array and it must be equal to or greater than the degrees of freedom. The interactions to be evaluated will require an even larger orthogonal array. Once the appropriate orthogonal array has been selected, the factors and interactions can be assigned to the various columns.

1(A) --------------- 2(B)

LINEAR GRAPH FOR L18

1 2 3 4

--------- * *

can study interaction 1 X 2

Interaction between any two columns (from 3 - to - 4) is confounded with the remaining columns and cannot be studied

Factor A has been assigned to column 1, factor B to column 2. The connecting line is representing interaction and also the column merged for the purpose. The remaining factor C and D were assigned to column 3 and 4 respectively.

Table: 7.3 L18 Mixed Experimental Design

Trail No:	Slurry Concentration	Abrasive Slurry	Power Rate (%)	Grit Size
1	20	Al_2O_3	20	280
2	20	Al_2O_3	40	400
3	20	Al_2O_3	60	600
4	20	SiC	20	280
5	20	SiC	40	400
6	20	SiC	60	600
7	20	Mixture	20	400
8	20	Mixture	40	600
9	20	Mixture	60	280
10	30	Al_2O_3	20	600
11	30	Al_2O_3	40	280
12	30	Al_2O_3	60	400
13	30	SiC	20	400
14	30	SiC	40	600
15	30	SiC	60	280
16	30	Mixture	20	600
17	30	Mixture	40	280
18	30	Mixture	60	400

To ensure that the abrasive in not settle down on the sump tank, to remove it take a brush and wash out from the sump tank. If abrasive is settled down in the sump tank then it affected the concentration of slurry.

7.7 EXPERIMENTAL SETUP

An experimental set-up having a provision for variation in process parameters was designed and fabricated. The dimension of the tool were decided keeping in view the limitation of the horn shape to economize the machining the machining operation. The Fig:7.1 represent the detailed drawing of the tool.

An electronic balance (Metler, Least count 0.1mg) and stop watch (Least count: 0.01min) were used to determine MRR and TWR. For measuring surface roughness (Pertho meter M4Pi, Least count: 0.01 micron) was used. For repetitions were made for the entire experimentation and corresponding MRR, TWR, SR and hardness. Detail drawing of the tool is shown in the Fig 7.1

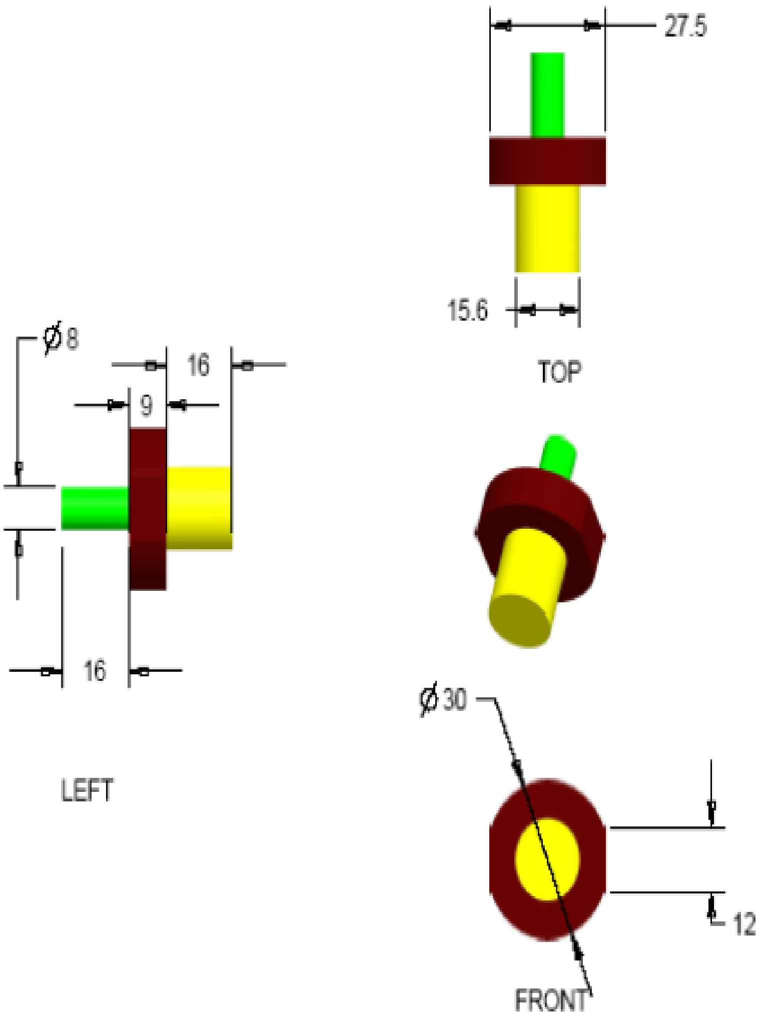

Fig 7.1 Detail Drawing of the tool

7.8 DESCRIPTION OF ULTRASONIC MACHINE

The USM machine tool used for the study is of 500w capacity, which consists of an ultrasonic spindle kit: a constant pressure feed system and slurry flow system. The ultrasonic spindle kit comprises an ultrasonic spindle, mounted with cylinder horn of 25.4mm diameter, a power supply unit. The Fig:7.2 represent the ultrasonic machine tool (type: Sonic mill, USA) used in the experimental work.

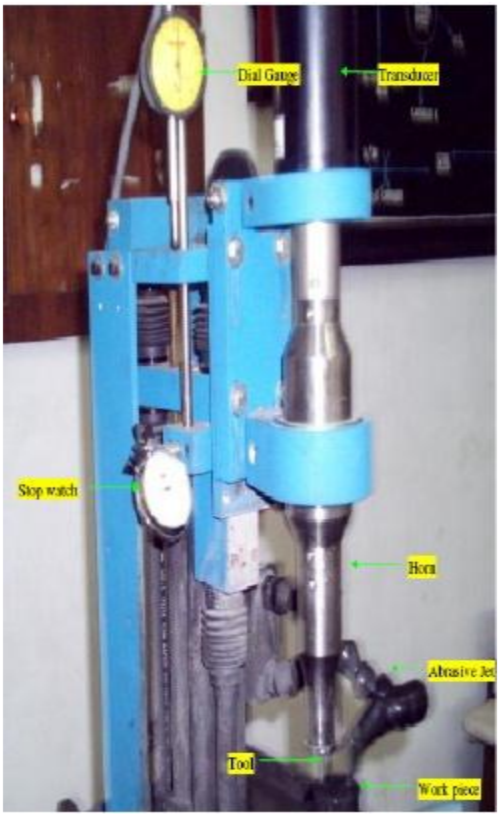

Fig:7.2 Ultrasonic Machine tool
(Type: Sonic Mill, USA)

Fig:7.3 Amplitude coupling for compact
500W Ultrasonic Machine

Fig:7.4 Ultrasonic Transducer for
Compact 500W Ultrasonic Machine

Fig: 7.5 Pump for Re-circulation
of Abrasive slurry

Fig:7.6 Power rating set-up for Ultrasonic machine

Fig:7.7 Ultrasonic Tool

Fig: 7.8 Work-piece after machining

The power supply converts 50 Hz electric supply to high frequency 20 kHz AC output. This is fed to piezoelectric transducer located in the spindle. The transducer converts the electric input into mechanical vibration. The amplitude of vibration is made fixed in range of 0.0253-0.0258 mm with a frequency of 20 kHz +/- 200Hz. The static load for feed rate was fixed at 1.724 kg and slurry flow rate at 30.6 L/min. The replaceable tools used for machining were solid tools having same area of cross-section. The other parts of the experimental set-up, amplitude coupling Fig: 7.3, ultrasonic transducer Fig: 7.4, Pump for re-circulation of abrasive slurry Fig: 7.5, Power rating set-up Fig 7.6, the ultrasonic tool Fig:7.7and, Fig: 7.8.Work-piece after machining are shown.

7.9 MEASURING AND TEST EQUIPMENT USED

MRR was measured using a weighing machine; TWR was also measured using weighing machine. The surface roughness tests conducted on the entire sample. The details of important test equipment used in experiment study are given below.

7.9.1 SURFACE ROUGHNESS TESTER

Surface roughness was measured using the perthometer, modal SJ400 manufactured by Mitutoyo company, available in Metrology lab of Thapar University, Patiala. The equipment uses the stylus method of measurement, has profile resolution of 12 nm, and measure roughness up to 100µm. A tracing length of 4.8mm was used for analysis. Surface roughness of each sample was measured at the centre of the processing piece.

7.9.2 ROCKWELL HARDNESS TESTER

Rockwell Hardness tester was measured the hardness on B type, Indenter is used in the Rockwell Hardness is ball type, Load is applied on the work-piece is 100kgF, Three rotation is given to the initial load three rotation mean 10kgF initial load is apply on the work piece. Unit of the Rockwell Hardness is HRB.

7.10 ANALYSIS OF RESULTs.

Signal-to-noise ratio

The parameters that influence the output can be categorized into two classes, namely controllable (or design) factors and uncontrollable (or noise) factors. Controllable factors are those factors whose values can be set and easily adjusted by the designer. Uncontrollable factors are the sources of variation often associated with operational environment. The best

settings of control factors as they influence the output parameters are determined through experiments. From the analysis point of view, there are three possible categories of the response characteristics explained below.
r is the number of tests in a trial (noise of repetitions regardless of noise levels)

$$\sum_{i=0}^{r} y^2 i = \text{Summation of all response values under each trial} \quad \text{(Equation....7.1)}$$

MSD= Mean square deviation
Y_1= Observed value of the response characteristic
Y_0= nominal or target value of the results

The three different response characteristics are given by the following.

1) ***Higher is Better***. The S/N for higher the better is given by:

$$(\frac{S}{N})_{HB} = -10\log(MSD_{HB}) \quad \text{(Equation....7.2)}$$

$$\text{Where } MSD_{HB} = \frac{1}{r}\sum_{j=1}^{r}(\frac{1}{y_j^2}) \quad \text{(Equation....7.3)}$$

MSDHB = Mean Square Deviation for higher-the-better response.

2) ***Nominal is Better***. The S/N for nominal is better is:

$$(\frac{S}{N})_{HB} = -10\log(MSD_{HB}) \quad \text{(Equation....7.4)}$$

$$\text{Where } MSD_{NB} = \frac{1}{r}\sum_{j=1}^{r}(y_j - y_o)^{\ 2} \quad \text{(Equation....7.5)}$$

3) ***Lower is Better***. In this design situation, response is the type of ‘‘lower is better’’, which is a logarithmic function based on the mean square deviation (MSD), given by

$$(\frac{S}{N})_{HB} = -10\log(MSD_{LB}) = -10\log\frac{1}{r}\sum_{j=1}^{r}(y_i^2) \quad \text{(Equation....7.6)}$$

$$\text{Where } MSD_{LB} = \frac{1}{r}\sum_{j=1}^{r}(y_i^2) \quad \text{(Equation....7.7)}$$

Signal to noise ratio for response characteristics

The parameters that influence the output can be categorized in two categories, controllable factors and uncontrollable factors. The control factors that may contribute to reduced variation can be quickly identified by looking at the amount of variation present in response. The uncontrollable factors are the sources of variation often associated with operational environment. For this experimental work, response characteristics have given in the Table 7.4.

Table 7.4 Response Characteristics

Response Name	Response Type	Units
Material Removal Rate (MRR)	Higher the Better	mm^3/min
Tool Wear Rate (TWR)	Lower the Better	mm^3/min
Rockwell Hardness	Higher the Better	HRB
Surface Roughness	Lower the Better	Micron

Measurement of F-value of Fisher's F ratio

The principle of the F test is that the larger the F value for a particular parameter, the greater the effect on the performance characteristic due to the change in that process parameter. F value is defined as:

F= (MS for a term/ MS for the error term) (Equation....7.8)

Computation of average performance:

Average performance of a factor at certain level is the influence of the factor at this level on the mean response of the experiments.

Analysis of variance

The knowledge of the contribution of individual factors is critically important for the control of the final response. The analysis of variance (ANOVA) is a common statistical technique to determine the percent contribution of each factor for results of the experiment. It calculates parameters known as sum of squares (SS), pure SS, degree of freedom (DOF), variance, F-ratio and percentage of each factor. Since the procedure of ANOVA is a very complicated and employs a considerable of statistical formulae, only a brief description of is given as following.

The Sum of Squares (SS) is a measure of the deviation of the experimental data from the mean value of the data.

Let '*A*' be a factor under investigation

$$SS_T = \sum_{i=1}^{N}(y_i - T)^2 \qquad \text{(Equation....7.9)}$$

Where N = Number of response observations, T is the mean of all observations y_i is the i th response

Factor Sum of Squares (SS_A) - Squared deviations of factor (A) averages from overall average

$$SS_A = [\sum_{i=1}^{k_a}(\frac{A_i^2}{n_{Ai}})] - T^2/N \qquad \text{(Equation....7.10)}$$

Where

Average of all observations under A_i level = A_i/n_{Ai}

T = sum of all observations

T Average of all observations = *T* / *N*

n_{Ai} = Number of observation under A_i level

Error Sum of Squares (SS_e) - Squared deviations of observations from factor (A) averages

$$SS_e = \sum_{j=1}^{k_A}\sum_{i=1}^{n_{Ai}}(y_i - A_j)^2 \qquad \text{(Equation....7.11)}$$

Sum of Squares (SS_{AxB}) for interactions

$$SS_{AxB} = [\sum_{i=1}^{c}(AxB)_i^2/n_{(AxB)i})] - T^2/N - SS_A - SS_B \quad \text{(Equation ....7.12)}$$

Sum of Squares of factors for dummy treatment level

The level symbols for A_1 & $A_{1^{**}}$, both indicate the same test condition w.r.t. factor A.

Therefore

$$SS_A = \frac{(A_1 + A_1^{**})^2}{n_{A1}+n_{A1}^{**}} + \frac{A_2^2}{n_{A2}} - T^2/N \qquad \text{(Equation ....7.13)}$$

$$SS_e = \frac{(A_1 - A_1^{**})^2}{n_{A1}+n_{A1}^{**}} \qquad \text{(Equation ....7.14)}$$

$$SS_{AxB} = [\sum_{i=1}^{c}(AxB)_i^2/n_{(AxB)i})] - T^2/N - SS_A - SS_B - SS_e \quad \text{(Equation ....7.15)}$$

CHAPTER 8

RESULTS AND ANALYSIS OF MRR

8.1 INTRODUCTION

The effect of parameters i.e. concentration, abrasive, power rate and grit size and some other interaction were evaluated using ANOVA and factorial design analysis. A confidence interval of 95% has been used for the analysis. One repetition for each 18 trails was completed to measure the Signal to Noise ratio (S/N Ratio).

8.2 RESULTS FOR MRR

The results for MRR for each of the 18 treatment condition with repetition are given in Table 8.1. MRR of each sample is calculated from weight difference of work-piece before and after the performance trial, which is given by:

$$MRR = \frac{W_i - W_f}{\rho \, X \, t} 1000 \; (mm^3/min) \qquad \text{(Equation....8.1)}$$

Where W_i = Initial weight of work-piece material (gm)

W_f = Final weight of work-piece material (gm)

t = Time period of trails in minutes

ρ = Density of work-piece in gm/cc (2.8 gm/cm^3)

Table 8.1 Result For MRR

Trail No:	Slurry Concentration	Abrasive	Power Rate (%)	Grit Size	MRR mm^3/min	S/N Ratio	Mean
1	20	Al_2O_3	20	280	27.956	28.9295	27.956
2	20	Al_2O_3	40	400	23.821	27.5392	23.821
3	20	Al_2O_3	60	600	22.689	27.1163	22.689
4	20	SiC	20	280	31.899	30.0755	31.899
5	20	SiC	40	400	28.998	29.2474	28.998
6	20	SiC	60	600	25.569	28.1543	25.569
7	20	Mixture	20	400	27.638	28.8301	27.638
8	20	Mixture	40	600	23.256	27.3307	23.256
9	20	Mixture	60	280	29.754	29.4709	29.754
10	30	Al_2O_3	20	600	24.268	27.7007	24.268
11	30	Al_2O_3	40	280	30.195	29.5987	30.195

12	30	Al_2O_3	60	400	26.985	28.6224	26.985
13	30	SiC	20	400	34.052	30.6429	34.052
14	30	SiC	40	600	31.032	29.8362	31.032
15	30	SiC	60	280	36.506	31.2473	36.506
16	30	Mixture	20	600	21.469	26.6362	21.469
17	30	Mixture	40	280	29.654	29.4417	29.654
18	30	Mixture	60	400	34.654	30.7951	34.654

8.3 ANALYSIS OF VARIANCE –MRR

The result of MRR was analyzed using ANOVA for identifying the significant factor affecting the performance measure. The analysis of variance (ANOVA) for the mean MRR at 80.167% confidence interval is given in Table 8.2. The various data for each factor and their interaction was P value find for the significant of each. The principal of the P value is that the value less than 0.05 that factors or interactions are significant if value is more than 0.05 then that factors or interactions are insignificant. From the ANOVA table for mean we see it Concentration P value is 0.013, Abrasive P value is 0.003, Power Rate P value is 0.041 and Grit Size P value is 0.001 these factors are significant, same concentration and Power rate interaction P value is more than 0.05 so that these are insignificant. In the table 8.3 the ranks are show for the different factor. 1^{st} rank is given to the grit size that mean grit size has the highest contribution to MRR. 2^{nd} rank is give to the type of abrasive, 3^{rd} rank is given to the power rate and the 4^{th} rank is given to the Concentration that mean power rate have the minimum contribution to the MRR.

Table 8.2 ANOVA for MRR

Source	DOF	Seq SS	Adj MS	F	P	SS'	% Contribution	Status
Concentration,A	1	37.66	37.657	10.26	0.013	36.551	9.148	Significant
Abrasive, B	2	94.03	47.015	12.82	0.003	91.812	22.979	Significant
Power Rate, C	2	35.88	17.940	4.89	0.041	33.662	8.205	Significant
Grit Size, D	2	191.54	79.691	21.72	0.001	189.322	47.381	Significant
A x C	2	11.09	5.544	1.51	0.278	8.872	2.2205	Insignificant
Residual Error	8	29.35	3.669	--	--	--	---	---
Total	17	399.54	--	--	--	--	---	---
e-Pooled	10	11.09	1.109	--	--	--	12.283	---

Table 8.3 Response table for means of MRR

Level	Concentration	Abrasive	Power Rate	Grit Size
1	27.06	25.49	28.79	31.75
2	29.96	31.01	26.66	29.73
3	---	29.04	30.08	24.05
Delta	2.89	5.52	3.42	7.70
Rank	4	2	3	1

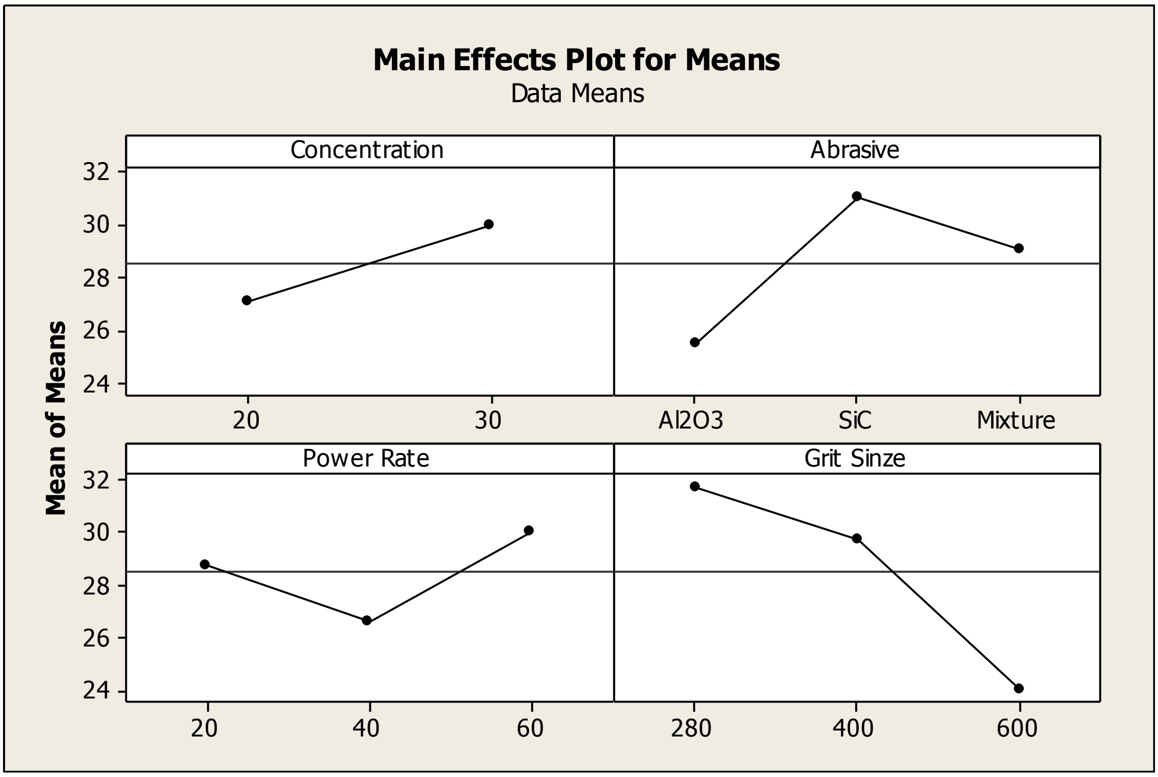

Fig:8.1 Main effects plot of MRR for means

In fig: 8.1 we see it the MRR is more of 30% concentration as compare to 20% concentration. From the Aluminium Oxide, Silicon Carbide and Mixture (Aluminium Oxide + Silicon Carbide) slurry Silicon Carbide have the more effect on the MRR and the Mixture (Aluminium Oxide + Silicon Carbide) have some less effect and the Aluminium Oxide have the less effect on MRR. There are three power rate 20, 40 and 60 the maximum effective is 60, similarly the grit size 280 grit size give the maximum MRR the 400 give some less and 600 grit size give minimum MRR.

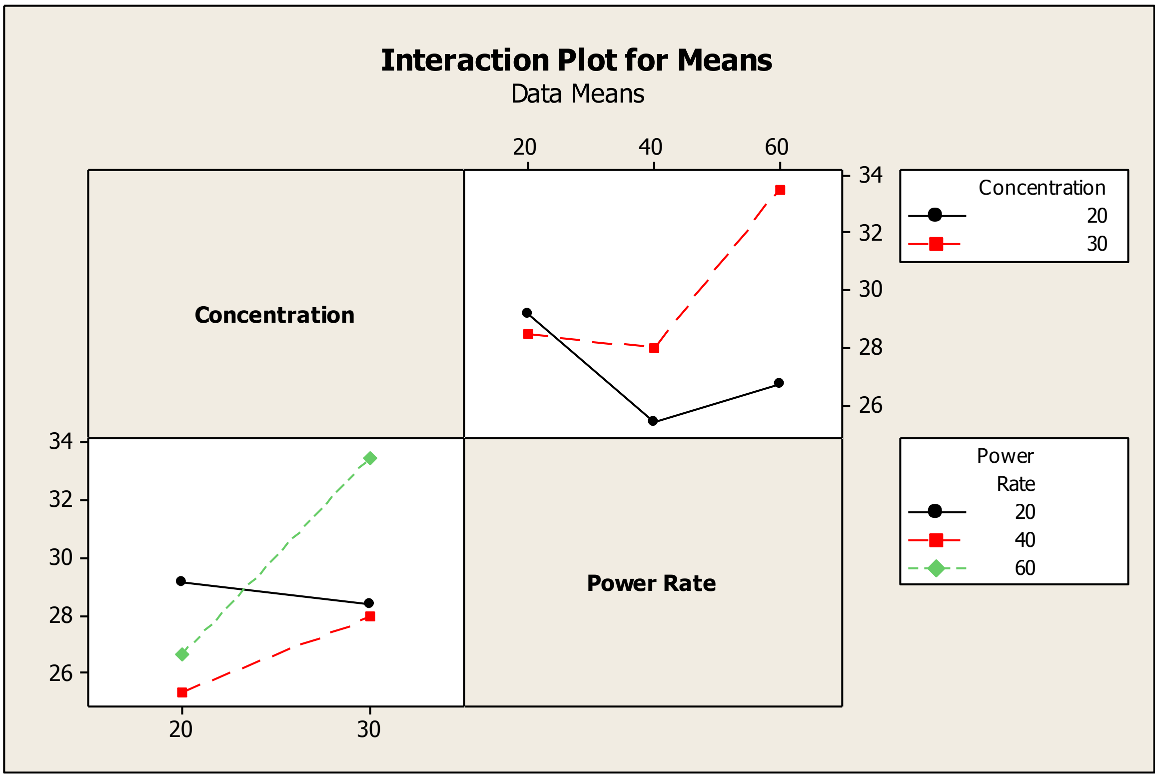

Fig: 8.2 Interaction plot for MRR

8.4 RESULTS FOR S/N RATIO OF MRR

The S/N ratio consolidates several repetitions into one value and is an indication of the amount of variation present. The S/N ratios have been calculated to identify the major contributing factors and interactions that cause variation in the MRR. MRR is "Higher is better" type response which is given by:

$$(\frac{S}{N})_{HB} = -10\log(MSD_{HB}) \qquad \text{(Equation....8.2)}$$

$$\text{Where } MSD_{HB} = \frac{1}{r}\sum_{j=1}^{r}(\frac{1}{y_j^2}) \qquad \text{(Equation....8.3)}$$

MSD_{HB} = Mean Square Deviation for higher-the-better response.

Table 8.4 shows the ANOVA results for S/N ratio of MRR at 95% confidence interval. Concentration, Abrasive Power Rate Grit Size p value is less the 0.05 so these are significant and AxC is in significant. Main effects plot and interaction plot of S/N ratio for MRR are shown in the figure 8.3 and 8.4 respectively.

Table 8.4 ANOVA for S/N Ratio of MRR

Source	DOF	Seq SS	Adj MS	F	P	SS,	% Contribution	Status
Concentration,A	1	3.0354	3.0354	11.46	0.010	2.7694	7.9091	Significant
Abrasive, B	2	8.2160	4.1080	15.51	0.002	7.6720	21.957	Significant
Power Rate, C	2	2.6901	1.3450	5.08	0.038	2.1461	6.1423	Significant
Grit Size, D	2	18.2781	7.3070	27.59	0.000	17.7341	50.756	Significant
A x C	2	0.6012	0.3006	1.13	0.368	0.0572	0.1637	Insignificant
Residual Error	8	2.1189	0.2649	--	--	--	---	---
Total	17	34.9396	--	--	--	--	---	---
e-Pooled	10	2.7201	0.2720	--	--	--	13.2353	---

Table 8.5 Response table for S/N ratio of MRR

Level	Concentration	Abrasive	Power Rate	Grit Size
1	28.58	28.08	29.08	29.98
2	29.40	29.70	28.47	29.37
3	--	29.18	29.40	27.61
Delta	0.82	1.62	0.93	2.38
Rank	4	2	3	1

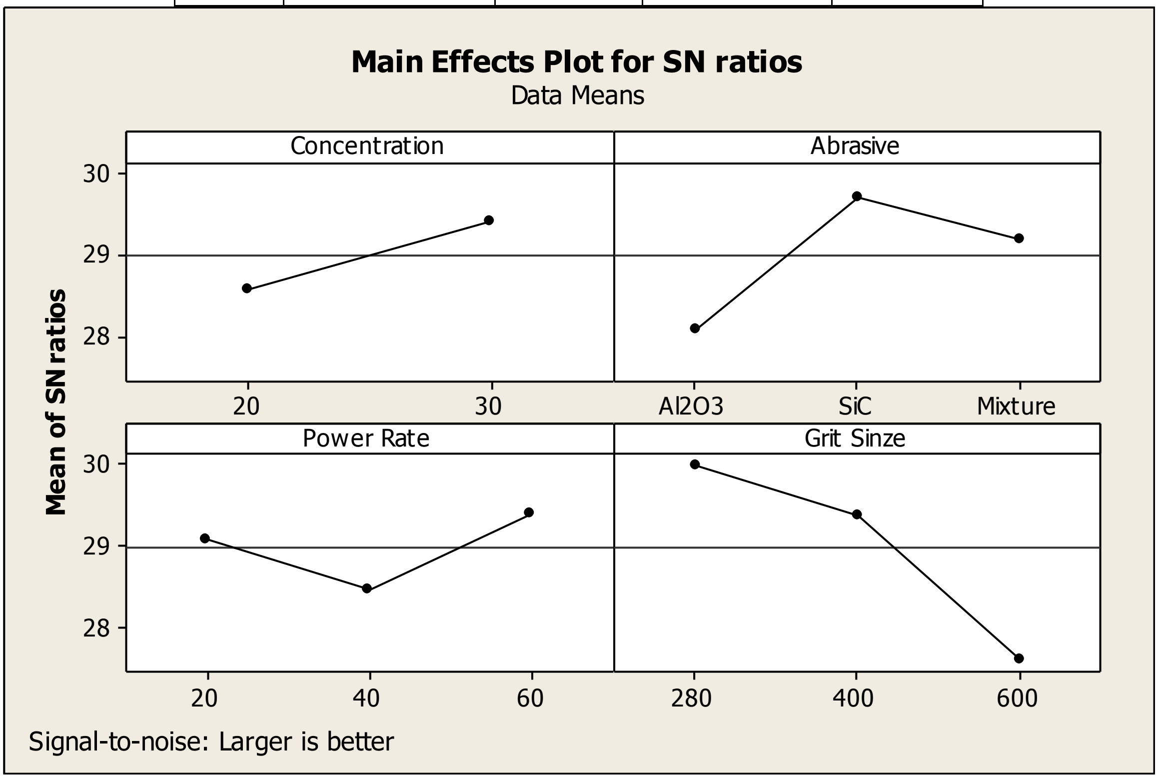

Fig: 8.3 Main effects plot for MRR of S/N ratio

In fig: 8.3 we see it the MRR is more of 30% concentration as compare to 20% concentration. From the Aluminium Oxide, Silicon Carbide and Mixture (Aluminium Oxide + Silicon Carbide) slurry Silicon Carbide have the more effect on the MRR and the Mixture (Aluminium Oxide + Silicon Carbide) have some less effect and the Aluminium Oxide have the less effect on MRR. There are three power rates 20, 40 and 60 the maximum effective is 60, similarly the grit size 280 grit sizes give the maximum MRR the 400 give some less and 600 grit sizes give minimum MRR.

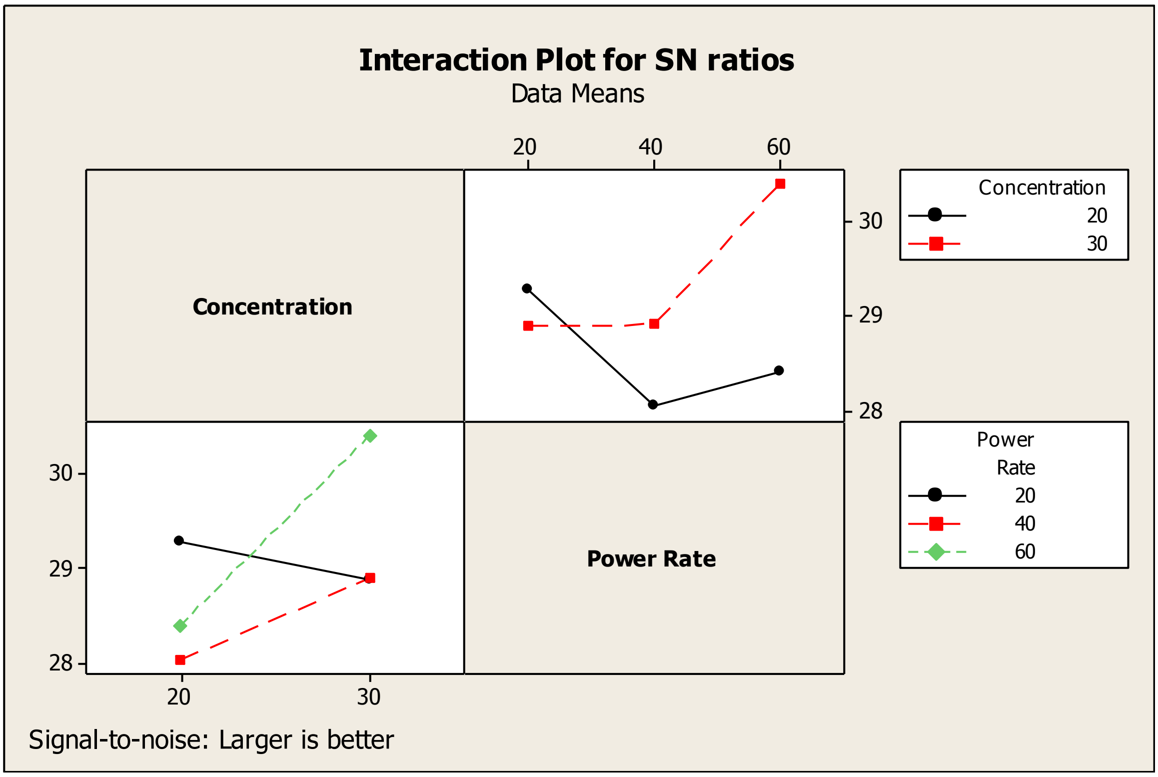

Fig;8.4 Interaction plot for MRR of S/N ratio

8.5 OPTIMAL DESIGN FOR MRR

The same level of all the significant factors provide a higher mean value and reduced variability so nothing has to be compromised. The level of factors which improves average and uniformity may conflict, so a compromise may have to be reached. Also a compromise has to occur when multiple responses are considered and the same factor level may cause one response to improve and other to deteriorate.

In this experiment analysis, the main effect plot and interaction plot in Fig: 8.1 and Fig: 8.2 used to estimate the mean MRR. From the table:8.6 it is concluded that highest MRR was observed when work-piece is machined on concentration 30%, abrasive Silicon Carbide, Power Rate 60 and Grit Size 280. It also observes that the interaction AxC is not any effect on the MRR. The best MRR value was compromised to get best results. MRR Assumed to be achieved best result if Glass work piece is machined at concentration 30% of abrasive and water slurry, abrasive Silicon Carbide, Power Rate 60 and Grit Size 280.

Table 8.6 Significant factor and interaction

Factor	Affecting Mean		Affecting Variation	
	Contribution	Best Level	Contribution	Best Level
Concentration,A	Significant	Level-2(30%)	Significant	Level-2(30%)
Abrasive, B	Significant	Level-2(SiO)	Significant	Level-2(SiO)
Power Rate, C	Significant	Level-3(60)	Significant	Level-3(60)
Grit Size, D	Significant	Level-1(280)	Significant	Level-1(280)
A x C	Insignificant	---	Insignificant	---

Estimating the mean

In experimental analysis, the MRR is a higher average response is better (HB) characteristic. Depending on the characteristic, different treatment combinations has chosen to obtain satisfactory results. After conducting the experiments the optimum treatment condition within the experiments determined on the basis of prescribed combination of factor levels is determined to one of those in the experiment.

Mean Value for MRR

$$\mu_{A_2B_2C_3D_1} = A_2 + B_2 + C_3 + D_1 - 4T \qquad \text{(Equation....8.4)}$$

$$= 29.96 + 29.04 + 30.08 + 31.75 - 3 \times 28.35 = 35.78 \text{ mm}^3/\text{min}$$

Confidence Interval around the Estimated Mean

The confidence interval is a maximum and minimum value between which the true average should fall at some stated percentage of confidence. The estimate of the mean μ is only a point estimate based on the averages of results obtained from the experiment. Statistically this provides a 50% chance of the true averages being greater than μ and a 50% chance of the true average being less than μ .

Confidence Interval around the estimated MRR mean

$$CI_1 = \sqrt{(F_{\alpha,V_1,V_2} V_e)/n_{eff}}$$

Where $F_{\alpha V_1 V_2}$ = F ratio

α = Risk (0.01) Confidence = 1- α

V_1 = DOF for mean which is always = 1

V_2 = DOF for error = Ve

η_{eff} = Number of tests under that condition using the participating factors

η_{eff} = (N/ 1+ $DOF_{A2B2C3D1}$) = 18/ 1+1+2+2+2 = 2.25

$$CI_1 = \sqrt{\frac{4.512\ X\ 5.54}{2.25} = 1.5}$$

So the confidence interval around the MRR is given by 35.78 ± 1.5 mm^3/min.

CHAPTER 9

RESULT AND ANALYSIS OF TWR

9.1 INTRODUCTION

The effects of parameters i.e. Concentration, Abrasive, Power Rate and Grit Size and the interaction between Concentration and Power Rate were evaluated using ANOVA analysis. A confidence interval of 95% has been used for the analysis. One repetition for each of 18 trails was completed to measure the Signal to Noise ratio(S/N Ratio).

9.2 RESULTS FOR TWR

The results for TWR for each of the 18 treatment conditions with repetition are given in Table 9.1. The TWR is calculated from the weight difference of Tool before and after the performance trial, which is given by:

$$TWR = \frac{T_i - T_f}{\rho\, X\, t}\, 1000\ (mm^3/min) \qquad \text{(Equation....9.1)}$$

Where T_i = Initial weight of Tool material (gm)

T_f = Final weight of Tool material (gm)

t = Time period of trails in minutes

ρ = Density of Tool in gm/cc (7.8 gm/cm^3)

Table 9.1 Results for TWR

Trail No:	Slurry Concentration	Abrasive	Power Rate (%)	Grit Size	MRR mm^3/min	S/N Ratio	Mean
1	20	Al_2O_3	20	280	0.2860	10.8727	0.2860
2	20	Al_2O_3	40	400	0.2620	11.6340	0.2620
3	20	Al_2O_3	60	600	0.2503	12.0308	0.2503
4	20	SiC	20	280	0.3902	8.1743	0.3902
5	20	SiC	40	400	0.3350	9.4991	0.3350
6	20	SiC	60	600	0.3540	9.0199	0.3540
7	20	Mixture	20	400	0.3199	9.8997	0.3199
8	20	Mixture	40	600	0.3630	8.8019	0.3630
9	20	Mixture	60	280	0.3902	8.1743	0.3902
10	30	Al_2O_3	20	600	0.2452	12.2096	0.2452
11	30	Al_2O_3	40	280	0.2869	10.8454	0.2869

12	30	Al_2O_3	60	400	0.3181	9.9487	0.3181
13	30	SiC	20	400	0.4098	7.7486	0.4098
14	30	SiC	40	600	0.3690	8.6595	0.3690
15	30	SiC	60	280	0.4915	6.1695	0.4915
16	30	Mixture	20	600	0.3452	9.2386	0.3452
17	30	Mixture	40	280	0.4301	7.3286	0.4301
18	30	Mixture	60	400	0.3805	8.3929	0.3805

9.3 ANALYSIS OF VARIANCE TWR

The result of MRR was analyzed using ANOVA for identifying the significant factor affecting the performance measure. The analysis of variance (ANOVA) for the mean MRR at 82.35% confidence interval is given in Table 9.2. The various data for each factor and their interaction was P value find for the significant of each. The principal of the P value is that the value less than 0.05 that factors or interactions are significant if value is more than 0.05 then that factors or interactions are insignificant. From the ANOVA table for mean we see it Concentration P value is 0.014, Abrasive P value is 0.001 and Grit Size P value is 0.013 these factors are significant, same Power rate and concentration and Power rate (AxC) interaction P value is more than 0.05 so that these are insignificant. In the table 9.3 the ranks are show for the different factor. 1st rank is given to the type of Abrasive that mean grit size has the highest contribution to TWR. 2nd rank is give to the Grit Size, 3rd rank is given to the Concentration and the 4th rank is given to the Power rate that mean power rate have the minimum contribution to the TWR.

Table 9.2 ANOVA for TWR

Source	DOF	Seq SS	Adj MS	F	P	SS'	% Contribution	Status
Concentration,A	1	0.00589	0.00589	9.69	0.014	0.0051	7.22640	Significant
Abrasive, B	2	0.04682	0.02341	38.49	0.001	0.0456	62.1745	Significant
Power Rate, C	2	0.00317	0.00158	2.61	0.134	-0.003	---	Insignificant
Grit Size, D	2	0.01073	0.00472	7.77	0.013	0.0095	12.9530	Significant
A x C	2	0.00184	0.00092	1.52	0.276	-0.001	---	Insignificant
Residual Error	8	0.00486	0.00060	--	--	--	---	---
Total	17	0.07334	--	--	--	--	---	---
e-Pooled	4	0.0099	0.00247	--	--	--	17.6461	---

Table 9.3 Response table for means of TWR

Level	Concentration	Abrasive	Power Rate	Grit Size
1	0.3278	0.2747	0.3327	0.3791
2	0.3640	0.3916	0.3410	0.3376
3	--	0.3715	0.3641	0.3211
Delta	0.0362	0.1168	0.0314	0.0580
Rank	3	1	4	2

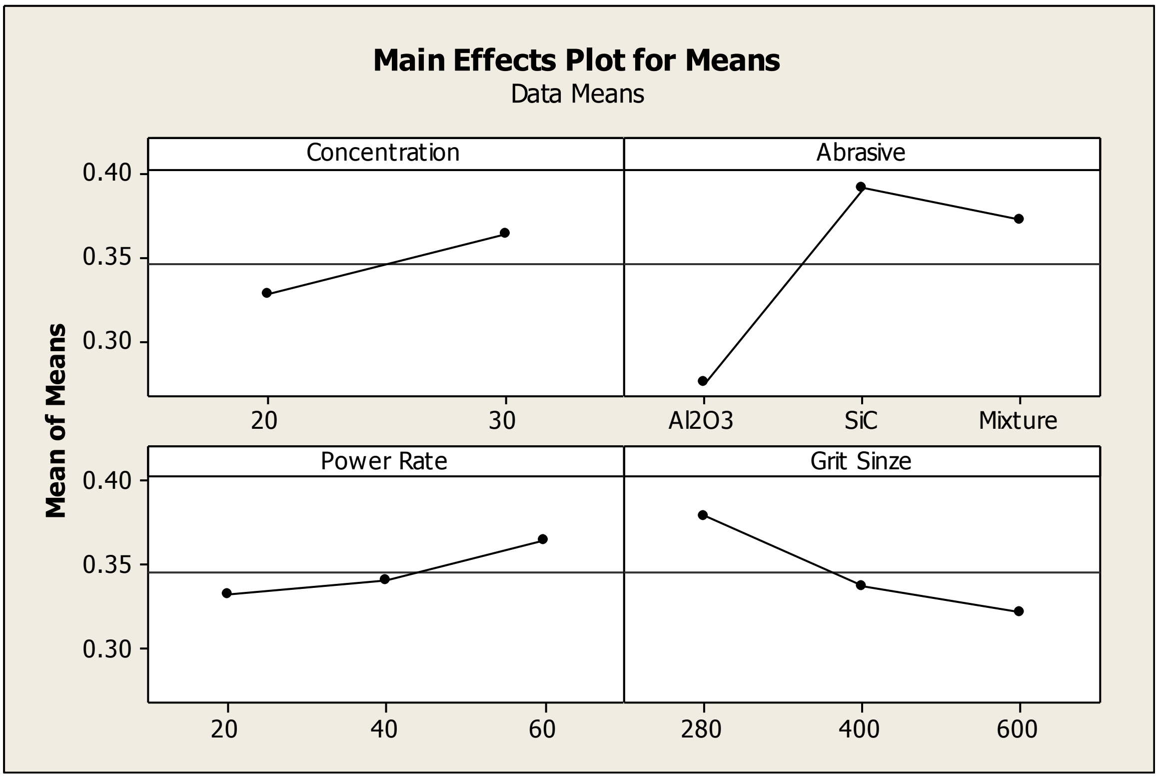

Fig 9.1 Main effect plot of TWR for mean

In fig: 9.1 we see it the TWR is more of 30% concentration as compare to 20% concentration. From the Aluminium Oxide, Silicon Carbide and Mixture (Aluminium Oxide + Silicon Carbide) slurry Silicon Carbide have the more effect on the TWR and the Mixture (Aluminium Oxide + Silicon Carbide) have some less effect and the Aluminium Oxide have the less effect on TWR. There are three power rate 20, 40 and 60 the maximum effective is 60, similarly the grit size 280 grit size give the maximum TWR the 400 give some less and 600 grit size give minimum TWR.

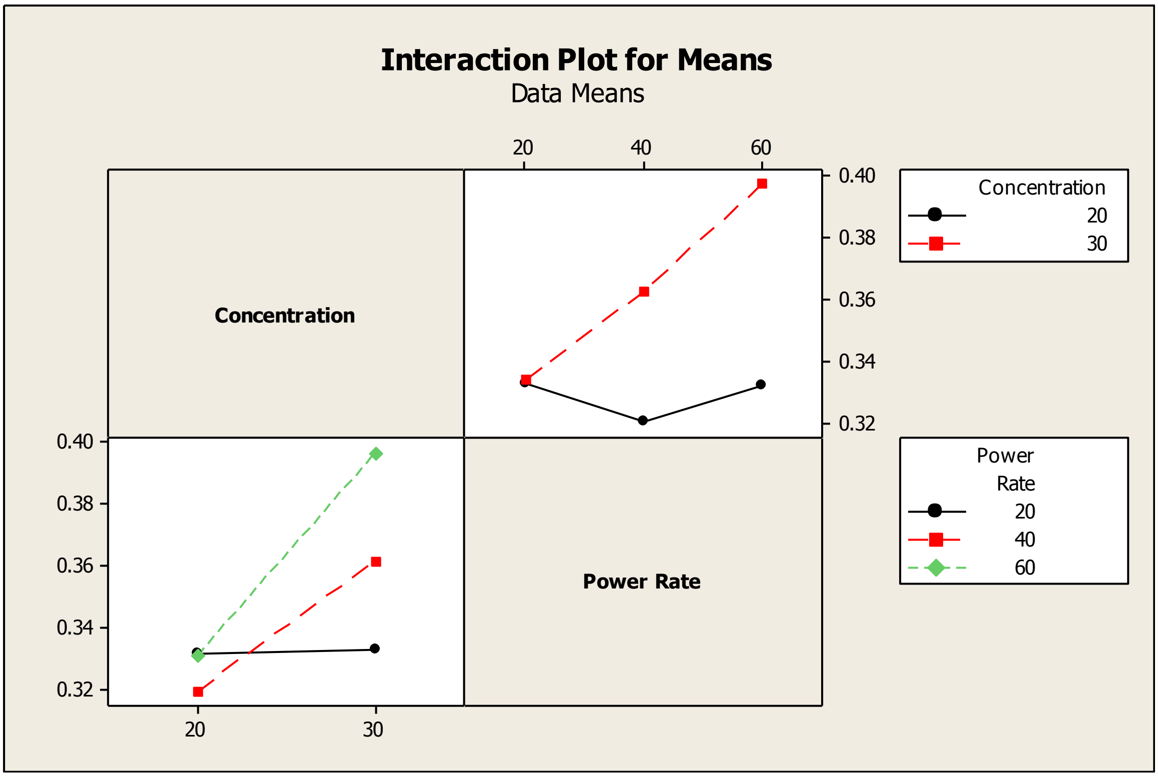

Fig 9.2 Interaction Plot for TWR

9.4 ANOVA FOR S/N RATIO FOR TWR

The S/N ratio consolidates several repetitions into one value and is an indication of the amount of variation present. The S/N ratios have been calculated to identify the major contributing factors and interactions that cause variation in the TWR. TWR is 'Lower is better' type response which is given by:

$$(\frac{S}{N})_{HB} = -10\log(MSD_{LB}) = -10\log\frac{1}{r}\sum_{j=1}^{r}(y_i^2) \quad \text{(Equation....9.2)}$$

$$\text{Where } MSD_{LB} = \frac{1}{r}\sum_{j=1}^{r}(y_i^2) \quad \text{(Equation....9.3)}$$

Table 9.4 shows the ANOVA results for S/N ratio of MRR at 95% confidence interval. Concentration, Abrasive Power Rate Grit Size p value is less the 0.05 so these are significant and AxC is in significant. Main effects plot and interaction plot of S/N ratio for TWR are shown in the figure 9.3 and 9.4 respectively.

Table 9.4 ANOVA for S/N ratio of TWR

Source	DOF	Seq SS	Adj MS	F	P	SS’	% Contribution	Status
Concentration,A	1	3.1796	3.1796	9.10	0.017	1.9353	4.1040	Significant
Abrasive, B	2	32.6131	16.3066	46.66	0.001	30.1245	63.881	Significant
Power Rate, C	2	1.6950	0.8475	2.42	0.150	-1.149	---	Insignificant
Grit Size, D	2	6.0794	2.3678	6.77	0.019	3.5908	7.6146	Significant
A x C	2	0.7960	0.3968	1.14	0.368	-2.391	---	Insignificant
Residual Error	8	2.7960	0.3495	--	--	--	---	---
Total	17	47.1567	--	--	--	--	---	---
e-Pooled	4	5.2870	1.5938	--	--	--	24.4004	---

Table 9.5 Response table for S/N ratio of TWR

Level	Concentration	Abrasive	Power Rate	Grit Size
1	9.790	11.257	9.691	8.594
2	8.949	8.212	9.461	9.520
3	--	8.639	8.956	9.993
Delta	0.841	3.045	0.735	1.399
Rank	3	1	4	2

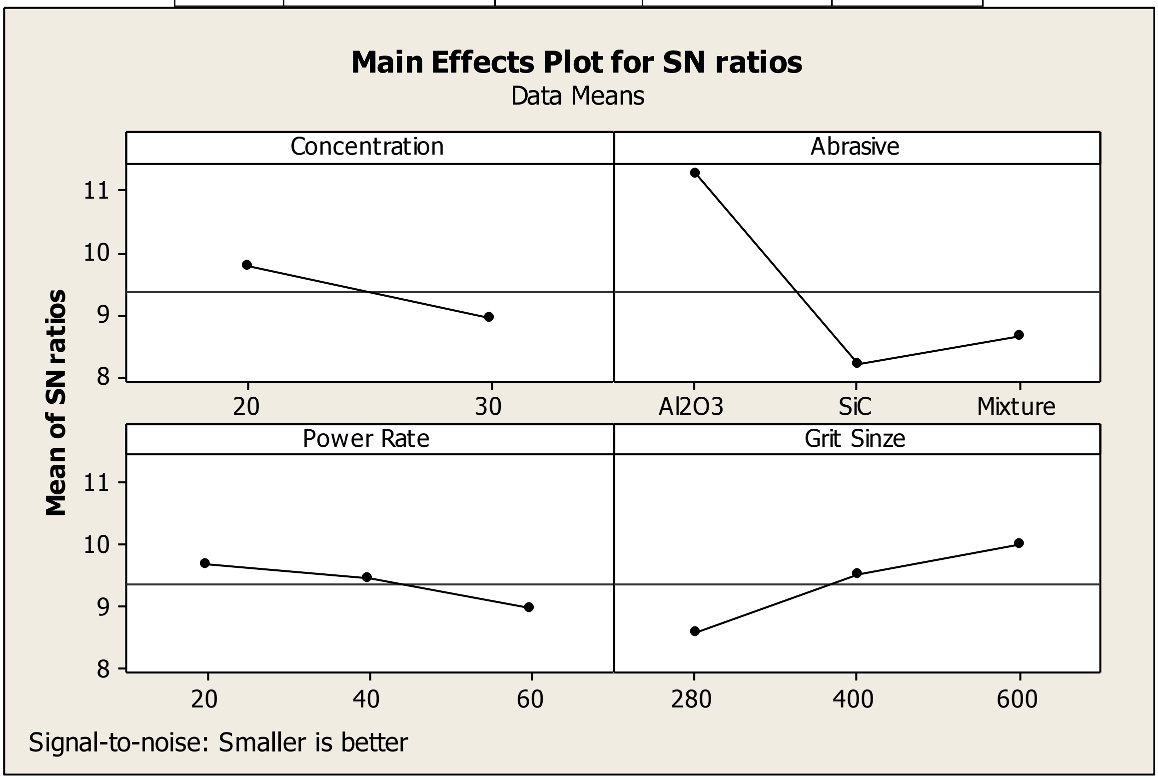

Fig 9.3 Main effects plot of TWR for S/N ratio

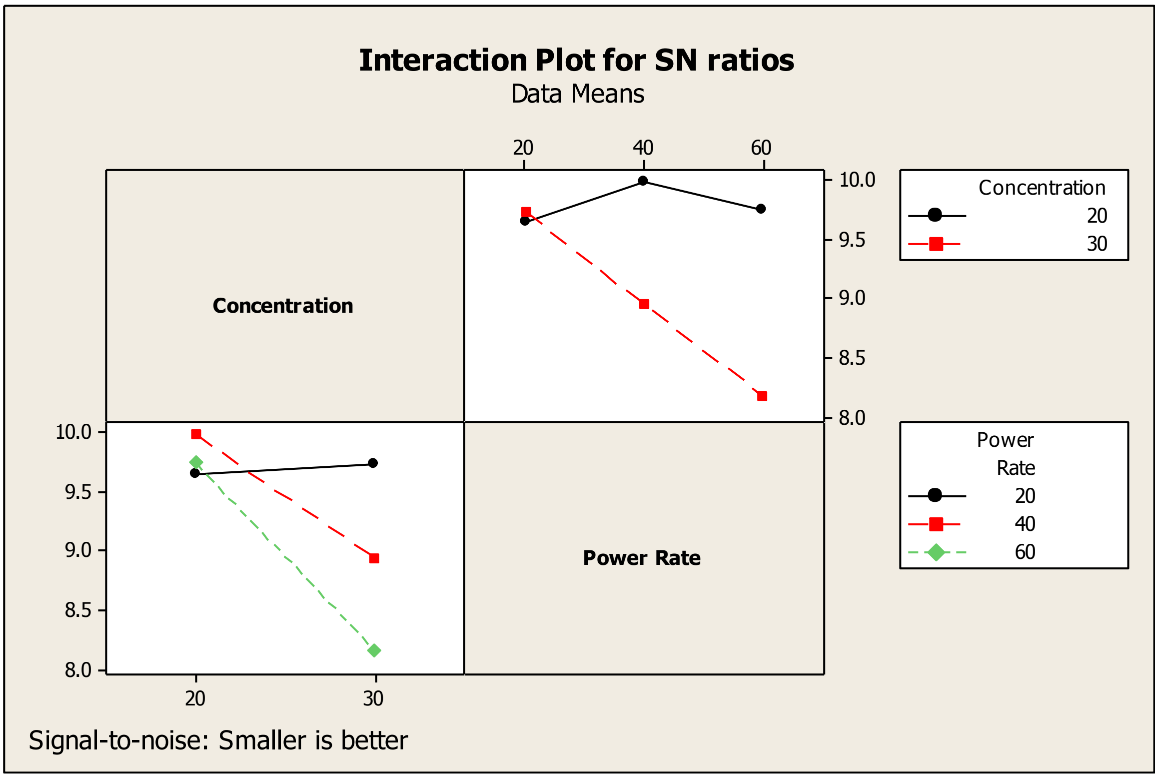

Fig:9.4 Interaction plot of TWR for S/N ratio

9.5 OPTIMAL DESIGN FOR TWR

In this experimental analysis, the main effect plot and interaction plot in Figure 9.1 and Figure 9.2 used to estimate the mean TWR. From the, Table 9.6 it is concluded that the lowest TWR was to be observed when work-piece was machined with Concentration 30% Abrasive Silicon Carbide and Grit Size 280. In S/N ratio highest TWR was to be observed when work-piece material was machined with Concentration 20%, Abrasive Aluminium Oxide and Grit Size 600.

Table 9.6 Significant factors and interactions

Factor	Affecting Mean		Affecting Variation	
	Contribution	Best Level	Contribution	Best Level
Concentration,A	Significant	Level-1 (30%)	Significant	Level-1(20%)
Abrasive, B	Significant	Level-2 (SiO)	Significant	Level-1(Al_2O_3)
Power Rate, C	Insignificant	---	Insignificant	---
Grit Size, D	Significant	Level-1(280)	Significant	Level-3(600)
A x C	Insignificant	---	Insignificant	---

Estimating the mean foe TWR

In experimental analysis, the TWR is a lower average response is better (LB) characteristic. Depending on the characteristic, different treatment combinations has chosen to obtain satisfactory results. After conducting the experiments the optimum treatment condition within the experiments determined on the basis of prescribed combination of factor levels was determined to one of those in the experiment.

Mean Value for TWR

$$\mu_{A_1B_2D_1} = A_1 + B_2 + D_1 - 3T \qquad \text{(Equation....9.4)}$$

Confidence Interval around the Estimated Mean

The confidence interval is a maximum and minimum value between which the true average should fall at some stated percentage of confidence. Confidence Interval around the estimated TWR mean

$$CI_1 = \sqrt{(F_{\alpha,V_1,V_2} V_e)/n_{eff}}$$

Where $F_{\alpha V1V2}$ = F ratio

α = Risk (0.01) Confidence = 1- α

V_1 = DOF for mean which is always = 1

V_2 = DOF for error = Ve

η_{eff} = Number of tests under that condition using the participating factors

η_{eff} = (N/ 1+ DOF_{A1B2D1}) = 18/ 1+1+2+2 = 3.00

$$CI_1 = \sqrt{\frac{4.585\ X\ 0.0008}{3.00}} = 0.0381$$

So the confidence interval around the TWR is given by 0.0970±0.0381mm^3/min.

CHAPTER 10

RESULT AND ANALYSIS OF SURFACE ROUGHNESS

10.1 INTRODUCTION

The effects of parameters i.e. Concentration, Abrasive, Power Rate and Grit Size and the interaction between Concentration and Power Rate were evaluated using ANOVA analysis. A confidence interval of 95% has been used for the analysis. One repetition for each of 18 trails was completed to measure the Signal to Noise ratio(S/N Ratio). In this experiment work surface roughness (Ra) has measured at position center.

10.2 RESULTS OF SURFACE ROUGHNESS

Table 10.1 Results for Surface Roughness

Trail No:	Slurry Concentration	Abrasive	Power Rate (%)	Grit Size	MRR mm^3/min	S/N Ratio	Mean
1	20	Al_2O_3	20	280	0.55	5.19275	0.55
2	20	Al_2O_3	40	400	0.70	3.09804	0.70
3	20	Al_2O_3	60	600	1.08	-0.66848	1.08
4	20	SiC	20	280	1.15	-1.21396	1.15
5	20	SiC	40	400	1.24	-1.86843	1.24
6	20	SiC	60	600	1.52	-3.63687	1.52
7	20	Mixture	20	400	0.99	0.08730	0.99
8	20	Mixture	40	600	1.41	-2.98438	1.41
9	20	Mixture	60	280	1.09	-0.74853	1.09
10	30	Al_2O_3	20	600	0.98	0.17548	0.98
11	30	Al_2O_3	40	280	1.02	-0.17200	1.02
12	30	Al_2O_3	60	400	1.01	-0.08643	1.01
13	30	SiC	20	400	1.24	-1.86843	1.24
14	30	SiC	40	600	1.63	-4.24375	1.63
15	30	SiC	60	280	1.48	-3.40523	1.48
16	30	Mixture	20	600	1.49	-3.46373	1.49
17	30	Mixture	40	280	1.30	-2.27887	1.30
18	30	Mixture	60	400	1.62	-4.19030	1.62

The results for surface roughness were analyzed using ANOVA for identifying the significant factors affecting the performance measures. ANOVA for the mean surface roughness at 95% confidence interval is given in Table 10.2. The Concentration, Power Rate, Type of Abrasive (Aluminium Oxide, Silicon Carbide and Mixture) is input parameters which affects the surface roughness. Main effect plots had shown in the Figure 10.1 shows that the surface roughness increases with increase in the Concentration, Power Rate, Abrasive and Grit Size.

10.3 ANALYSIS OF VARIANCE SURFACE ROUGHNESS

The work-piece material also affects the surface roughness. Table 10.3 shows ranks to various input parameters in terms their relative significance. 1st rank is given to Abrasive slurry, 2nd rank is given to Grit Size, 3rd Rank is given to Power Rate and 4th rank is given to Concentration.

Table 10.2 ANOVA for Surface Roughness

Source	DOF	Seq SS	Adj MS	F	P	SS'	% Contribution	Status
Concentration,A	1	0.2312	0.23120	30.54	0.002	0.2238	14.4813	Significant
Abrasive, B	2	0.8449	0.42248	55.80	0.001	0.8302	53.7193	Significant
Power Rate, C	2	0.1677	0.08388	11.08	0.005	0.1530	9.9001	Significant
Grit Size, D	2	0.2261	0.10465	13.82	0.003	0.2114	13.6790	Significant
A x C	2	0.0147	0.00738	0.98	0.418	-0.002	---	Insignificant
Residual Error	8	0.0605	0.00757	--	--	--	---	---
Total	17	1.5454	--	--	--	--	---	---
e-Pooled	10	0.0753	0.0075	--	--	--	8.2203	---

Table 10.3 Response table for means of Surface Roughness

Level	Concentration	Abrasive	Power Rate	Grit Size
1	1.0811	0.8900	1.0667	1.0983
2	1.3078	1.3767	1.2167	1.1333
3	--	1.3167	1.3000	1.3517
Delta	0.2267	0.4867	0.2333	0.2533
Rank	4	1	3	2

In the Table 10.2 Concentration, Abrasive (Aluminium Oxide, Silicon Carbide and Mixture), Power Rate, Grit Size have P value is less than 0.005 that means these are significant and interaction AxC is more than 0.005 that means it is insignificant. From Table 10.3 we see it 1st rank is given to the Abrasive that mean it have high contribution in the Surface Roughness, 2nd rank is given to Grit Size, 3rd rank is given to Power Rate and 4th rank is given to concentration that mean it have less contribution in the Surface Roughness.

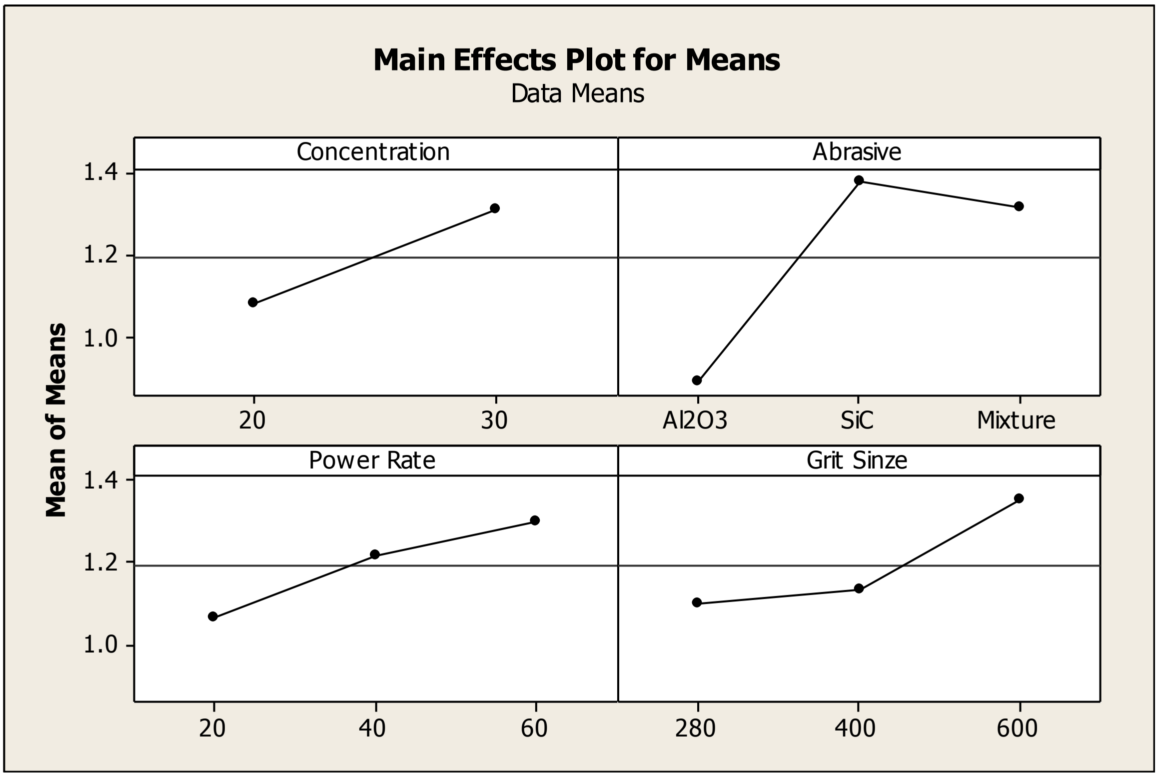

Fig: 10.1 Main effects plot for surface roughness

Figure 10.1 is shows that Surface roughness is maximum on 30% concentration, and Silicon gives the better Surface Roughness. From 20, 40 and 60 power rate maximum Surface Roughness given by the 60, and from 280, 400 and 600 grit size of abrasive 600 grit size give the good surface roughness.

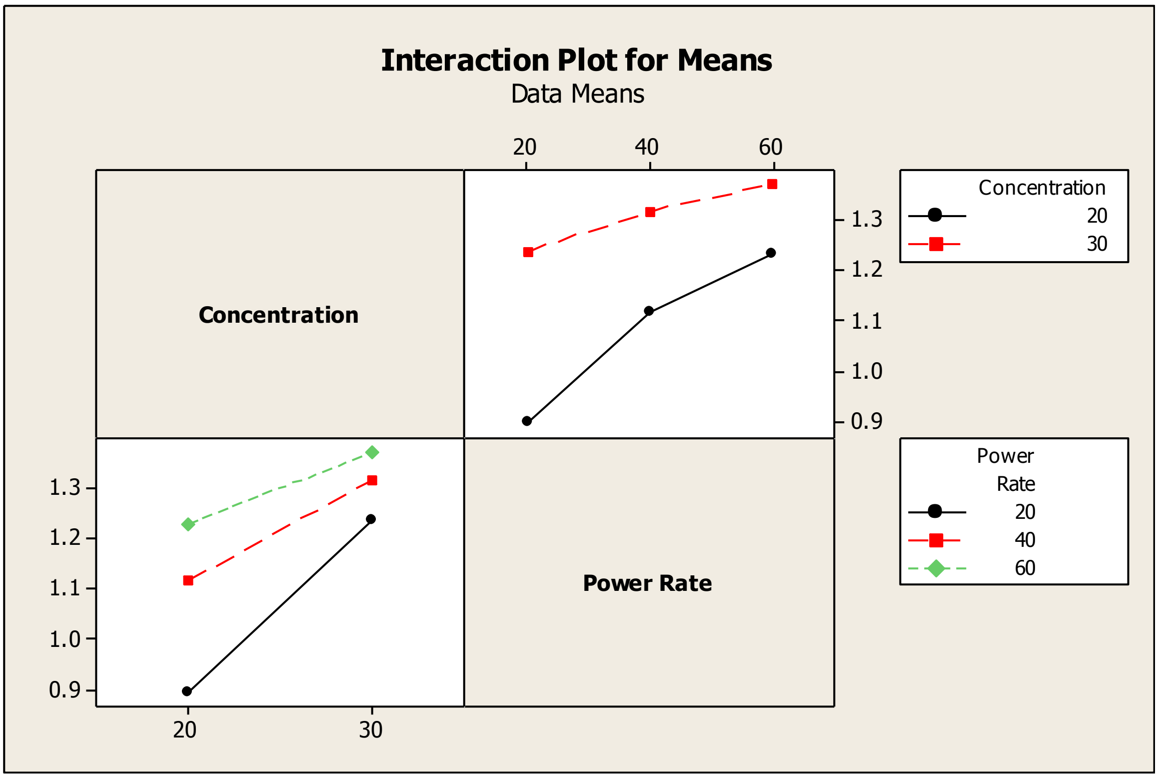

Fig 10.2 Interaction plot surface roughness

10.4 ANOVA FOR S/N RATIO FOR SURFACE ROUGHNESS (Ra)

The S/N ratio several repetitions into one value which reflects the amount of variation present. The values of all the results according to Taguchi array parameter design layout are presented in this section. The S/N ratios have been calculated to identify the major contributing factors and interactions for variation in the roughness values at position Center In this design Surface roughness is the type of 'lower is better', which is a logarithmic function based on the mean square deviation (MSD), given by

$$(\frac{S}{N})_{HB} = -10\log(MSD_{LB}) = -10\log\frac{1}{r}\sum_{j=1}^{r}(y_i^2) \quad \text{(Equation....10.1)}$$

$$\text{Where } MSD_{LB}= \frac{1}{r}\sum_{j=1}^{r}(y_i^2) \quad \text{(Equation....10.2)}$$

Table 7.4 shows the ANOVA for S/N ratio for roughness at 87.32% confidence interval. Among all the factors Concentration, Power Rate, Abrasive and Grit Size are significant factor. Abrasive has most significant which has highest contribution in roughness. The interaction between Concentration and Power Rate is insignificant.

Table 10.4 ANOVA for S/N ratio of TWR

Source	DOF	Seq SS	Adj MS	F	P	SS'	% Contribution	Status
Concentration,A	1	15.663	15.6626	17.75	0.003	14.7808	14.0741	Significant
Abrasive, B	2	56.574	28.2870	32.06	0.001	54.8096	52.1892	Significant
Power Rate, C	2	11.563	5.7816	6.55	0.021	9.7986	9.3301	Significant
Grit Size, D	2	14.081	5.2158	5.91	0.027	12.3166	11.7277	Significant
A x C	2	0.083	0.0413	0.05	0.955	-1.346	---	Insignificant
Residual Error	8	7.058	0.8822	--	--	--	---	---
Total	17	105.021	--	--	--	--	---	---
e-Pooled	10	7.1410	0.7141	--	--	--	12.6789	---

Table 10.5 Response table for S/N ratio of TWR

Level	Concentration	Abrasive	Power Rate	Grit Size
1	-0.3047	1.2566	-0.1818	-0.4376
2	-2.1704	-2.7061	-1.4082	-0.8047
3	--	-2.2631	-2.1226	-2.4703
Delta	1.8656	3.9627	1.9409	2.0326
Rank	4	1	3	2

From Table 10.5, 1st rank is given to Abrasive that means it higher contribution in the Surface Roughness, 2nd rank is given to Grit Size, 3rd rank is given to Power Rate and the 4th rank is given to Concentration that means it have less contribution in the Surface roughness.

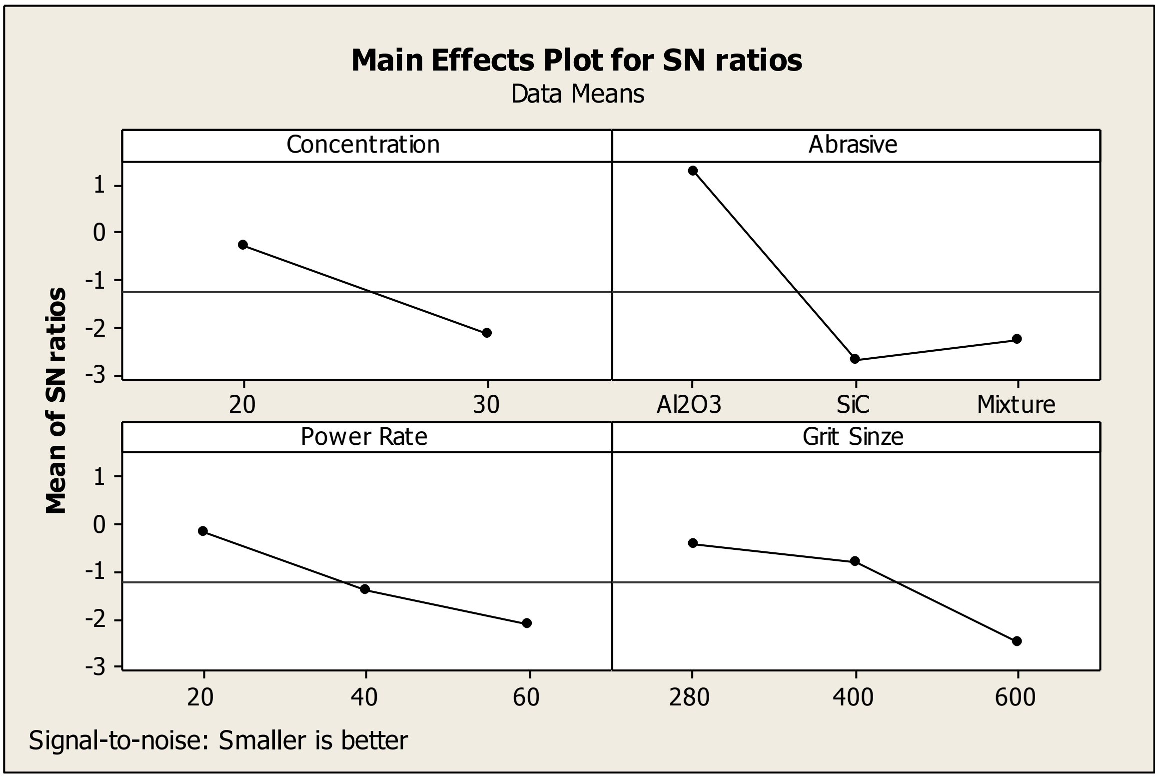

Fig 10.3 Main effects plot for S/N ratio of surface roughness

In fig 10.3 Main effects plot for S/N ratio of surface roughness shows that maximum Surface roughness is at 20% concentration, abrasive is Aluminium Oxide and Power Rate is 20 and the Grit Size is 280.

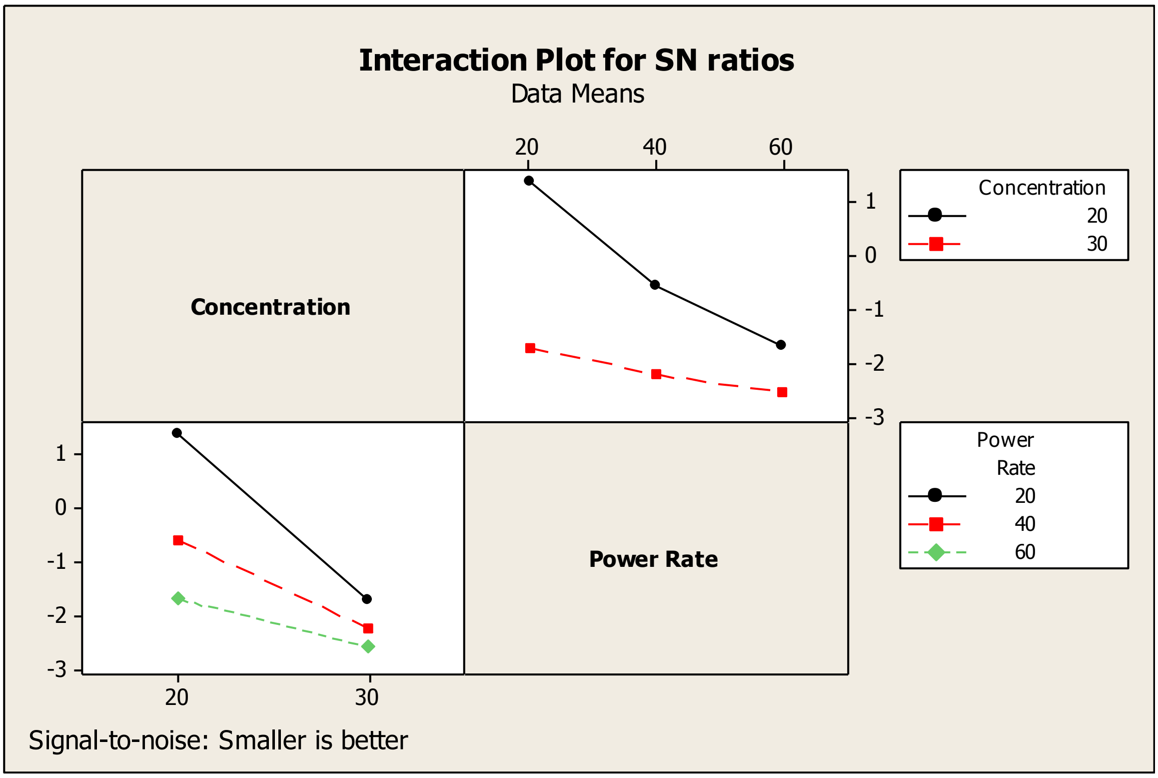

Fig 10.4 Interaction plot for of S/N ratio for Surface roughness

10.5 OPTIMAL DESIGN FOR SURFACE ROUGHNESS

In this experimental analysis, the main effect plot and interaction plot in Figure 10.1 and Figure 10.2 used to estimate the mean surface roughness. From the, Table 10.6 it was concluded that lowest roughness value was to be observed when Glass Work piece was machined Concentration 30%, abrasive Silicon Carbide, Power Rate 60 and Grit Size 600. In S/N ratio was to be observed at lowest roughness value when work-piece material was machined at Concentration 20%, Abrasive Aluminium Oxide, Power Rate 20 and Grit Size 280.

Table 10.6 **Significant factors and interactions**

Factor	Affecting Mean		Affecting Variation	
	Contribution	Best Level	Contribution	Best Level
Concentration,A	Significant	Level-2(30%)	Significant	Level-1(20%)
Abrasive, B	Significant	Level-2 (SiO)	Significant	Level-1(Al_2O_3)
Power Rate, C	Significant	Level-3(60)	Significant	Level-1(20)
Grit Size, D	Significant	Level-3 (600)	Significant	Level-1(280)
A x C	Insignificant	---	Insignificant	---

Mean Value for Surface Roughness

$$\mu_{A_2B_2C_3D_3} = A_2 + B_2 + C_3 + D_3 - 3T \qquad \text{(Equation....10.3)}$$

$$=1.3078+1.3767+1.3000+1.3517-3 \times 1.333=1.3422 \text{ micron}$$

Confidence Interval around the Estimated Mean

The confidence interval is a maximum and minimum value between which the true average should fall at some stated percentage of confidence. Confidence Interval around the estimated TWR mean

$$CI_1 = \sqrt{(F_{\alpha,V_1,V_2} V_e)/n_{eff}}$$

Where $F_{\alpha V1V2}$ = F ratio

α = Risk (0.01)   Confidence = 1- α

V_1 = DOF for mean which is always = 1

V_2 = DOF for error = Ve

η_{eff} = Number of tests under that condition using the participating factors

η_{eff} = (N/ 1+ DOF$A_2B_2C_3D_3$) = 18/ 1+1+2+2+2 = 2.25

$$CI_1 = \sqrt{(4.561\ X\ 0.0075)/2.25} = 0.082$$

So the confidence interval around the Surface Roughness is given by 1.3422±0.082 micron.

CHAPTER 11

RESULTS AND ANALYSIS OF ROCKWELL HARDNESS

11.1 INTRODUCTION

The effect Parameters i.e. Concentration, Type of Abrasive, Power Rate and Grit Size and the interaction between Concentration and Power Rate (AxC) were evaluated ANOVA and optimum design analysis. The Confidence interval of 95% has been used for the analysis. One repetition for each of 18 trails was completed to measure the Signal to Noise Ratio (S/N Ration).

11.2 RESULTS FOR ROCKWELL HARDNESS

The Rockwell hardness is measured on B type load and indenter type is steel ball, load applies for the 20 sec on the work-piece, and the units of Rockwell Hardness are HRB.

Table 11.1 Results for Rockwell Hardness

Trail No:	Slurry Concentration	Abrasive	Power Rate (%)	Grit Size	MRR mm^3/min	S/N Ratio	Mean
1	20	Al_2O_3	20	280	23.05	27.2534	23.05
2	20	Al_2O_3	40	400	25.15	28.0108	25.15
3	20	Al_2O_3	60	600	27.65	28.8339	27.65
4	20	SiC	20	280	26.05	28.3162	26.05
5	20	SiC	40	400	27.02	28.6337	27.02
6	20	SiC	60	600	29.01	29.2510	29.01
7	20	Mixture	20	400	26.23	28.3760	26.23
8	20	Mixture	40	600	28.45	29.0816	28.45
9	20	Mixture	60	280	29.59	29.4229	29.59
10	30	Al_2O_3	20	600	26.42	28.4387	26.42
11	30	Al_2O_3	40	280	25.58	28.1580	25.58
12	30	Al_2O_3	60	400	27.36	28.7423	27.36
13	30	SiC	20	400	26.24	28.3793	26.24
14	30	SiC	40	600	27.85	28.8965	27.85
15	30	SiC	60	280	28.95	29.2330	28.95
16	30	Mixture	20	600	28.06	28.9618	28.06
17	30	Mixture	40	280	29.99	29.5395	29.99
18	30	Mixture	60	400	30.13	29.5800	30.13

11.3 ANALYSIS OF VARIANCE FOR ROCKWELL HARDNESS

ANOVA Table 11.2 shows that factor Concentration, Abrasive and Power rate have P value less than 0.05 that means these are the significant, similarly Grit Size and interaction between Concentration and Power Rate have the P Value more than 0.05 that means the factor and the interaction is insignificant. Table 11.3 Response table for Means 1st is given to type of abrasive that means it has more contribution in Rockwell Hardness, 2nd rank given to the Power Rate, 3rd rank is given to the Concentration and the 4th rank is given to the Grit Size that means it has very less contribution in the Rockwell Hardness.

Table 11.2 ANOVA for means of Rockwell Hardness

Source	DOF	Seq SS	Adj MS	F	P	SS'	% Contribution	Status
Concentration,A	1	3.9014	3.9014	8.76	0.018	3.456	5.888	Significant
Abrasive, B	2	24.9530	12.4765	28.01	0.001	24.062	41.001	Significant
Power Rate, C	2	23.0862	11.5431	25.92	0.003	22.195	37.820	Significant
Grit Size, D	2	2.6253	0.4644	1.04	0.396	-0.569	---	Insignificant
A x C	2	0.5569	0.2784	0.63	0.559	-0.577	---	Insignificant
Residual Error	8	3.5630	0.4454	--	--	--	---	---
Total	17	58.6858	--	--	--	--	---	---
e-Pooled	12	6.7452	0.5621	--	--	--	15.291	---

Table 11.3 Response table for Means

Level	Concentration	Abrasive	Power Rate	Grit Size
1	26.91	25.87	26.01	27.20
2	27.84	27.52	27.34	27.02
3	--	28.74	28.78	27.91
Delta	0.93	2.87	2.77	0.89
Rank	3	1	2	4

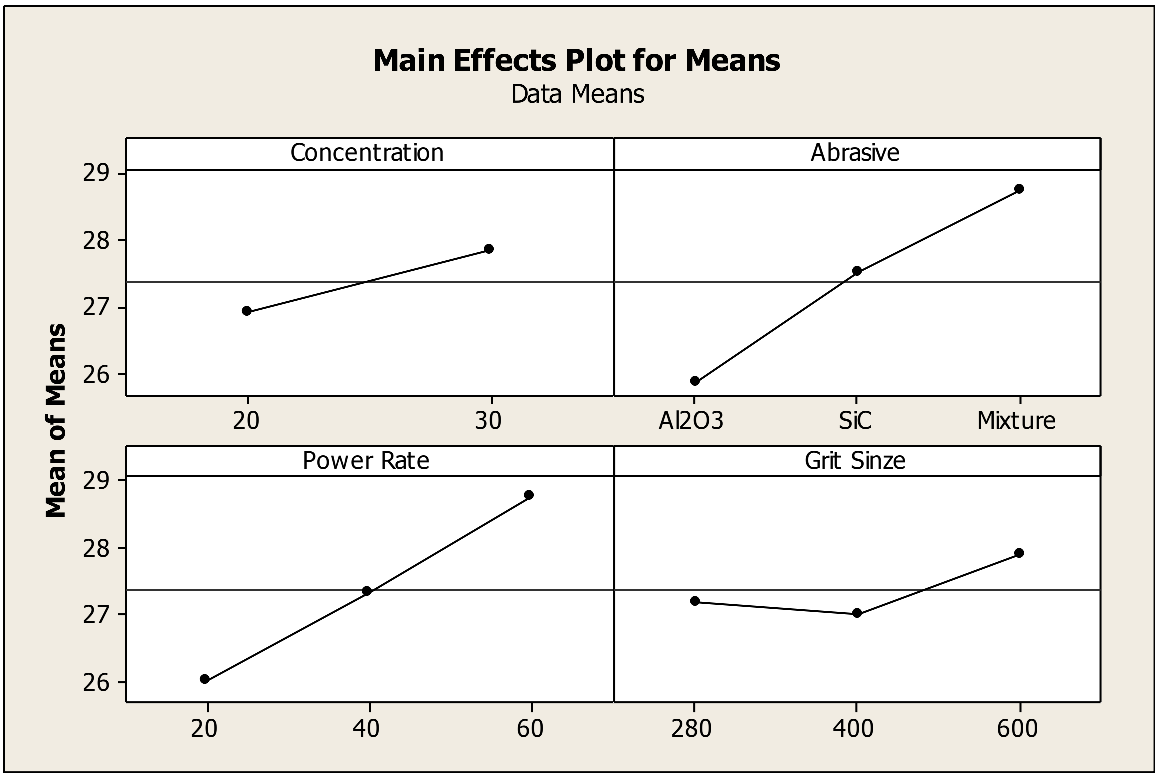

Fig11.1 Main effect plot for Mean of Rockwell Hardness

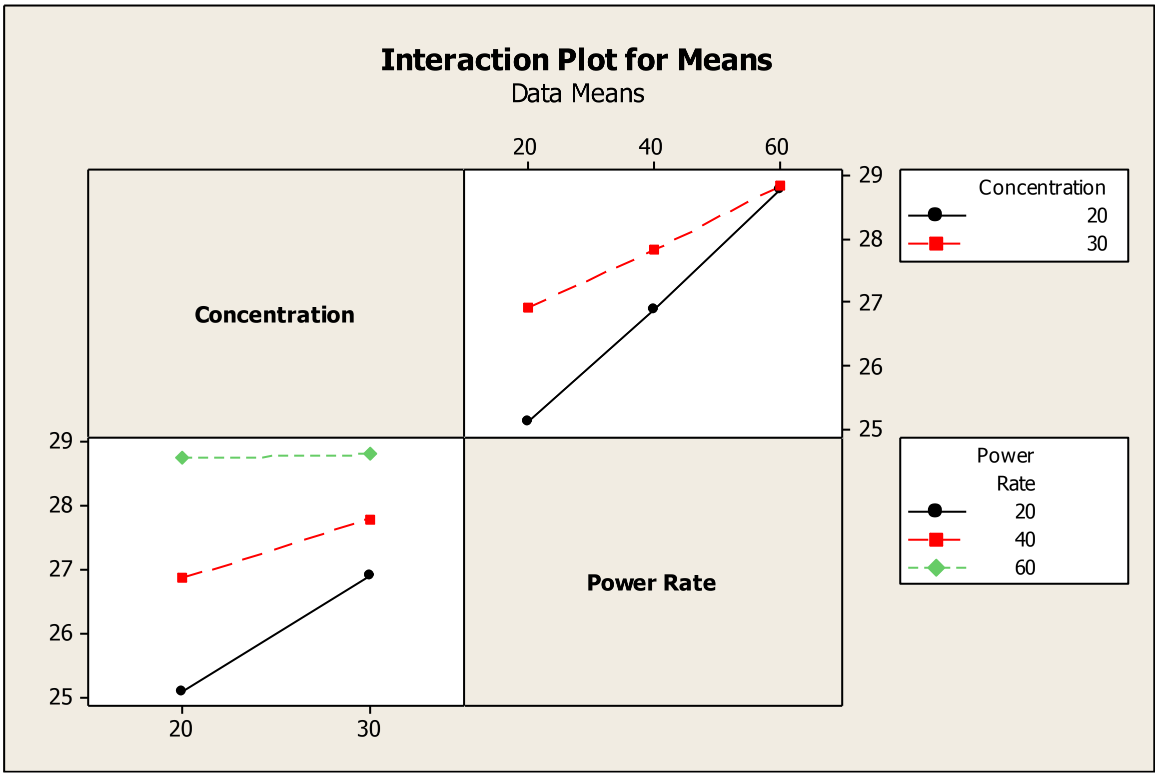

Fig11.2 Interaction plot for Means

11.4 ANOVA FOR S/N RATIO OF ROCKWELL HARDNESS

Rockwell hardness is "Higher is Better" type response, for which S/N ratio was calculated by using equation 11.1 and 11.2

$$(\frac{S}{N})_{HB} = -10\log(MSD_{HB}) \quad \text{(Equation....11.1)}$$

$$\text{Where } MSD_{HB} = \frac{1}{r}\sum_{j=1}^{r}(\frac{1}{y_j^2}) \quad \text{(Equation....11.2)}$$

MSDHB = Mean Square Deviation for higher-the-better response.

Table 11.4 shows the ANOVA for S/N ratio for Rockwell Hardness as 95% confidence interval. There Concentration, Abrasive and power Rate have P Value Less than 0.05 that means these are significant and the Grit Size and the interaction between Concentration and Abrasive have P Value Less the 0.005 That means these are insignificant. From Table 11.5 Response table for S/N Ratio 1st rank is given to Abrasive that mean it have higher contribution in the Rockwell Hardness, 2nd rank is given to Power Rate, 3rd rank is given to Concentration and the 4th rank is given to Grit Size that means it have the less contribution in the Rockwell Hardness.

Table11.4 ANOVA table of S/N ratio for Rockwell Hardness

Source	DOF	Seq SS	Adj MS	F	P	SS'	% Contribution	Status
Concentration,A	1	0.42002	0.42002	8.36	0.020	0.36979	6.025	Significant
Abrasive, B	2	2.57245	1.28622	25.61	0.002	2.47199	40.281	Significant
Power Rate, C	2	2.37496	1.18748	23.64	0.012	2.27450	37.063	Significant
Grit Size, D	2	0.41024	0.52056	9.02	0.021	0.30982	5.048	Significant
A x C	2	0.06499	0.03249	0.62	0.549	0.05559	0.0905	Insignificant
Residual Error	8	0.40186	0.05023	--	--	--	---	---
Total	17	6.13681	--	--	--	--	---	---
e-Pooled	1	0.42002	0.42002	8.36	0.020	0.36979	6.025	---

Table 11.5 Response table for S/N Ratio

Level	Concentration	Abrasive	Power Rate	Grit Size
1	28.58	28.24	28.29	28.65
2	28.88	28.78	28.72	28.62
3	--	29.16	29.18	28.91
Delta	0.31	0.92	0.89	0.29
Rank	3	1	2	4

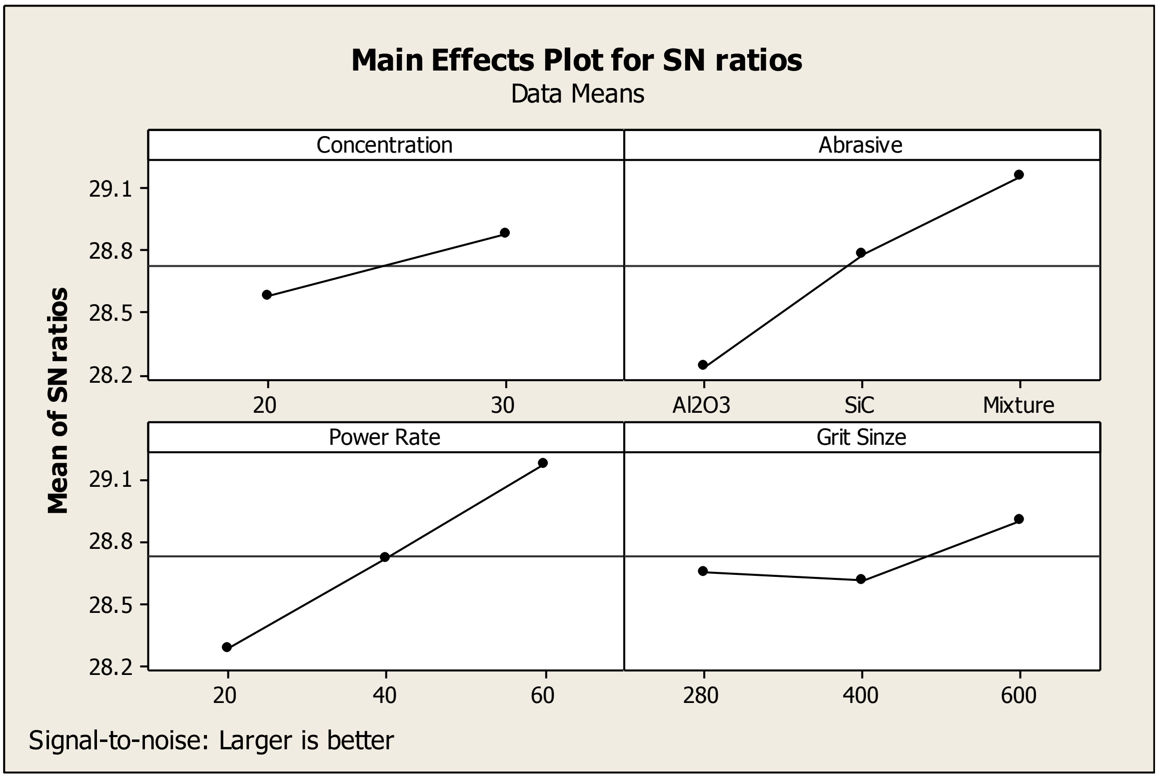

Fig11.3 Main Effects plot for S/N ration

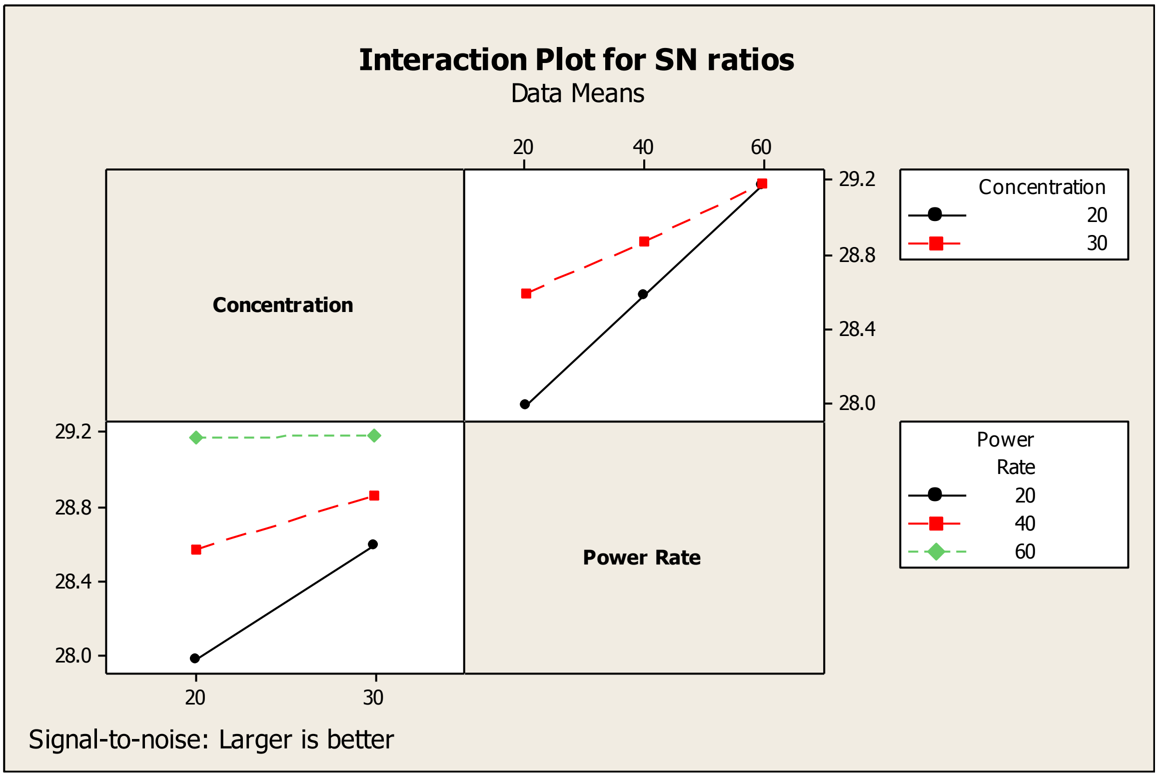

Fig11.4 Interaction plot for S/N ratio

11.5 OPTIMAL DESIGN FOR ROCKWELL HARDNESS

In this experiment analysis, the main effect plot and interaction plot in Fig11.1 and 11.2 used to estimate the main Rockwell Hardness was observed that when work-piece was machined at Concentration 30%, Abrasive Mixture (Aluminium Oxide and Silicon Carbide) and Power Rate 60. In S/N ratio highest Rockwell Hardness was obtained when the work-piece was machined at Concentration 30%, Abrasive Mixture (Aluminium Oxide and Silicon Carbide) and Power Rate 60. So to achieve higher Rockwell Hardness the best design was suggested that Work piece Glass machined at Concentration 30%, Abrasive Mixture (Aluminium Oxide and Silicon Carbide) and Power Rate 60.

Table 11.6 Significant factors and interactions

Factor	Affecting Mean		Affecting Variation	
	Contribution	Best Level	Contribution	Best Level
Concentration,A	Significant	Level-2 (30)	Significant	Level-2 (30)
Abrasive, B	Significant	Level-3 (Mix)	Significant	Level-3 (Mix)
Power Rate, C	Significant	Level-3 (60)	Significant	Level-3 (60)
Grit Size, D	Insignificant	---	Significant	Level-3 (600)
A x C	Insignificant	---	Insignificant	---

Estimating the mean for Rockwell Hardness In experiment analysis, the Rockwell Hardness is a higher average response is better (HB) characteristic. Different treatment combinations have been chosen to get satisfactory results. After conducting the experiments the optimum treatment condition within the experiments determined on the basis of prescribed combination of factor levels is determined to one of those in the experiment.

Mean Value for TWR

$$\mu_{A_2B_3C_3} = A_2 + B_3 + C_3 + D_3 - 4T \qquad \text{(Equation....11.3)}$$

$$= 27.84 + 28.74 + 28.78 + 27.91 - 3 \times 27.37 = 31.16$$

The confidence interval is a maximum and minimum value between which the true average should fall at some stated percentage of confidence. Confidence Interval around the estimated Rockwell Hardness mean

$$CI_1 = \sqrt{(F_{\alpha,V_1,V_2} V_e)/n_{eff}}$$

Where $F_{\alpha V1V2}$ = F ratio

α = Risk (0.01) Confidence = 1- α

V_1 = DOF for mean which is always = 1

V_2 = DOF for error = V_e

η_{eff} = Number of tests under that condition using the participating factors

η_{eff} = (N/ 1+ $DOFA_2B_3C_3D_3$) = 18/ 1+1+2+2+2 = 2.25

$$CI_1 = \sqrt{(4.895\ X\ 0.0047)/2.25} = 0.0102$$

So the confidence interval around the Rockwell Hardness is given by 31.16 ± 0.0102 HRB

CHAPTER 12

REGRESSION ANALYSIS

12.1 INTRODUCTION

A statistical procedure used to find relationships among a set of variables. In regression analysis, there is a **dependent variable**, which is the one you are trying to explain, and one or more **independent variables** that are related to it. You can express the relationship as a linear equation, such as:

$$y = a + bx \qquad \text{(Equation….12.1)}$$

- y is the dependent variable
- x is the independent variable
- a is a constant
- b is the slope of the line

For every increase of 1 in x, y changes by an amount equal to b.

Regression finds the line that best fits the observations. It does this by finding the line those results in the lowest sum of squared errors. Since the line describes the mean of the effects of the independent variables, by definition, the sum of the actual errors will be zero. If you add up all of the values of the dependent variable and you add up all the values predicted by the model, the sum is the same.That is, the sum of the negative errors (for points below the line) will exactly offset the sum of the positive errors (for points above the line). Summing just the errors wouldn't be useful because the sum is always zero. So, instead, regression uses the sum of the squares of the errors. An Ordinary Least Squares (OLS) regression finds the line those results in the lowest sum of squared errors.

Multiple Regressions

When, several factors affecting the independent variable. Each of these factors has a separate relationship with the price of a home. The equation that describes a multiple regression relationship is:

$$y = a + b_1x_1 + b_2x_2 + b_3x_3 + \dots b_nx_n + e \qquad \text{(Equation….12.2)}$$

- y is the dependent variable
- $x_1, x_2, x_3 \dots x_n$ are the independent variables
- a is a constant
- $b_1,b_2,b_3 \dots b_n$ slope of the line

This equation separates each individual independent variable from the rest, allowing each to have its own coefficient describing its relationship to the dependent variable.

"p-values" and Significance Levels

Each independent variable has another number attached to it in the regression result its "p-value" or significance level. The p-value is a percentage. It tells you how likely it is that the coefficient for that independent variable emerged by chance and does not describe a real relationship. P-value of .05 means that there is a 5% chance that the relationship emerged randomly and a 95% chance that the relationship is real. It is generally accepted practice to consider variables with a p-value of less than .1 as significant, though the only basis for this cutoff is convention.

12.2REGRESSIONS ANALYSIS FOR MRR

In the regression analysis for MRR there are four input parameter Concentration, Abrasive, Power Rate and Grit Size and the output parameters are MRR, TWR, Surface Roughness and Rockwell Hardness. The equation that describes a multiple regression relationship for the MRR is:

$$MRR = 27.0 + 2.89\ A + 1.78\ B + 0.647\ C - 3.85 \qquad \text{(Equation...12.3)}$$

Where A is Concentration, B is Type of Abrasive, C is Power Rate and D is Grit Size.

Where R-Sq Value is 64.7% that means the equation is:

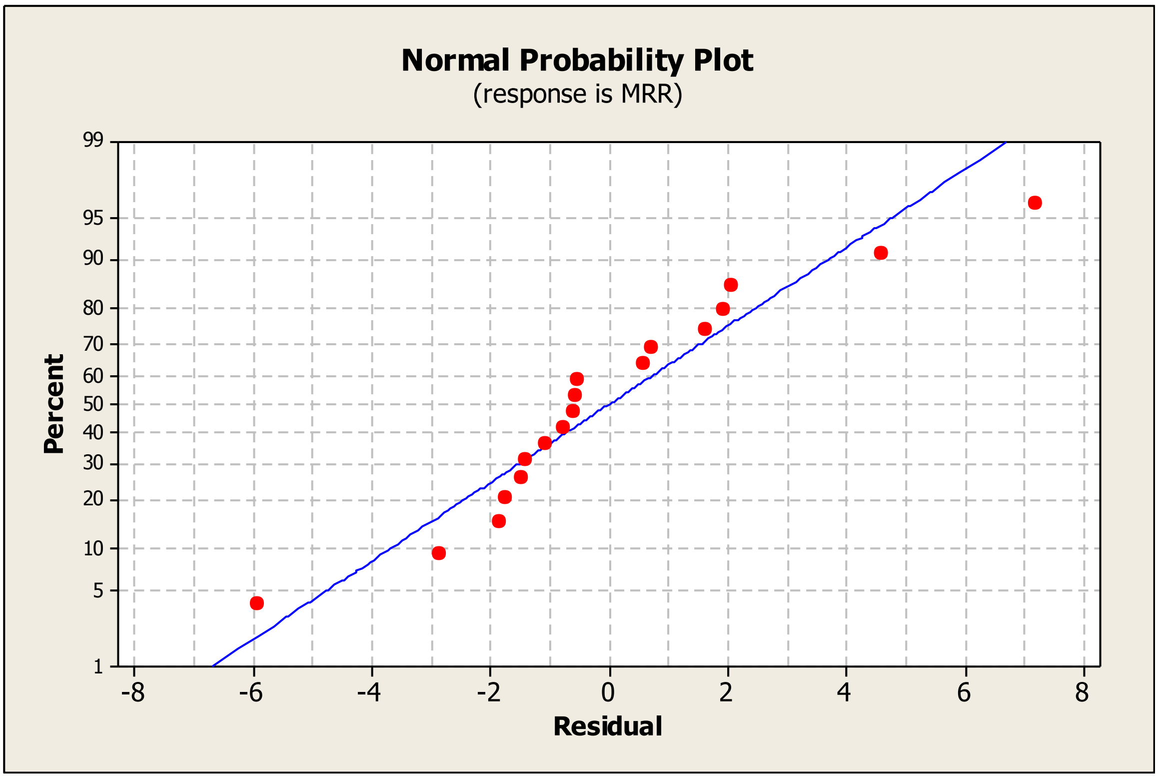

Fig 12.1 Normal Probability plot for MRR

In the Fig 12.1 we see it the maximum value of the experiment work are located near the line of slop that means the equation is suitable with the input and output parameters

12.3 REGRESSIONS ANALYSIS FOR TWR

In the regression analysis for MRR there are four input parameter Concentration, Abrasive, Power Rate and Grit Size and the output parameters are MRR, TWR, Surface Roughness and Rockwell Hardness. The equation that describes a multiple regression relationship for the TWR is:

Tool wear = 0.222 + 0.0362 A + 0.0484 B + 0.0157 C - 0.0290 D (Equation....12.4)

Where A is Concentration, B is Type of Abrasive, C is Power Rate and D is Grit Size. Where R-Sq Value is 64.1% that means the equation is:

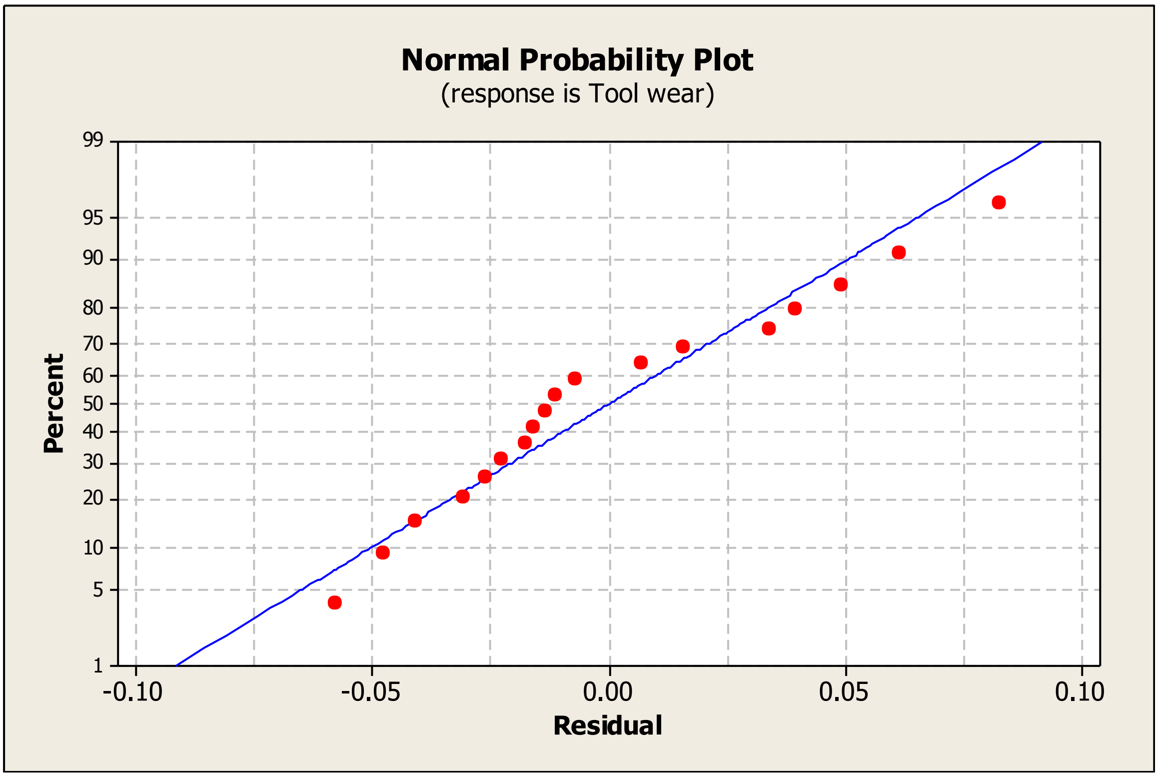

Fig 12.2 Normal Probability of TWR

In the Fig 12.2 we see it the maximum value of the experiment work are located near the line of slop that means the equation is suitable with the input and output parameters

12.4 REGRESSIONS ANALYSIS FOR SURFACE ROUGHNESS

In the regression analysis for MRR there are four input parameter Concentration, Abrasive, Power Rate and Grit Size and the output parameters are MRR, TWR, Surface Roughness and Rockwell Hardness. The equation that describes a multiple regression relationship for the Surface Roughness is:

Surface Roughness = - 0.059 + 0.227 A + 0.213 B + 0.117 C + 0.127 D (Equation....12.5)

Where A is Concentration, B is Type of Abrasive, C is Power Rate and D is Grit Size. Where R-Sq Value is 73.3% that means the equation is:

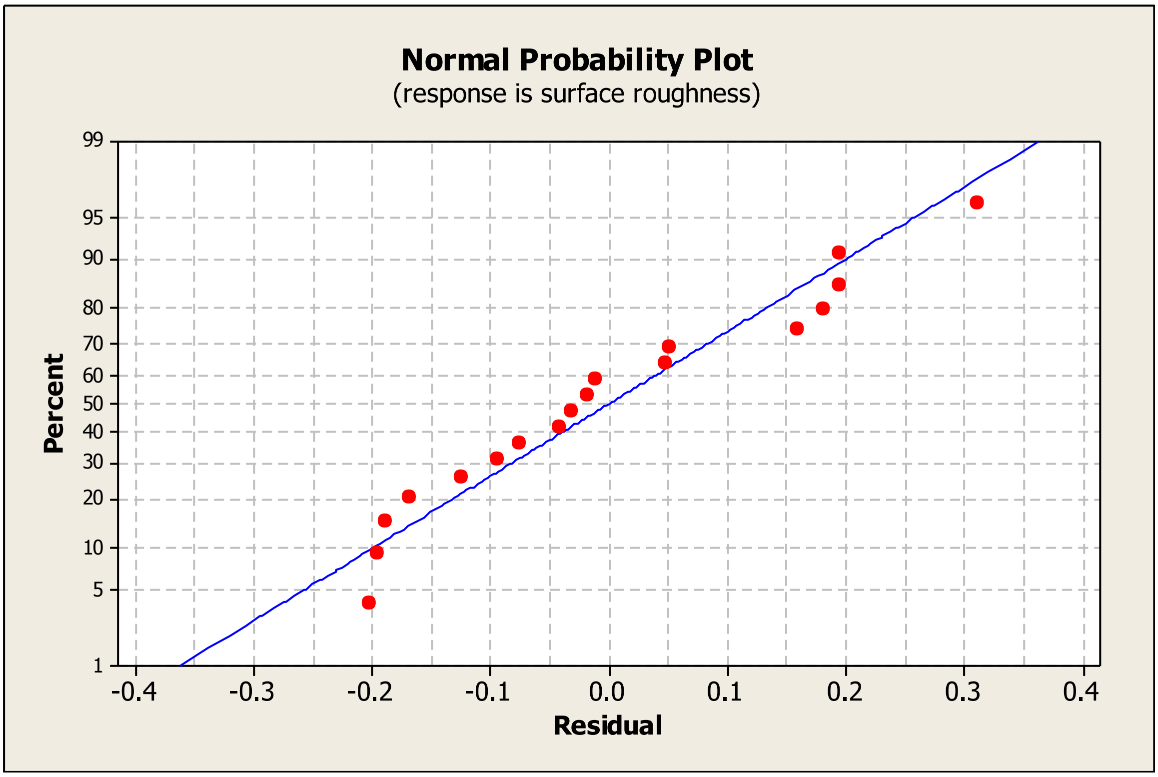

Fig 12.3 Normal Probability plot for Surface Roughness

In the Fig 12.3 we see it the maximum value of the experiment work are located near the line of slop that means the equation is suitable with the input and output parameters

12.5 REGRESSIONS ANALYSIS FOR ROCKWELL HARDNESS

In the regression analysis for MRR there are four input parameter Concentration, Abrasive, Power Rate and Grit Size and the output parameters are MRR, TWR, Surface

Roughness and Rockwell Hardness. The equation that describes a multiple regression relationship for the Rockwell Hardness is:

Rockwell hardness = 19.6 + 0.931 A + 1.44 B + 1.39 C + 0.353 D (Equation....12.6)

Where A is Concentration, B is Type of Abrasive, C is Power Rate and D is Grit Size. Where R-Sq Value is 90.7% that means the equation is:

)

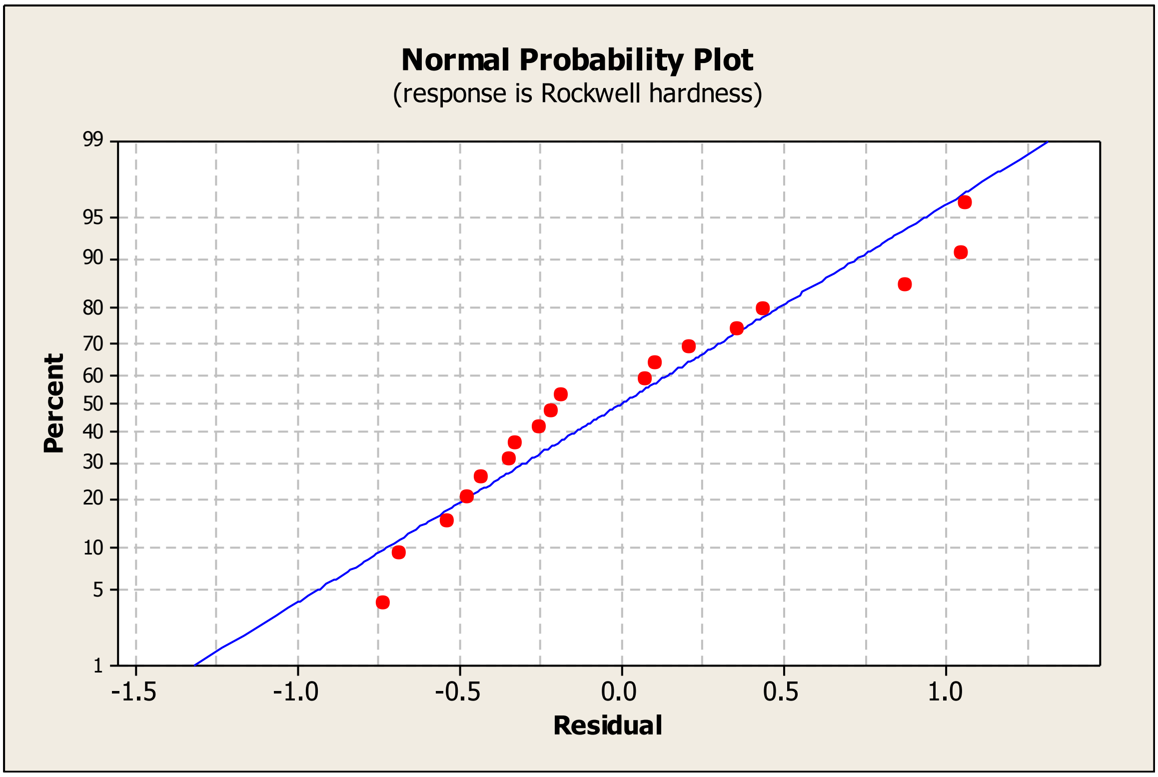

Fig 12.4 Normal Probability plot of Rockwell Hardness

In the Fig 12.4 we see it the maximum value of the experiment work are located near the line of slop that means the equation is suitable with the input and output parameters.

CHAPTER 13

RESULTS, CONCLUSIONS AND RECOMMENDATIONS

13.1 RESULTS

The effect of parameters i.e. Concentration, Type of Abrasive, Power Rate and Grit Size and interactions between concentration and power rate evaluated using ANOVA design analysis and Regression analysis. The purpose of the ANOVA was to identify the important parameters in prediction of MRR, TWR, Surface Roughness and Rockwell Hardness. Some results consolidated from ANOVA and plots are given below:

13.1.1 MRR

The effect of parameters i.e, concentration, abrasive, power rate and grit size and some other interaction were evaluated using ANOVA and factorial design analysis. A confidence interval of 80.167% has been used for the analysis. One repetition for each 18 trails was completed to measure the Signal to Noise ratio (S/N Ratio).

The various data for each factor and their interaction was P value find for the significant of each. The principal of the P value is that the value less than 0.05 that factors or interactions are significant if value is more than 0.05 then that factors or interactions are insignificant. From the ANOVA table for mean we see it Concentration P value is 0.013, Abrasive P value is 0.003, Power Rate P value is 0.041 and Grit Size P value is 0.001 these factors are significant, same concentration and Power rate interaction P value is more than 0.05 so that these are insignificant. In the table 8.3 the ranks are show for the different factor. 1st rank is given to the grit size that mean grit size has the highest contribution to MRR. 2nd rank is give to the type of abrasive, 3rd rank is given to the power rate and the 4th rank is given to the Concentration that mean power rate have the minimum contribution to the MRR.

Highest MRR was observed when Work-piece is machined on concentration 30%, abrasive Silicon Carbide, Power Rate 60 and Grit Size 280. It also observes that the interaction AxC is not any effect on the MRR. The best MRR value was compromised to get best results. MRR Assumed to be achieved best result if Glass work piece is machined at concentration 30% of abrasive and water slurry, abrasive Silicon Carbide, Power Rate 60 and

Grit Size 280. With 95% confidence interval mean value of MRR was found to be 35.78 ± 0.221 mm^3/min.

13.1.2 TWR

The effects of parameters i.e. Concentration, Abrasive, Power Rate and Grit Size and the interaction between Concentration and Power Rate were evaluated using ANOVA analysis. A confidence interval of 82.35% has been used for the analysis. One repetition for each of 18 trails was completed to measure the Signal to Noise ratio(S/N Ratio).

The various data for each factor and their interaction was P value find for the significant of each. The principal of the P value is that the value less than 0.05 that factors or interactions are significant if value is more than 0.05 then that factors or interactions are insignificant. From the ANOVA table for mean we see it Concentration P value is 0.014, Abrasive P value is 0.001 and Grit Size P value is 0.013 these factors are significant, same Power rate and concentration and Power rate (AxC) interaction P value is more than 0.05 so that these are insignificant. In the table 9.3 the ranks are show for the different factor. 1^{st} rank is given to the type of Abrasive that mean grit size has the highest contribution to TWR. 2^{nd} rank is give to the Grit Size, 3^{rd} rank is given to the Concentration and the 4^{th} rank is given to the Power rate that mean power rate have the minimum contribution to the TWR.

The lowest TWR was to be observed when workpiece was machined with Concentration 30% Abrasive Silicon Carbide and Grit Size 280. In S/N ratio highest TWR was to be observed when workpiece material was machined with Concentration 20%, Abrasive Aluminium Oxide and Grit Size 600. With 95% confidence interval mean value of TWR was found to be 0.0970±0.0065mm^3/min.

13.1.3 SURFACE ROUGHNESS

The effects of parameters i.e. Concentration, Abrasive, Power Rate and Grit Size and the interaction between Concentration and Power Rate were evaluated using ANOVA analysis. A confidence interval of 95% has been used for the analysis. One repetition for each of 18 trails was completed to measure the Signal to Noise ratio(S/N Ratio). In this experiment work surface roughness (Ra) has measured at position centre.

The Concentration, Power Rate, Type of Abrasive (Aluminium Oxide, Silicon Carbide and Mixture) is input parameters which affects the surface roughness. Main effect plots had shown in the Figure 10.1 shows that the surface roughness increases with increase in the Concentration, Power Rate, Abrasive and Grit Size.

The work-piece material also affects the surface roughness. Table 10.3 shows ranks to various input parameters in terms their relative significance. 1st rank is given to Abrasive slurry, 2nd rank is given to Grit Size, 3rd Rank is given to Power Rate and 4th rank is given to Concentration.

it was concluded that lowest roughness value was to be observed when Glass Work piece was machined Concentration 30%, abrasive Silicon Carbide, Power Rate 60 and Grit Size 600. In S/N ratio was to be observed at lowest roughness value when workpiece material was machined at Concentration 20%, Abrasive Aluminium Oxide, Power Rate 20 and Grit Size 280. With 95% confidence interval mean value of Surface Roughness was found to be 1.3422±0.018 micron.

13.1.4 ROCKWELL HARDNESS

The effect Parameters i.e, Concentration, Type of Abrasive, Power Rate and Grit Size and the interaction between Concentration and Power Rate (AxC) were evaluated ANOVA and optimum design analysis. The Confidence interval of 95% has been used for the analysis. One repetition for each of 18 trails was completed to measure the Signal to Noise Ratio (S/N Ration).

Factor Concentration, Abrasive and Power rate have P value less than 0.05 that means these are the significant, similarly Grit Size and interaction between Concentration and Power Rate have the P Value more than 0.05 that means the factor and the interaction is insignificant. Table 11.3 Response table for Means 1st is given to type of abrasive that means it has more contribution in Rockwell Hardness, 2nd rank given to the Power Rate, 3rd rank is given to the Concentration and the 4th rank is given to the Grit Size that means it has very less contribution in the Rockwell Hardness.

The main Rockwell Hardness was observed that when work-piece was machined at Concentration 30%, Abrasive Mixture (Aluminium Oxide and Silicon Carbide) and Power Rate 60. In S/N ratio highest Rockwell Hardness was obtained when the work-piece was machined at Concentration 30%, Abrasive Mixture (Aluminium Oxide and Silicon Carbide) and Power Rate 60. So to achieve higher Rockwell Hardness the best design was suggested that Work piece Glass machined at Concentration 30%, Abrasive Mixture (Aluminium Oxide and Silicon Carbide) and Power Rate 60. With 95% confidence interval mean value of MRR was found to be 31.16 ± 0.1731 HRB

13.2 CONCLUSIONS

The present study was carried out to study the effect of input parameters (Type of Abrasive, Power Rate and Grit Size and the interaction between Concentration and Power Rate (AxC)) on the MRR, TWR, Surface Roughness and Rockwell Hardness. The following conclusions have been drawn from the study:

- In Finite Element Analysis the maximum Stress was generated on the tip of the tool.
- With the help of stress value of USM tool and Glass work-piece Factor of Safety Calculated that was 4, that mean design was safe.
- With the help of stress analysis and safety factor tool material (High Carbon high Chromium steel) was selected.
- The MRR mainly affected by the Grit Size and Abrasive.
- Maximum MRR Obtained at Grit Size 280, 30% Concentration, Silicon Carbide Abrasive And 60% Power Rate.
- Maximum tool wear rate is occur when 30% Concentration, Abrasive Silicon Carbide, and Grit Size 280.
- Higher concentrations gives higher the MRR and TWR.
- Grit Site 280 of Silicon Carbide gives maximum MRR but, also increase the TWR.
- Minimum TWR is at 20% concentration, Abrasive Aluminium Oxide, Power Rate 20 and Grit Size 600.
- Maximum Surface Roughness is obtained with 30% Concentration, Abrasive Silicon Carbide, Power Rate 60 and Grit Size 600.
- Maximum effect on machined surface finish is due to type of Abrasive and Grit Size.
- Grit Size 600 of Silicon Carbide gives the maximum Surface finish.
- Rockwell Hardness is mainly effected by Type of Abrasive and Power Rate
- Maximum effect on the Rockwell Hardness is due to 30% Concentration, Abrasive Mixture (Aluminium Oxide and Silicon Carbide) and Power Rate 60.
- Maximum Rockwell Hardness is obtained by Mixture Slurry (Aluminium Oxide and Silicon Carbide) of concentration 30%.

REFRENCE

1. Z.C. Lia, Liang-Wu Caib Z.J, Peia C. (2006) Treadwellc Edge-chipping reduction in rotary ultrasonic machining of ceramics:Finite element analysis and experimental verification International Journal of Machine Tools & Manufacture 46 1469–1477.

2. *S. Aminia, H. Soleimanimehra, M.J. Nategha,, A. Abudollahb, M.H. Sadeghia*(2008) FEM analysis of ultrasonic-vibration-assisted turning and the vibratory tool, journal of materials processing technology 201 43–47.

3. Yu Liua,b, Lijun Wanga,b, Dongpo Wanga,b, (2011) Finite element modeling of ultrasonic surface rolling process Journal of Materials Processing Technology 211 2106–2113.

4. DeFu Liu , W.L.Cong , Z.J.Pei b,n, YongJunTang, (2012) A cutting force model for rotary ultrasonic machining of brittle materialsInternational Journal of Machine Tools & Manufacture 52 77–84.

5. J. Pujana , A.Rivero , A.Celaya , L.N.Lo pez deLacalle, (2009) Analysis of ultrasonic-assisted drilling of Ti_6Al_4V International Journal of Machine Tools & Manufacture 49 500–508

6. V.I. Babitsky, A.V. Mitrofanov, V.V. Silberschmidt (2004) Ultrasonically assisted turning of aviation materials: simulations and experimental study Ultrasonics 42, 81–86.

7. A.R. Jones , J.B. Hull (1998) Ultrasonic flow polishing, Ultrasonics 36 (1998)97- 101.

8. *Kei-Lin Kuo* (2008) Design of rotary ultrasonic milling tool using FEM simulation journal of materials processing technology 201, 48–52.

9 P. L. Guzzo and H. Shinohara(2004) A Comparative Study on Ultrasonic Machining of Hard and Brittle Vol. XXVI, No. 1.

10. Eng. Alexandru Sergiu nanu, prof. niculae ion marinescu,(2011) study on ultrasonic stepped horn geometry design and fem simulation *nonconventional technologies review – no. 4/2011*

*11. Javad Akbari, Hassan Borzoie, and Mohammad Hossein Mamduhi (2008)*Study on Ultrasonic Vibration Effects on Grinding Process of Alumina Ceramic (Al_2O_3), World Academy of Science, Engineering and Technology 41.

12. Vinod Kumar, Jatinder Kumar (2011) Prediction of Tool and Nozzle Flow Behavior in Ultrasonic Machining Process, World Academy of Science, Engineering and Technology 81.

13. Jatinder Kumar, J.S. Khamba (2008) An investigation into the machining characteristics of titanium using ultrasonic machining, *Int. J. Machining and Machinabiliy of Materials, Vol. 3, Nos. 1/2.*

14. *T.C.* Lee, C.W. Chan (1997) Mechanism of the ultrasonic machining of ceramic composites of Materials Processing Technology, 71,195-205.
15. Kei-Lin KUO, Ultrasonic vibrating system design and tool analysis (2009), Trans. Nonferrous Met.Soc.China 19,225-231.

16. M. Nad, Ultrasonic horn design for ultrasonic machining technologies, Applied and Computational Mechanics 4, 79–88.

17. Vinod Yadava & Aniruddha Deoghare, Design of horn for rotary ultrasonic machining using the finite element method (2008), Int J Adv Manuf Technol 39,9–20.

18. Aarati Sarwade, Study of micro rotary ultrasonic machining (2010), University of Nebraska – Lincoln

19. *Kumar.V , Khamba. J. S. (2009)* Parametric optimization of ultrasonic machining of co-based super alloy using the Taguchi multi-objective approach, Prod. Eng. Res. Devel, 3, 417–425.

20. Yang.K, Teo.E.C, Konstantin.F (2007) Application of Taguchi method in optimization of cervical ring cage, Journal of Biomechanics 40, 3251–3256.

21. Xiansheng.N, Zhenggan.Z, Xiongwei.W , Luming.L (2011) The use of Taguchi method to optimize the laser welding of sealing neuro-stimulator, Optics and Lasers in Engineering 49, 297–304.

22. Lin.Y.C, Chen.Y.F, WangD.A, Lee.H.S, (2009) Optimization of machining parameters in magnetic forceassisted EDM based on Taguchi method, journal of materials processing technology 209, 3374–3383.

23. Liu.Y.T, Chang.W.C, Yamagata.Y, (2010) A study on optimal compensation cutting for an aspheric surface using theTaguchi method, CIRP Journal of Manufacturing Science and Technology 3, 40–48.

24. Comakli.K,Simsek.F,Comakli.O, Sahin.B, (2009) Determination of optimum working conditions R22 and R404A refrigerant mixtures in heat-pumps using Taguchi method, Applied Energy 86, 2451–2458.

25. Hou.T.H, Hung S.C, Wang-L. L, (2007) Parameters optimization of a nano-particle wet milling process using theTaguchi method, response surface method and genetic algorithm. Powder Technology 173, 153–162.

26. Ming L.J , Lu.P.L, Weng.W.K, (2001) modifications of ITO surfaces in OLED devices by Taguchi methods, Materials Science and Engineering 85, 209–211.

27. Chang.C.W, Kuo.C.P(2007) Evaluation of surface roughness in laser-assisted machining of aluminum oxide ceramics with Taguchi method, International Journal of Machine Tools & Manufacture 47 141–147.

28. Tosun.N, Cogun.C, Tosun.G, (2004) A study on kerf and material removal rate in wire electrical discharge machining based on Taguchi method, Journal of Materials Processing Technology 152, 316–322.

29. Gologlu.C, Sakarya.N, (2008) The effects of cutter path strategies on surface roughness of pocket milling of 1.2738 steel based on Taguchi method, journal of materials processing technology 206, 7–15.

30. Kapsiz.M, Durat.M,Ficici.F, (2011) Friction and wear studies between cylinder liner and piston ring pair using Taguchi design method, Advances in Engineering Software 42, 595–603.

31. Rosa. J.L., Robin. A., Silva. M.B., Baldan. C.A., Peres. M.P. (2009) Electrodeposition of copper on titanium wires: Taguchi experimental design approach, journal of materials processing technology 209, 1181–1188.

32. Prihandana.G.S, Mahardika.M, Hamdi.M, Wong. Y.S.,Mitsui.K, (2009) Effect of micro-powder suspension and ultrasonic vibration of dielectric fluid in micro-EDM processes—Taguchi approach International Journal of Machine Tools & Manufacture 49, 1035–1041.

33. Thipprakmas.S, (2010) Application of Taguchi technique to investigation of geometry and position of V-ring indenter in fine-blanking process. Materials and Design 31,2496–2500.

34. Savas.O, Kayikci.R, (2007) Application of Taguchi's methods to investigate some factors affecting microporosity formation in A360 aluminium alloy casting, Materials and Design 28, 2224–2228.

35. Kishore. R.A., Tiwari. R., Dvivedi. A., Singh I, (2009) Taguchi analysis of the residual tensile strength after drilling in glass fiber reinforced epoxy composites, Materials and Design 30, 2186–2190.

36. George P.M., Raghunath B.K., Manocha L.M., Warrier A.M, (2004) EDM machining of carbon–carbon composite—a Taguchi approach, Journal of Materials Processing Technology 145, 66–71.

37. Yen.Y.T, Fang.T.H, Lin.Y.C, (2011) Optimization of screen-printing parameters of SN9000 ink for pinholes using Taguchi method in chip on film packaging, Robotics and Computer-Integrated Manufacturing 27, 531–537.

38. Kilickap.E (2010) Optimization of cutting parameters on delamination based on Taguchi method during drilling of GFRP composite. Expert Systems with Applications 37, 6116–6122.

39. Fung.P.C, Kang.P.K, (2005) Multiresponse optimization in friction properties of PBT composites using Taguchi method and principle component analysis, Journal of Materials Processing Technology 170, 602–610.

40. Jeang.A, Chung.C.P, Chen.C.W, Li. H.C, (2009) Optimizing process parameters of hot-bar soldering process through quality function deployment and Taguchi method, journal of materials processing technology 209, 2967–2977.

41. Anawa.E.M, Olabi A.G. (2008) Using Taguchi method to optimize welding pool of dissimilar laser-welded components, Optics & Laser Technology 40, 379–388

42. Pan.L.K, Wang.C.C,Hsiao.Y.C,Ho.K.C, (2004) Optimization of Nd:YAG laser welding onto magnesium alloy via Taguchi analysis, Optics & Laser Technology 37,33-42.

43. Aggarwal.A, Singh.H, Kumar.P, Manmohan Singh.M, (2008) Optimizing power consumption for CNC turned parts using response surface methodology and Taguchi's technique—A comparative analysis, journal of materials processing technology 200, 373–384.

44. Finite Element Analysis (2005) Dr.S.S Bhavikatti, New Age International Publishers, Volume 1.

45. Experimental and finite element modelling of ultrasonic cutting of food (2008)Euan McCulloch BEngAMIMechE, Department of Mechanical Engineering University of Glasgow.